

**Numerical Investigation of Convective Heat and Mass Transfer Flow  
along a Vertical Porous Plate with Soret and Dufour Effects  
in the Presence of Induced Magnetic Field**

by

**S. M. Mahathy Hasan**

Roll No: 1351551

Session: July-2013

A Thesis Submitted in partial fulfillment for the requirements for the degree of  
Master of Philosophy  
in Mathematics



**Khulna University of Engineering & Technology**

Khulna 9203, Bangladesh

**August 2017**

## **Declaration**

This is to certify that the thesis work entitled “*Numerical Investigation of Convective Heat and Mass Transfer Flow along a Vertical Porous Plate with Soret and Dufour Effects in the Presence of Induced Magnetic Field*” has been carried out by *S. M. Mahathy Hasan* in the Department of *Mathematics*, Khulna University of Engineering & Technology, Khulna, Bangladesh. The above thesis work or any part of this work has not been submitted anywhere for the award of any degree or diploma.

Signature of Supervisor

Signature of Candidate

## Approval

This is to certify that the thesis work submitted by *S. M. Mahathy Hasan* entitled “*Numerical Investigation of Convective Heat and Mass Transfer Flow along a Vertical Porous Plate with Soret and Dufour Effects in the Presence of Induced Magnetic Field*” has been approved by the board of examiners for the partial fulfillment of the requirements for the degree of *Master of Philosophy* in the Department of *Mathematics*, Khulna University of Engineering & Technology, Khulna, Bangladesh on 27 August 2017.

### BOARD OF EXAMINERS

1. \_\_\_\_\_  
Prof. Dr. M. M. Touhid Hossain  
Department of Mathematics  
Khulna University of Engineering & Technology  
Khulna-9203, Bangladesh. Chairman  
(Supervisor)
  
2. \_\_\_\_\_  
Head  
Department of Mathematics  
Khulna University of Engineering & Technology  
Khulna-9203, Bangladesh. Member
  
3. \_\_\_\_\_  
Prof. Dr. Mohammad Arif Hossain  
Department of Mathematics  
Khulna University of Engineering & Technology  
Khulna-9203, Bangladesh. Member
  
4. \_\_\_\_\_  
Prof. Dr. Md. Abul Kalam Azad  
Department of Mathematics  
Khulna University of Engineering & Technology  
Khulna-9203, Bangladesh. Member
  
5. \_\_\_\_\_  
Prof. Dr. Md. Yeakub Ali  
Department of Mathematics  
Chittagong University of Engineering & Technology  
Chittagong-4349, Bangladesh. Member  
(External)

## **Acknowledgement**

The author would like to express his deepest gratitude and appreciation to his Supervisor Dr. M. M. Touhid Hossain, Professor and Head, Department of Mathematics, Khulna University of Engineering & Technology (KUET), under whose guidance the work was accomplished. The author would like to thank Professor Dr. M. M. Touhid Hossain for his earnest feelings and help in matters concerning author's research affairs as well as personal affairs. I wish to express my sincere appreciation and gratitude to all the teachers of the Department of Mathematics, KUET, for their necessary advice and cordial cooperation during the period of study. I am thankful to all the research students of this Department for their help in many aspects. I am grateful to the Department of Mathematics, KUET, for providing me all kinds of supports and helps to accomplish my Master of Philosophy (M.Phil) degree.

The Author

## **Abstract**

In this study the thermal-diffusion (Soret) and diffusion-thermo (Dufour) effects on combined heat and mass transfer mixed convection flow of viscous incompressible MHD electrically conducting fluid along a vertical porous surface have been considered under the effects of induced magnetic fields. An implicit Finite Difference numerical technique is adopted to obtain the solutions regarding the velocity, temperature, mass concentration and induced magnetic field and are presented for different selected values of the established dimensionless parameters. The similarity equations of the above mentioned problem are obtained by employing the usual similarity technique and Bousinesq approximation. Then the transformed set of partial differential equations has been solved numerically using the implicit finite difference numerical method. Numerical solutions are obtained for the velocity and temperature fields as well as the concentration distribution and induced magnetic field for different values of the physical parameters entering into the problem. The effects of these various involved parameters on the velocity and temperature fields, the concentration distribution and induced magnetic field have been investigated. Finally, the obtained results involving the effects of these physical parameters on the flow phenomena have been discussed with the help of graphs and tables. The numerical results have shown that the above mentioned effects have to be taken into consideration in the flow fields and in the heat and mass transfer processes.

# Contents

	Page
Title Page	i
Declaration	ii
Approval	iii
Acknowledgements	iv
Abstract	v
Contents	vi
List of Figures	viii
List of Tables	xii
<b>CHAPTER I Introduction</b>	<b>1</b>
<b>CHAPTER II Literature Review</b>	<b>5</b>
2 Some Available information on MHD	
2.1 Magnetohydrodynamics (MHD)	5
2.2 Some Useful Dimensionless Parameters	7
2.3 MHD Boundary Layer and related Transfer Phenomena	9
2.4 Mass Transfer	10
2.5 MHD and Heat Transfer	11
2.6 Free Convection	12
2.7 Mixed Convection	14
2.8 Heat and Mass Transfer	15
2.9 Thermal Diffusion Effect	16
2.10 Diffusion-Thermo Effect	17
<b>CHAPTER III 3.1 The Basic Governing Equations</b>	<b>18</b>
3.1.1 Case-I: Unsteady MHD heat and mass transfer by mixed convection past an infinite vertical porous plate.	23
3.1.2 Case-II: Steady MHD heat and mass transfer by mixed convection flow past a semi-infinite vertical porous plate.	27
<b>CHAPTER IV The Finite Difference Numerical Scheme</b>	<b>32</b>
4.1 The Governing equations	32
4.2 Mathematical Formulation	33

4.3 The Finite Difference Numerical Solution	37
<b>CHAPTER V Numerical Solution and Results Discussions</b>	40
<b>CHAPTER VI Conclusions and Recommendations</b>	64
<b>References</b>	66

## LIST OF FIGURES

Figure No.	Description	Page
4.3.1	Implicit finite difference system grid	37
5.1	Velocity profiles for different values of $V_w$ (for $D_f = 2.0$ , $M = 1.0$ , $S_r = 2.0$ , $G_r = 5.0$ , $G_m = 2.0$ , $Pr = 0.71$ , $P_m = 1.0$ , $E_c = 0.5$ and $S_c = 0.6$ )	41
5.2	Temperature profiles for different values of $V_w$ (for $D_f = 2.0$ , $M = 1.0$ , $S_r = 2.0$ , $G_r = 5.0$ , $G_m = 2.0$ , $Pr = 0.71$ , $P_m = 1.0$ , $E_c = 0.5$ and $S_c = 0.6$ )	42
5.3	Variation of concentration for different values of $V_w$ (for $D_f = 2.0$ , $M = 1.0$ , $S_r = 2.0$ , $G_r = 5.0$ , $G_m = 2.0$ , $Pr = 0.71$ , $P_m = 1.0$ , $E_c = 0.5$ and $S_c = 0.6$ )	42
5.4	Variation of induced magnetic field for different values of $V_w$ (for $D_f = 2.0$ , $M = 1.0$ , $S_r = 2.0$ , $G_r = 5.0$ , $G_m = 2.0$ , $Pr = 0.71$ , $P_m = 1.0$ , $E_c = 0.5$ and $S_c = 0.6$ )	43
5.5	Velocity profiles for different values of $D_f$ (for $V_w = 0.5$ , $M = 1.0$ , $S_r = 2.0$ , $G_r = 5.0$ , $G_m = 2.0$ , $Pr = 0.71$ , $P_m = 1.0$ , $E_c = 0.5$ and $S_c = 0.6$ )	43
5.6	Temperature profiles for different values of $D_f$ (for $V_w = 0.5$ , $M = 1.0$ , $S_r = 2.0$ , $G_r = 5.0$ , $G_m = 2.0$ , $Pr = 0.71$ , $P_m = 1.0$ , $E_c = 0.5$ and $S_c = 0.6$ )	44
5.7	Variation of concentration for different values of $D_f$ (for $V_w = 0.5$ , $M = 1.0$ , $S_r = 2.0$ , $G_r = 5.0$ , $G_m = 2.0$ , $Pr = 0.71$ , $P_m = 1.0$ , $E_c = 0.5$ and $S_c = 0.6$ )	44
5.8	Variation of induced magnetic field for different values of $D_f$ (for $V_w = 0.5$ , $M = 1.0$ , $S_r = 2.0$ , $G_r = 5.0$ , $G_m = 2.0$ , $Pr = 0.71$ , $P_m = 1.0$ , $E_c = 0.5$ and $S_c = 0.6$ )	45
5.9	Velocity profiles for different values of $M$ (for $V_w = 0.5$ , $D_f = 1.0$ , $S_r = 2.0$ , $G_r = 5.0$ , $G_m = 2.0$ , $Pr = 0.71$ , $P_m = 1.0$ , $E_c = 0.5$ and $S_c = 0.6$ )	45
5.10	Temperature profiles for different values of $M$ (for $V_w = 0.5$ , $D_f = 1.0$ , $S_r = 2.0$ , $G_r = 5.0$ , $G_m = 2.0$ , $Pr = 0.71$ , $P_m = 1.0$ , $E_c = 0.5$ and $S_c = 0.6$ )	46



5.11	Variation of concentration for different values of $M$ (for $V_w = 0.5$ , $D_f = 1.0$ , $S_r = 2.0$ , $G_r = 5.0$ , $G_m = 2.0$ , $Pr = 0.71$ , $P_m = 1.0$ , $E_c = 0.5$ and $S_c = 0.6$ )	46
5.12	Variation of induced magnetic field for different values of $M$ (for $V_w = 0.5$ , $D_f = 1.0$ , $S_r = 2.0$ , $G_r = 5.0$ , $G_m = 2.0$ , $Pr = 0.71$ , $P_m = 1.0$ , $E_c = 0.5$ and $S_c = 0.6$ )	47
5.13	Velocity profiles for different values of $S_r$ (for $V_w = 0.5$ , $D_f = 1.0$ , $M = 1.0$ , $G_r = 5.0$ , $G_m = 2.0$ , $Pr = 0.71$ , $P_m = 1.0$ , $E_c = 0.5$ and $S_c = 0.6$ )	47
5.14	Temperature profiles for different values of $S_r$ (for $V_w = 0.5$ , $D_f = 1.0$ , $M = 1.0$ , $G_r = 5.0$ , $G_m = 2.0$ , $Pr = 0.71$ , $P_m = 1.0$ , $E_c = 0.5$ and $S_c = 0.6$ )	48
5.15	Variation of concentration for different values of $S_r$ (for $V_w = 0.5$ , $D_f = 1.0$ , $M = 1.0$ , $G_r = 5.0$ , $G_m = 2.0$ , $Pr = 0.71$ , $P_m = 1.0$ , $E_c = 0.5$ and $S_c = 0.6$ )	48
5.16	Variation of induced magnetic field for different values of $S_r$ (for $V_w = 0.5$ , $D_f = 1.0$ , $M = 1.0$ , $G_r = 5.0$ , $G_m = 2.0$ , $Pr = 0.71$ , $P_m = 1.0$ , $E_c = 0.5$ and $S_c = 0.6$ )	49
5.17	Velocity profiles for different values of $G_r$ (for $V_w = 0.5$ , $D_f = 1.0$ , $M = 1.0$ , $S_r = 2.0$ , $G_m = 2.0$ , $Pr = 0.71$ , $P_m = 1.0$ , $E_c = 0.5$ and $S_c = 0.6$ )	49
5.18	Temperature profiles for different values of $G_r$ (for $V_w = 0.5$ , $D_f = 1.0$ , $M = 1.0$ , $S_r = 2.0$ , $G_m = 2.0$ , $Pr = 0.71$ , $P_m = 1.0$ , $E_c = 0.5$ and $S_c = 0.6$ )	50
5.19	Variation of concentration for different values of $G_r$ (for $V_w = 0.5$ , $D_f = 1.0$ , $M = 1.0$ , $S_r = 2.0$ , $G_m = 2.0$ , $Pr = 0.71$ , $P_m = 1.0$ , $E_c = 0.5$ and $S_c = 0.6$ )	50
5.20	Variation of induced magnetic field for different values of $G_r$ (for $V_w = 0.5$ , $D_f = 1.0$ , $M = 1.0$ , $S_r = 2.0$ , $G_m = 2.0$ , $Pr = 0.71$ , $P_m = 1.0$ , $E_c = 0.5$ and $S_c = 0.6$ )	51
5.21	Velocity profiles for different values of $G_m$ (for $V_w = 0.5$ , $D_f = 1.0$ , $M = 1.0$ , $S_r = 2.0$ , $G_r = 5.0$ , $Pr = 0.71$ , $P_m = 1.0$ , $E_c = 0.5$ and $S_c = 0.6$ )	51
5.22	Temperature profiles for different values of $G_m$ (for $V_w = 0.5$ , $D_f = 1.0$ , $M = 1.0$ , $S_r = 2.0$ , $G_r = 5.0$ , $Pr = 0.71$ , $P_m = 1.0$ , $E_c = 0.5$ and $S_c = 0.6$ )	52

5.23	Variation of concentration for different values of $G_m$ (for $V_w = 0.5$ , $D_f = 1.0$ , $M = 1.0$ , $S_r = 2.0$ , $G_r = 5.0$ , $Pr = 0.71$ , $P_m = 1.0$ , $E_c = 0.5$ and $S_c = 0.6$ )	52
5.24	Variation of induced magnetic field for different values of $G_m$ (for $V_w = 0.5$ , $D_f = 1.0$ , $M = 1.0$ , $S_r = 2.0$ , $G_r = 5.0$ , $Pr = 0.71$ , $P_m = 1.0$ , $E_c = 0.5$ and $S_c = 0.6$ )	53
5.25	Velocity profiles for different values of $Pr$ (for $V_w = 0.5$ , $D_f = 1.0$ , $M = 1.0$ , $S_r = 2.0$ , $G_r = 5.0$ , $G_m = 2.00$ , $P_m = 1.0$ , $E_c = 0.5$ and $S_c = 0.6$ )	53
5.26	Temperature profiles for different values of $Pr$ (for $V_w = 0.5$ , $D_f = 1.0$ , $M = 1.0$ , $S_r = 2.0$ , $G_r = 5.0$ , $G_m = 2.00$ , $P_m = 1.0$ , $E_c = 0.5$ and $S_c = 0.6$ )	54
5.27	Variation of concentration for different values of $Pr$ (for $V_w = 0.5$ , $D_f = 1.0$ , $M = 1.0$ , $S_r = 2.0$ , $G_r = 5.0$ , $G_m = 2.00$ , $P_m = 1.0$ , $E_c = 0.5$ , and $S_c = 0.6$ )	54
5.28	Variation of induced magnetic field for different values of $Pr$ (for $V_w = 0.5$ , $D_f = 1.0$ , $M = 1.0$ , $S_r = 2.0$ , $G_r = 5.0$ , $G_m = 2.00$ , $P_m = 1.0$ , $E_c = 0.5$ and $S_c = 0.6$ )	55
5.29	Velocity profiles for different values of $P_m$ (for $V_w = 0.5$ , $D_f = 1.0$ , $M = 1.0$ , $S_r = 2.0$ , $G_r = 5.0$ , $G_m = 2.00$ , $Pr = 0.71$ , $E_c = 0.5$ , and $S_c = 0.6$ )	55
5.30	Temperature profiles for different values of $P_m$ (for $V_w = 0.5$ , $D_f = 1.0$ , $M = 1.0$ , $S_r = 2.0$ , $G_r = 5.0$ , $G_m = 2.00$ , $Pr = 0.71$ , $E_c = 0.5$ and $S_c = 0.6$ )	56
5.31	Variation of concentration for different values of $P_m$ (for $V_w = 0.5$ , $D_f = 1.0$ , $M = 1.0$ , $S_r = 2.0$ , $G_r = 5.0$ , $G_m = 2.00$ , $Pr = 0.71$ , $E_c = 0.5$ and $S_c = 0.6$ )	56
5.32	Variation of induced magnetic field for different values of $P_m$ (for $V_w = 0.5$ , $D_f = 1.0$ , $M = 1.0$ , $S_r = 2.0$ , $G_r = 5.0$ , $G_m = 2.00$ , $Pr = 0.71$ , $E_c = 0.5$ and $S_c = 0.6$ )	57
5.33	Velocity profiles for different values of $E_c$ (for $V_w = 0.5$ , $D_f = 1.0$ , $M = 1.0$ , $S_r = 2.0$ , $G_r = 5.0$ , $G_m = 2.00$ , $Pr = 0.71$ , $P_m = 1.0$ and $S_c = 0.6$ )	57

5.34	Temperature profiles for different values of $E_c$ (for $V_w = 0.5$ , $D_f = 1.0$ , $M = 1.0$ , $S_r = 2.0$ , $G_r = 5.0$ , $G_m = 2.00$ , $Pr = 0.71$ , $P_m = 1.0$ and $S_c = 0.6$ )	58
5.35	Variation of concentration for different values of $E_c$ (for $V_w = 0.5$ , $D_f = 1.0$ , $M = 1.0$ , $S_r = 2.0$ , $G_r = 5.0$ , $G_m = 2.00$ , $Pr = 0.71$ , $P_m = 1.0$ and $S_c = 0.6$ )	58
5.36	Variation of induced magnetic field for different values of $E_c$ (for $V_w = 0.5$ , $D_f = 1.0$ , $M = 1.0$ , $S_r = 2.0$ , $G_r = 5.0$ , $G_m = 2.00$ , $Pr = 0.71$ , $P_m = 1.0$ and $S_c = 0.6$ )	59
5.37	Velocity profiles for different values of $S_c$ (for $V_w = 0.5$ , $D_f = 1.0$ , $M = 1.0$ , $S_r = 2.0$ , $G_r = 5.0$ , $G_m = 0.6$ , $Pr = 0.71$ , $P_m = 1.0$ and $E_c = 0.5$ )	59
5.38	Temperature profiles for different values of $S_c$ (for $V_w = 0.5$ , $D_f = 1.0$ , $M = 1.0$ , $S_r = 2.0$ , $G_r = 5.0$ , $G_m = 0.6$ , $Pr = 0.71$ , $P_m = 1.0$ and $E_c = 0.5$ )	60
5.39	Variation of concentration for different values of $S_c$ (for $V_w = 0.5$ , $D_f = 1.0$ , $M = 1.0$ , $S_r = 2.0$ , $G_r = 5.0$ , $G_m = 0.6$ , $Pr = 0.71$ , $P_m = 1.0$ and $E_c = 0.5$ )	60
5.40	Variation of induced magnetic field for different values of $S_c$ (for $V_w = 0.5$ , $D_f = 1.0$ , $M = 1.0$ , $S_r = 2.0$ , $G_r = 5.0$ , $G_m = 0.6$ , $Pr = 0.71$ , $P_m = 1.0$ and $E_c = 0.5$ )	61

## LIST OF TABLES

<b>Table No.</b>	<b>Description</b>	<b>Page</b>
5.1	Values proportional to the coefficients of skin-friction and heat transfer for different values of suction parameter ( $V_w$ )	61
5.2	Values proportional to the coefficients of skin-friction and heat transfer for different values of Dufour parameter ( $D_f$ )	62
5.3	Values proportional to the coefficients of skin-friction and heat transfer for different values of Grashof number ( $G_r$ )	62
5.4	Values proportional to the coefficients of skin-friction and heat transfer for different values of modified Grashof number ( $G_m$ )	62
5.5	Values proportional to the coefficients of skin-friction and heat transfer for different values of Prandtl number (Pr)	62
5.6	Values proportional to the coefficients of skin-friction and heat transfer for different values of Schmidt number ( $S_c$ )	63

# CHAPTER I

## Introduction

Many transfer process can be found in natural, scientific and technological system, in which heat and mass transfer by mixed convection flow occurs due to the buoyancy force caused by thermal diffusion (temperature difference) and mass diffusion (concentration difference). The heat and mass transfer by mixed convection flow has great importance in stellar, planetary and magnetospheric studies and also in the field of aeronautics, chemical engineering and electronics. Besides, there are natural phenomena and engineering problems susceptible to MHD analysis. The generation of electric power with flow of electrically conducting fluid through a transverse magnetic field is one of the important applications of MHD. Recently, the experiments with ionized gases have been performed with the hope of producing power on large scale in stationary plants with large magnetic fields. Considerable attention has been paid to the study of MHD heat and mass transfer flows because of the applications in geophysics, aeronautics, and chemical engineering.

The thermal and mass transfer caused by the convection process takes place due to the buoyancy effects owing to the differences of temperature and concentration are of considerable interest in practice. Further, heat and mass transfer in the presence of magnetic field, which is the subject matter of magnetohydrodynamics (MHD), has different applications in natural phenomena and in many engineering problems. Again the stabilizing effect of the boundary layer development has been well known for several years and till to date it is still the most of efficient, simple and common method of boundary layer control. The boundary layer control is often necessary to prevent separation of the boundary layer to reduce the drag and to attain high lift values. Thus, the effect of suction on MHD boundary layer is of great interest in astrophysics. Considering these numerous applications, MHD free convective heat and mass transfer flow in a porous medium have been studied by among others Raptis and Kafoussias (1982), Alam (1995) etc. Mohammed *et al.* (2005) investigated the effect of similarity solution for MHD flow through vertical porous plate with suction. Gundagani *et al.* (2013) presented a

numerical solution to the problem of unsteady MHD free convective flow past a vertical porous plate with variable suction. Choudhary and Sharma (2006) studied the laminar mixed Convection flow of an incompressible electrically conducting viscous fluid over a continuously moving porous vertical plate with inclined magnetic field. Sattar *et al.* (2006) numerically studied a steady two-dimensional MHD free convective heat and mass transfer flow past an inclined semi-infinite surface with heat generation. However, Pantokratoras (2007) showed that a moving electrically conducting fluid induced a new magnetic field, which interacts with the applied external magnetic fields and the relative importance of this induced magnetic field depends on the relative value of the magnetic Reynolds number. Sattar (1993) analyzed the effect of free and forced convection boundary layer flow through a porous medium with large suction. Mohammed *et al.* (2005) investigated the effect of similarity solution for MHD flow through vertical porous plate with suction. The effect of viscous dissipation is usually characterized by the Eckert number and has played a very important role in geophysical flow and in nuclear engineering that was studied by Alim *et al.* (2007). Similarly, Mansour *et al.* (2008) described the influence of chemical reaction and viscous dissipation on MHD natural convection flow. Palani and Srikanth (2009) studied the MHD flow of an electrically conducting fluid over a semi-infinite vertical plate under the influence of the transversely applied magnetic field. Makinde (2010) investigated the MHD boundary layer flow with heat and mass transfer over a moving vertical plate in the presence of magnetic field and convective heat exchange at the surface. The effects of suction or injection on boundary layer flow also play an important role in various processes of engineering applications and have been widely investigated by numerous researchers. Various researchers have studied the effects of viscous dissipation and constant suction in different surface geometries. Khaleque and Samad (2010) described the effects of radiation, heat generation, and viscous dissipation on MHD free convection flow along a stretching sheet.

In the presence of induced magnetic field, Hossain *et al.* (2013) studied the steady MHD free convection heat and mass transfer flow about a vertical porous surface with thermal diffusion. Khan *et al.* (2014) investigate the effects of heat generation, radiation and chemical reaction on unsteady mixed convection flow from a moving vertical porous plate

with induced magnetic field, time dependent suction velocity at the plate, thermal diffusion, constant heat and mass fluxes. Wahiduzzaman *et al.* (2015) presented a numerical solution to investigate the influence of the hall current and constant heat flux on the MHD natural convection boundary layer viscous incompressible fluid flowing in the manifestation of transverse magnetic field near an inclined vertical permeable flat plate. In their analysis they assumed that the induced magnetic field is negligible compared with the imposed magnetic field.

Asaduzzaman *et al.* (2016) considered the transient heat transfer flow along a vertical plate with induced magnetic field. The effect of thermal diffusion on the combined MHD heat transfer in an unsteady flow past a continuously moving semi-infinite vertical porous plate under the action of strong applied magnetic field has been investigated numerically by Islam *et al.* (2016) taking into account the induced magnetic field. Recently, Opiyo *et al.* (2017) considered the effects of MHD on two-dimensional steady free convection boundary layer heat and mass transfer flow of viscous, incompressible, electrically conducting fluid on an inclined plate with a varying angle of inclination.

Uwanta (2012) studied the effects of chemical reaction and radiation on heat and mass transfer flow past a semi-infinite vertical porous plate with constant mass flux and dissipation. Govardhan *et al.* (2012) presented a theoretical study on the influence of radiation on a steady free convection heat and mass transfer over an isothermal stretching sheet in the presence of a uniform magnetic field with viscous dissipation effect. Jai (2012) presented the study of a viscous dissipation and chemical reaction effects on flow past a stretching porous surface in a porous medium.

When heat and mass transfer occur simultaneously in a moving fluid, affecting each other, causes a cross diffusion effect, the mass transfer caused by temperature gradient is called the Soret effect, while the heat transfer caused by concentration effect is called the Dufour effect. Soret and Dufour effects are important phenomena in areas such as hydrology, petrology and geosciences. The Soret effect, for instance, has been utilized for separation of isotope in a mixture between gases with very light molecular weight (He, H<sub>2</sub>) and of medium molecular weight (N<sub>2</sub>, air). The Dufour effect was recently found to be of order of considerable magnitude so that it cannot be neglected (Eckert, and Drake (1974)). Many researchers studied Soret and Dufour effects; for example, Kafousiasis and Williams

(1995) examined Soret and Dufour effects on mixed free-forced convective and mass transfer boundary layer flow with temperature dependent viscosity, Uwanta et al. (2008) have analyzed MHD fluid flow over a vertical plate with Dufour and Soret effects. Postelnicu (2010) analyzed the effect of Soret and Dufour effects on heat and mass transfer. Later, Usman and Uwanta (2013) have considered the effect of thermal conductivity on MHD heat and mass transfer flow past an infinite vertical plate with Soret and Dufour effects. Recently, the effects of Soret and Dufour on an unsteady MHD free convection flow past a vertical porous plate in the presence of suction or injection have been investigated by Sarada and Shankar (2013), Most recently, using implicit finite difference scheme of Crank-Nicolson, Uwatana and Usman (2014) investigated the combined effects of Soret and Dufour on free convective heat and mass transfer on the unsteady boundary layer flow over a vertical channel in the presence of viscous dissipation and constant suction.

In view of the above studies, the present study will deal with the numerical investigation of convective heat and mass transfer flow along a vertical porous plate with Soret and Dufour effects in existence with an induced magnetic field. Computations will be performed for a wide range of the non-dimensional parameters such as thermal Grashof number, modified Grashof number, Prandtl number, Soret number, Dufour number, Schmidt number, Eckert number, magnetic parameter, Magnetic Diffusion parameter and other driving parameters.

The present thesis is composed of Six Chapters. An introduction of the problem is given in CHAPTER I. The basic literature review including, some available information on MHD and useful dimensionless parameters regarding our problem are presented in CHAPTER II. Basic equations governing the problems with some simplifying assumptions are given in CHAPTER III. CHAPTER IV deals with the mathematical model of the problem with dimensional analysis. A brief description of the implicit Finite Difference numerical method and the calculation technique has been given here. The numerical solution including the graphs and tables and results and discussions have been given in CHAPTER V. The conclusions gained from this research have been discussed in CHAPTER VI.



## **CHAPTER II**

### **Literature Review**

#### **2 Some Available Information on MHD**

##### **2.1 Magnetohydrodynamics (MHD)**

Magneto hydrodynamics (MHD) is the branch of magneto fluid dynamics, which deals with the flow of electrically conducting fluid in electric and magnetic field. Probably, the largest advancement towards an understanding of such phenomena comes from the field of astrophysics. It has long been suspected that most of the matter in the universe is in the form of plasma of highly ionized gaseous state and much of the basic knowledge in the area of electromagnetic fluid dynamics evolved from these studies. The field of MHD consists of the study of a continuous, electrically conducting fluid under the influence electromagnetic fields. Originally MHD included only the study of partially ionized gases as well as the other names have been suggested, such as magneto fluid mechanics or magneto aerodynamics, but the original nomenclature has persisted. The essential requirement for problem to be analyzed under MHD is that the continuum approach be applicable.

There are many natural phenomena and engineering problems susceptible to MHD analysis. It is useful in astrophysics because much of the universe is filled with widely spaced charged particles and permeated by magnetic field and so the continuum assumption becomes applicable. Engineers employ MHD principles in the design of heat exchangers, pumps and flow meters, in solving space vehicle propulsion, control and reentry problem, in designing communications and radar system, in creating noble power generating systems, and in developing confinement schemes for controlled fusion. The MHD in the generation of electrical power with the flow of electrically conducting fluid through a transverse magnetic field is one of the most important applications. Recently, these experiments with ionized gases have been performed with the hope of producing power on large scale in stationary plants with large magnetic fields. Generation of MHD power on a smaller scale is of interest of space applications. Generally we known that, to

convert the heat energy in to the electricity, several intermediate transformations are necessary. Each of these steps means a loss of energy. This naturally limits the overall efficiency, reliability and compactness of the conversion process. Method for the direct conversion to energy is now increasingly receiving attention. Of these, the fuel converts the chemical energy of fuel directly into electrical energy, fusion energy utilizes the energy released when two hydrogen molecules fuse into a heavier one, and thermoelectrically power generation uses a thermocouple. MHD power generation is another new process that has received worldwide attention. The principal MHD effects were first demonstrated in the experiments of Faraday & Ritchie. Faraday (1832) find out experiments with flow of mercury in glass Tubes placed between poles of a magnet and discovered that a voltage was induced across the tube by the motion of the mercury across the magnetic field, perpendicular to the direction of flow and to the magnetic field. Faraday observed that the current generated by this induced voltage interacted with the magnetic field to slow down the motion of the fluid and he was aware of the fact that the current produced its own magnetic field that obeyed Ampere's right-hand rule and thus, in turn distorted the field of magnet. Ritchie contemporary of Faraday, discovered in 1832 that when an electric field was applied to a conducting fluid perpendicularly to a magnetic field it pumped the fluid in a direction perpendicular to both fields. Faraday also suggested that electrical power could be generated in a load circuit by the interaction of a flowing conducting fluid and a magnetic field. The first astronomical application of the MHD theory occurred in 1899, when Bigelow suggested that the sun as a gigantic magnetic system. It remained, however, for Alfven (1942) to make a most significant contribution by discovering MHD waves in the sun. These waves are produced by disturbances which propagate simultaneously in the conducting fluid and the magnetic field. The analogy that explains the generation of an Alfven wave is that of a harp string plucked while submerged in a fluid. The string provides the elastic force and the fluid provides the inertia force, and they combine to propagate a perturbing wave through the fluid and the string. In summary, MHD phenomena result from the mutual effect of a magnetic field and conducting fluid flowing across it. Thus, an electromagnetic force is produced in a fluid flowing across a transverse magnetic field, and the resulting current and magnetic

field combine to produce a force that resists the fluid's motion. The current also generates its own magnetic field which distorts the original magnetic field. An opposing or pumping force on the fluid can be produced by applying an electric field perpendicularly to the magnetic field. Disturbance in either the magnetic field or the fluid can propagate in both to produce MHD waves, as well as upstream and downstream-wake phenomena. The science of MHD is the detailed study of these phenomena, which occur in nature and are produced in engineering devices.

## 2.2 Some Useful Dimensionless Parameters

### Reynolds number ( $R_e$ )

The Reynolds number  $R_e$  is the most important parameter of the fluid dynamics of a viscous fluid, which is defined by the following ratio

$$R_e = \frac{\text{inertia force}}{\text{viscous force}} = \frac{\rho L^3 \times \frac{U}{T}}{\mu \times \frac{U}{L} \times L^2} = \frac{\rho L U}{\mu} = \frac{L U}{\nu}$$

where  $L$  and  $U$  denotes the characteristic length and velocity respectively and  $\nu = \frac{\mu}{\rho}$  is the kinematic viscosity ( $\mu$  is the viscosity and  $\rho$  is the density). If  $R_e$  is small, the viscous force will be pre-dominant and the effect of viscosity will be felt in the whole flow field. On the other hand if  $R_e$  is large the inertia force will be predominant and in such case the effect of viscosity to be confined in a thin layer, near to the solid wall or other restricted region, which is known as boundary layer. However if  $R_e$  is very large, the flow ceases to be laminar and becomes turbulent. The Reynolds number at which translation from laminar to turbulent occurs is known as critical Reynolds number. Reynolds in 1883 found that for flow in a circular pipe becomes turbulent when  $R_e$  exceeds the critical value 2300, i.e.,  $R_e = \left[ \frac{\bar{U}d}{\nu} \right]_{\text{crit}} = 2300$ , where  $\bar{U}$  is the mean velocity and 'd' is the diameter of the pipe. When the viscous force is pre-dominating force, Reynolds number must be similar for dynamic similarity of two flows.

### **Prandtl number ( $P_r$ )**

The Prandtl number  $P_r$  is the ratio of the kinematic viscosity to the thermal diffusivity and is defined by

$$P_r = \frac{\text{Kinematic viscosity}}{\text{Thermal diffusivity}} = \frac{\frac{\mu}{\rho}}{\frac{k}{\rho c_p}} = \frac{\mu c_p}{k}$$

where  $c_p$  is the specific heat at constant pressure and  $k$  is the thermal conductivity. The value of  $\frac{k}{\rho c_p}$  is the thermal diffusivity due to the heat conduction. The smaller value of  $\frac{k}{\rho c_p}$  is, the narrower is the region which affected by the heat conduction and it is known as the thermal boundary layer. The value of  $\nu = \frac{\mu}{\rho}$  show the effect of viscosity of the fluid and thus the Prandtl number shows the relative importance of heat conduction and viscosity of a fluid. Evidently  $P_r$  varies from fluid to fluid. For air  $P_r = 0.72$  (approx.), for water at  $15.5^\circ \text{C}$ ,  $P_r = 7.00$  (approx.), for mercury  $P_r = 0.044$ , but for high viscous fluid it may be very large, e.g. for glycerin  $P_r = 7250$ .

### **Magnetic Parameter ( $M$ )**

The magnetic force number is the ratio of the magnetic force to the inertia force and is defined by  $M = \frac{\text{Magnetic force}}{\text{Inertia force}} = \frac{\mu^3 H_0^2 \sigma' L}{\rho U}$

### **Schmidt number ( $S_c$ )**

The Schmidt number is the ratio of the viscous diffusivity to the chemical molecular diffusivity and is defined by  $S_c = \frac{\text{Viscous diffusivity}}{\text{Chemical molecular diffusivity}} = \frac{\nu}{D_m}$ .

### **Grashof number ( $G_r$ )**

The Grashof number is defined by  $G_r = \frac{g \beta L^3 \Delta T}{\nu^2 T}$  and is a measure of the relative importance of the buoyancy and viscous forces. The larger it is, stronger is the convective current. Here  $g$  is the local acceleration due to gravity,  $\beta$  is the thermal expansion coefficient and  $\Delta T$  be the temperature difference.

### **Modified Grashof number ( $G_m$ )**

The Modified Grashof number is defined by  $G_m = \frac{g \beta^* L^3 \Delta C}{\nu^2}$ , where  $\beta^*$  is the concentration expansion coefficient and  $\Delta C$  be the concentration difference.

### **Magnetic diffusivity ( $P_m$ )**

The magnetic diffusivity is defined by  $P_m = \mu_e \sigma' \nu$

### **Eckert number ( $E_c$ )**

The Eckert number is defined by  $E_c = \frac{kU_0}{\sigma q c_p}$ , which is the ratio of the kinetic energy at the wall to the specific enthalpy difference between wall and fluid. Eckert number phenomena are being the result of dissipation created by shear stress in the fluid at the wall. In other words, it is the kinetic energy of the flow relative to the enthalpy difference.

### **Soret number ( $S_r$ )**

The Soret number is generally defined by  $S_r = \frac{D_m K_T (T_w - T_\infty)}{T_m \nu (C_w - C_\infty)}$ .

where  $K_T$  is the thermal diffusion ratio,  $T_m$  is the mean fluid temperature,  $T_w$  and  $T_\infty$  are temperature of the fluid at the wall and far away from the plate respectively as well as  $C_w$  and  $C_\infty$  are concentration of the species at the wall and far away from the plate respectively.

### **Dufour number ( $D_f$ )**

A dimensionless number used in studying thermo-diffusion, equal to the increase in enthalpy of a unit mass during isothermal mass transfer divided by the enthalpy of a unit mass of mixture. The Dufour number is generally defined by  $D_f = \frac{D_m K_T (C_w - C_\infty)}{C_s c_p \nu (T_w - T_\infty)}$ .

## **2.3 MHD Boundary Layer and Related Transfer Phenomena**

Boundary layer phenomena occur when the viscous effect may be considered to be confined in a very thin layer near to the boundaries and the non-dimensional diffusion parameter such as the Reynolds number, Grashof number, the Magnetic Reynolds number etc, are very large. The boundary layers are then the velocity and thermal (or magnetic) boundary layers and each of its thickness is inversely proportional to the square root of the associated diffusion number. Prandtl observed, in classical fluid dynamics boundary layer theory, from experimental flows that for large Reynolds number, the viscosity and the thermal conductivity appreciably influences the flow only near the wall. When distance

measurements in the flow direction are compared with a characteristic dimension in that direction, transverse measurement compared with the boundary layer thickness and velocities compared with the free stream velocity, the Navier-Stokes and energy equations can be considerably simplified through neglecting small quantities. The flow directive components are only remain in the boundary layer equations and pressure is then only a function of the flow direction and can be determined from the non-viscous flow solution. There are two types of MHD boundary layer flows, by considering the limiting cases of a very large and a negligible small magnetic Reynolds number. When the magnetic Reynolds number is large, the magnetic boundary layer thickness is small and is of nearly the same size of the viscous and thermal boundary layers and then the equations of the MHD boundary layer must be solved simultaneously. On the other hand, when the magnetic Reynolds number is very small and the magnetic field is oriented in an arbitrary direction relative to a confining surface, the flow directive component of the magnetic interaction and the corresponding joule heating is only a function of the transverse magnetic field component and the local velocity in the flow direction. Changes in the transverse magnetic boundary layer are negligible. The thickness of the magnetic boundary layer is very large and the induced magnetic field is negligible. In this case the magnetic field moves with the flow and is called frozen mass.

## **2.4 Mass Transfer**

Mass transfer problems are of importance in many processes and have therefore received a considerable amount of attention. In many mass transfer processes, heat transfer considerations arise owing to chemical reaction and are often due to the nature of the process. In processes such as drying, evaporation at the surface water body, energy transfer in a wet cooling tower and the flow in a desert cooler, heat and mass transfer occur simultaneously. In many of these processes, the interest lies in the determination of the total energy transfer, although in processes such as drying, the interest lies mainly in the overall mass transfer

for moisture removal. Natural convection processes involving the combined mechanisms are also encountered in many natural processes, such as evaporation, condensation and agricultural drying, in many industrial applications involving solutions and mixtures in the absence of an externally induced flow and in many chemical processing systems. In many processes such as the curing of plastics, cleaning and chemical processing of materials relevant to the manufacture of printed circuitry, manufacture of pulp-insulated cables etc., the combined buoyancy mechanisms arise and the total energy and material transfer resulting from the combined mechanisms, has to be determined. The basic heat and mass transfer problem is governed by the combined buoyancy effects rising from the simultaneous diffusion of thermal energy and of chemical species. Therefore the continuity, momentum, energy and concentration equations are coupled through the buoyancy terms alone, if the other effects, such as the Dufour effects are neglected. This would again be valid for low species concentration levels.

## **2.5 MHD and Heat Transfer**

With the advent of hypersonic flight, the field of MHD, as define above, which has attracted the interest of aero dynamists and associated largely with liquid metal pumping. It is possible to alter the flow and the heat transfer around high velocity vehicles provided that the air is sufficiently ionized. Furthermore, the invention of high temperature facilities such as the shock tube plasma jet has provided laboratory sources of following ionized gas, which provide an incentive for the study of plasma accelerators and generators. As a result of this, many of the classical problems of fluid mechanics have been reinvestigated. Some of these analyses awake out of the natural tendency of scientists to search a new subject. In this case it was the academic problem of solving the equations of fluid mechanics with a new body force and another source of dissipation in the energy equation. Some time there were no practical applications for these results. As for example, natural

convection MHD flows have been of interest to the engineering community only since the investigations, directly applicable to the problem in geophysics and astrophysics. But it was in the field of aerodynamic heating that the largest interest was awakened. Rossow (1957) presented the first paper on this subject. His result for incompressible constant property flat plate boundary layer flow indicated that the skin friction and heat transfer were reduced substantially when a transverse magnetic field was applied to the fluid. This encouraged a multitude analysis for every imaginable type of aerodynamic flow, and most of the research centered on the stagnation point, where in hypersonic flight, the highest degree of ionization could be expected. The result of these studies were sometimes contradictory concerning the amount by which the heat transfer would be reduced (some of this was due to misinterpretations and invalid comparison). Eventually, however, it was concluded that the field strength, necessary to provide sufficient against heat fluxes during atmospheric flight, were not competitive (in terms of weight) with other method of cooling (Sutton and Gloersen, 1961). However the invention of new light weight super conducting magnets has revived interests in the problem of providing heat projection during the very high velocity re-entry from orbital and super orbital flight (Levy and Petschek, (1962)

## **2.6 Free Convection**

In the studies related to heat transfer, considerable effort has been directed towards the convective mode, in which the relative motion of the fluid provides an additional mechanism for the transfer of energy and material, the later being a more important consideration in case where mass transfer, due to a concentration difference, occurs. Convection is inevitable coupled with the conductive mechanisms, since, although the fluid motion modifies the transport process, the eventual transfer of energy from one fluid element to another in its neighborhood is thorough conduction. Also, at the surface the process is predominantly that of conduction because the relative fluid motion is brought to zero at the surface. A study of the convective heat transfer therefore involves the mechanisms of conduction and sometimes those of radiative processes as well, coupled



with that fluid flow. These make the study of this mode of heat or mass transfer very complex, although its importance in technology and in nature can hardly be exaggerated.

The heat transfer in convective mode is divided into two basic processes. If no externally induced flow is provided and flow arises naturally simply owing to the effect of a density difference, resulting from a temperature or concentration difference in a body force field, such as the gravitational field, the process is referred to the natural convection. On the other hand if the motion of the fluid is caused by an external agent such as the externally imposed flow of a fluid stream over a heated object, the process is termed as forced convection. In the forced convection, the fluid flow may be the result of, for instance, a fan, a blower, the wind or the motion of the heated object itself. Such problems are very frequently encountered in technology where the heat transfer to or from a body is often due to an imposed flow of a fluid at a different temperature from that of a body. On the other side, in the natural convection, the density difference gives rise to buoyancy effects, owing to which the flow is generated. A heated body cooling in ambient air generates such a flow in the region surrounding it. Similarly the buoyant flow arising from heat rejection to the atmosphere and to other ambient media, circulations arising in heated rooms, in the atmosphere, and in bodies of water, rise of buoyant flow to cause thermal stratification of the medium, as in temperature inversion and many other such heat transfer processes in our natural environment, as well as in many technological applications, are included in the area of natural convection. The flow may also arise owing to concentration differences such as those caused by salinity differences in the sea and by composition differences in a chemical processing unit, and these cause a natural convection mass transfer.

Practically some time both processes, natural and forced convection are important and heat transfer is by mixed convection, in which neither mode is truly predominant. The main difference between the two really lies in the word external. A heated body lying in still air loses energy by natural convection. But it also generates a buoyant flow above it and a body placed in that flow is subjected to an external flow and it becomes necessary to determine the natural, as well as the forced convection effects and the regime in which the heat transfer mechanisms lie.

When MHD become a popular subject, it was normal that these flows would be investigated with the additional ponder motive body force as well as the buoyancy force. At a first glance there seems to be no practical applications for these MHD solutions, for most heat exchangers utilize liquids, whose conductivity is so small that prohibitively large magnetic fields are necessary to influence the flow. But some nuclear power plants employ heat exchangers with liquid metal coolants, so the application of moderate magnetic fields to change the convection pattern appears feasible. Another classical natural convection problem is the thermal instability that occurs in a liquid heated from below. This subject is of natural interest to geophysicists and astrophysicists, although some applications might arise in boiling heat transfer.

The basic concepts involved in employing the boundary layer approximation to natural convection flows are very similar to those in forced flows. The main difference lies in the fact the pressure in the region beyond the boundary layer is hydrostatic instead of being imposed by an external flow, and that the velocity outside the layer is zero. However the basic treatment and analysis remain the same, the book by Schlichting (1968) is an excellent collection of the boundary layer analysis. There are several methods for the solution of the boundary layer equations namely the similarity variable method, the perturbation method, analytical method, numerical method etc. and their details are available in the books by Rosenberg (1969), Patanker and Spalding (1970) and Spalding (1977).

## **2.7 Mixed Convection**

Practically sometimes both the processes, natural and forced convection, are important and heat transfer is by mixed convection, in which neither mode is truly predominant. The main difference between the two really lies in the word external. A heated body lying on stagnant air loses energy by natural convection. But it also generates a buoyant flow above it and body placed on a moving air flow is subjected to an external flow and it becomes necessary to determine the natural, as well as the forced convection effects in the regime in which the heat transfer mechanisms lie.

When the study of MHD became a popular subject, it was normal that these flows would be investigated with the additional ponderomotive body force as well as the buoyancy force. At a first glance there seems to be no practical applications for these MHD solutions, for most heat exchangers utilize liquids, whose conductivity is so small that prohibitively large magnetic fields are necessary to influence the flow. But some nuclear power plants employ heat exchangers with liquid metal coolants, so the application of moderate magnetic fields to change the convection pattern appears feasible. Another classical natural convection problem is the thermal instability that occurs in a liquid heated from below. This subject is of natural interest to geophysicists and astrophysicists, although some applications might arise in boiling heat transfer.

The basic concepts involved in employing the boundary layer approximation to natural convection flows are very similar to those in forced flows. The main difference lies in the fact that pressure in the region beyond the boundary layer is hydrostatic instead of being imposed by an external flow and that the velocity outside the layer is zero. However the basic treatment and analysis remain the same, the book by Schlichting (1968) is an excellent collection of the boundary layer analysis. There are several methods for the solution of the boundary layer equations namely the similarity variable method, the perturbation method, analytical method, numerical method etc. and their details are available in the books written by Rosenberg (1969) and Patankar and Spalding (1970).

## **2.8 Heat and Mass Transfer**

The basic heat and mass transfer problem is governed by the combined buoyancy effects arising from the simultaneous diffusion of thermal energy and chemical species. Therefore, the equations of continuity, momentum, energy, mass diffusion are coupled through the buoyancy terms alone, if the other effects, such as the Soret and Duffour effects are neglected. This would again be valid for low species concentration levels. These additional effects have also been considered in several investigations, for example, the work of Caldwell (1974), Groot and Mozart (1962), Hurel and Jakeman (1971) and Legros, *et al.* (1968).

Somers (1956) considered combined buoyancy mechanisms for flow adjacent to a wet isothermal vertical surface in an unsaturated environment. Uniform temperature and uniform species concentration at the surface were assumed and an integral analysis was carried out to obtain the result which is expected to be valid for  $P_r$  and  $S_c$  values around 1.0 with one buoyancy effect being small compared with the other. Adams and McFadden (1966) presented experimental measurements of heat and mass transfer parameters, with opposed buoyancy effects. Gebhart and Pera (1971) studied laminar vertical natural convection flows resulting from the combined buoyancy mechanisms in terms of similarity solutions.

Nanousis and Goudas (1979) have studied the effects of mass transfer on free convection problem in the Stokes problem for an infinite vertical limiting surface. Georgantopolous and Nanousis (1980) have considered the effects of the mass transfer on free convection flow of an electrically conducting viscous fluid (e. g. of a stellar atmosphere of star) in the presence of transverse magnetic field. Solution for the velocity and skin friction in closed form are obtained with the help of the Laplace transformation technique, and the results obtained for the various values of the parameters  $P_r$ ,  $S_c$  and  $M$  are given in graphical form. Raptis and Kafoussias (1982) presented the analysis of free convection and mass transfer steady hydro magnetic flow of an electrically conducting viscous incompressible fluid, through a porous medium, occupying a semi-infinite region of the space bounded by an infinite vertical porous plate under the action of transverse magnetic field. Agrawal *et al.* (1983) have investigated the effect of Hall current on the combined effect of thermal and mass diffusion of an electrically conducting liquid past an infinite vertical porous plate, when the free stream oscillates about constant nonzero mean. The velocity and temperature distributions are shown on graphs for different values of parameters.

## **2.9 Thermal Diffusion Effect**

When heat and mass transfer occur simultaneously in a moving fluid, the relations between the fluxes and driving potentials are of more complicated in nature. If mass fluxes being created due to the temperature gradients then this is known as thermal diffusion

effect or Soret effect. Thus, Soret effect is a mass flux due to a temperature gradient and appears in the species continuity equation when we have a multi-component mixture where each species has its own diffusional velocity. The Soret coefficient is the ratio of the thermal diffusion coefficient divided by the ordinary diffusion coefficient. If  $D$  is the diffusion coefficient and  $D_T$  is the thermo-diffusion coefficient, then quotient of both coefficients is called Soret coefficient, that is,  $S_T = \frac{D_T}{D}$ . In general the thermal diffusion effects is of a small order of magnitude, described by Fourier or Flick's law, is often neglected in heat and mass transfer processes.

There are however, exceptions. The thermal diffusion effect for instance has been utilized for isotope separation and in mixtures between gases with very light molecular weight ( $H_2$ ,  $He$ ) and of medium molecular, weight ( $N_2$ , air). Kafoussias (1992) studied the MHD free convection and mass transfer flow, past an infinite vertical plate moving on its own plane, taken into account the thermal diffusion when the plate surface is (i) impulsively started moving in its own plane (I. S. P) and (ii) uniformly accelerated (U. A. P). The problem is solved with the help of Laplace transformation method and analytical expressions are given for the velocity field as well as for the skin friction for the above-mentioned two different cases.

## **2.10 Diffusion-Thermo Effect**

It is also known that an energy flux can be generated not only by temperature gradients but by composition gradients as well. This type of energy flux is called the diffusion-thermo effect or Dufour effect. The Dufour effect describes the energy (heat) flux created when a chemical system is under a concentration gradient. This effect is found in the energy equation. In isothermal mixtures of two or more species (gases, liquids and even solids), mass diffusion occurs if the species are initially distributed unevenly, i.e., when a concentration gradient exists.

## CHAPTER III

### 3.1 The Basic Governing Equations

The generalized Continuity equation, Momentum equation, Energy equation, Magnetic induction equation, Concentration equation together with the Ohm's law and Maxwell equations form the basis of studying of Magneto fluid dynamics (MFD). These equations are as follows:

Continuity equation for viscous compressible electrically conductive fluid is

$$\frac{\partial \rho}{\partial t} + \nabla \cdot (\rho \mathbf{q}) = 0 \quad (3.1)$$

where  $\rho$  the fluid density and  $\mathbf{q}$  is the fluid velocity.

For incompressible fluid ( $\rho = \text{constant}$ ) the equation yields

$$\nabla \cdot \mathbf{q} = 0 \quad (3.2)$$

where  $\mathbf{q} = (u, v, w)$ .

Momentum equation for viscous compressible fluid is

$$\frac{d\mathbf{q}}{dt} = \mathbf{F} - \frac{1}{\rho} \nabla p + \nu \nabla^2 \mathbf{q} + \frac{\nu}{3} \nabla (\nabla \cdot \mathbf{q}) \quad (3.3)$$

For incompressible ( $\nabla \cdot \mathbf{q} = 0$ ) the equation (3.3) yields

$$\frac{\partial \mathbf{q}}{\partial t} + (\mathbf{q} \cdot \nabla) \mathbf{q} = \mathbf{F} - \frac{1}{\rho} \nabla p + \nu \nabla^2 \mathbf{q} \quad (3.4)$$

When the fluid moves through a magnetic field, then the equation (3.4) becomes to be Magneto hydrodynamic (MHD) equation as

$$\frac{\partial \mathbf{q}}{\partial t} + (\mathbf{q} \cdot \nabla) \mathbf{q} = \mathbf{F} - \frac{1}{\rho} \nabla p + \nu \nabla^2 \mathbf{q} + \frac{\mu_e}{\rho} (\mathbf{J} \wedge \mathbf{H}) \quad (3.5)$$

Magnetic induction equation for a viscous incompressible electrically conducting fluid is

$$\frac{\partial \mathbf{H}}{\partial t} + (\mathbf{q} \cdot \nabla) \mathbf{H} = (\mathbf{H} \cdot \nabla) \mathbf{q} + \frac{1}{\mu_e \sigma'} \nabla^2 \mathbf{H} \quad (3.6)$$

Energy equation for a viscous incompressible electrically conducting fluid is

$$\frac{\partial T}{\partial t} + (\mathbf{q} \cdot \nabla) T = \frac{k}{\rho c_p} \nabla^2 T + \frac{1}{\rho c_p} \phi + \frac{\mathbf{J}^2}{\rho c_p \sigma'} + \frac{D_m K_T}{c_s c_p} \nabla^2 C \quad (3.7)$$

The Concentration equation for a viscous incompressible electrically conductive fluid (in the absence of heat source viscous dissipation and Joule heating term) is

$$\frac{\partial C}{\partial t} + (\mathbf{q} \cdot \nabla)C = D_m \nabla^2 C + \frac{D_m K_T}{T_m} \nabla^2 T \quad (3.8)$$

Generalized Ohm's law is of the form  $\mathbf{J} = \sigma'(\mathbf{E} + \mathbf{q} \wedge \mathbf{B}) - \frac{\sigma'}{en_e}(\mathbf{J} \wedge \mathbf{B} - \nabla p_e)$

$$\text{or, } \mathbf{J} = \sigma'(\mathbf{E} + \mathbf{q} \wedge \mathbf{B}) - \frac{\sigma'}{en_e} \mathbf{J} \wedge \mathbf{B} + \frac{\sigma'}{en_e} \nabla p_e$$

$$\therefore \mathbf{J} + \frac{\sigma'}{en_e} \mathbf{J} \wedge \mathbf{B} = \sigma'(\mathbf{E} + \mathbf{q} \wedge \mathbf{B}) + \frac{\sigma'}{en_e} \nabla p_e \quad (3.9)$$

The Maxwell's equations are

$$\nabla \wedge \mathbf{H} = \mathbf{J} \quad (3.10)$$

$$\nabla \wedge \mathbf{H} = \mathbf{0} \quad (3.11)$$

$$\nabla \cdot \mathbf{B} = 0 \quad (3.12)$$

where  $\mathbf{F}$  is the body force per unit mass,  $p$  is the fluid pressure,  $p_e$  is the pressure of electron,  $\mu_e$  is the magnetic permeability,  $\mathbf{J}$  is the current density vector,  $\mathbf{B}$  is the magnetic field vector,  $\mathbf{E}$  is the electric field vector,  $\mathbf{H}$  is the magnetic field intensity,  $T$  is the fluid Temperature,  $T_m$  is the mean fluid Temperature,  $C$  is the species concentration variable,  $\sigma'$  is the electrical conductivity,  $e$  is the charge of electron,  $D_m$  is the coefficient of mass diffusivity,  $D_T$  is the thermal diffusivity,  $c_p$  is the specific heat at constant pressure,  $c_s$  is the concentration susceptibility,  $n_e$  is the number of density electron,  $k$  is the thermal conductivity,  $K_T$  is the thermal diffusion ratio. Also  $\phi$  denotes the dissipation function, involving the viscous stress and it represents the rate at which energy is being dissipated per unit volume through the action of viscosity. In fact the energy is dissipated in a viscous fluid in motion on account of internal friction and for incompressible fluid.

$$\phi = \mu \left[ \left( \frac{\partial u}{\partial x} \right)^2 + \left( \frac{\partial v}{\partial y} \right)^2 + \left( \frac{\partial w}{\partial z} \right)^2 + \left( \frac{\partial u}{\partial y} + \frac{\partial v}{\partial x} \right)^2 + \left( \frac{\partial w}{\partial y} + \frac{\partial v}{\partial z} \right)^2 + \left( \frac{\partial w}{\partial x} + \frac{\partial u}{\partial z} \right)^2 \right] \quad (3.13)$$

which is always positive, since all the terms are quadratic; where  $\mu$  is the coefficient of viscosity.

Let us consider a heat and mass transfer by mixed convection flow of an incompressible electrically conducting viscous fluid past an electrically non-conducting vertical porous plate  $y = 0$ . Introducing the Cartesian co-ordinate system  $x$ - axis is chosen along the direction of flow and  $y$ - axis is normal to it. A uniform magnetic field is applied normal to the flow direction. In addition the analysis is based on the following assumptions:

The magnetic Reynolds number of the flow is taken to be large so that the induced magnetic field is not negligible. The magnetic field is of the form:  $\mathbf{H} = (H_x, H_y, 0)$

The equation of the conservation of electric charge is  $\nabla \cdot \mathbf{J} = 0$  where  $\mathbf{J} = (J_x, J_y, 0)$ , the direction of propagation is considered only along the y-axis and does not have any variation along the y- axis and the y derivative of  $\mathbf{J}$  namely  $\frac{\partial J_y}{\partial y} = 0$ , resulting in  $J_y = 0$  constant. Since the plate electrically non-conducting, this constant is zero and hence  $J_y = 0$  everywhere in the flow.

The divergence equation of Maxwell equations is  $\nabla \cdot \mathbf{H} = 0$  which gives  $\frac{\partial H_y}{\partial y} = 0 \Rightarrow H_y = \text{constant} = H_0(\text{say})$ . So  $\mathbf{H} = (H_x, H_0, 0)$ .

Now, from equation (3.10), we have

$$\mathbf{J} = \nabla \wedge \mathbf{H} = \begin{vmatrix} \hat{i} & \hat{j} & \hat{k} \\ \frac{\partial}{\partial x} & \frac{\partial}{\partial y} & \frac{\partial}{\partial z} \\ H_x & H_0 & 0 \end{vmatrix} = \left(0 - \frac{\partial}{\partial z} H_0\right) \hat{i} - \left(0 - \frac{\partial}{\partial z} H_x\right) \hat{j} + \left(0 - \frac{\partial}{\partial y} H_x\right) \hat{k}$$

$$\text{or, } \mathbf{J} = (0 - 0) \hat{i} - \left(0 - \frac{\partial H_x}{\partial z}\right) \hat{j} + \left(0 - \frac{\partial H_x}{\partial y}\right) \hat{k}$$

$$\text{or, } \mathbf{J} = 0 \cdot \hat{i} + \frac{\partial H_x}{\partial z} \hat{j} - \frac{\partial H_x}{\partial y} \hat{k}$$

$$\therefore \mathbf{J} = \left(0, \frac{\partial H_x}{\partial z}, -\frac{\partial H_x}{\partial y}\right) \quad (3.14)$$

$$\begin{aligned} \text{Therefore, } \frac{\mu_e}{\rho} (\mathbf{J} \wedge \mathbf{H}) &= \frac{\mu_e}{\rho} \begin{vmatrix} \hat{i} & \hat{j} & \hat{k} \\ 0 & \frac{\partial H_x}{\partial z} & -\frac{\partial H_x}{\partial y} \\ H_x & H_0 & 0 \end{vmatrix} \\ &= \frac{\mu_e}{\rho} \left[ \left(0 - H_0 \frac{\partial H_x}{\partial z}\right) \hat{i} - \left(0 + H_x \frac{\partial H_x}{\partial y}\right) \hat{j} + \left(0 - H_x \frac{\partial H_x}{\partial z}\right) \hat{k} \right] \\ &= \frac{\mu_e}{\rho} \left( H_0 \frac{\partial H_x}{\partial y} \hat{i} - H_x \frac{\partial H_x}{\partial y} \hat{j} - H_x \frac{\partial H_x}{\partial z} \hat{k} \right) \end{aligned}$$

$$\text{i.e., } \frac{\mu_e}{\rho} (\mathbf{J} \wedge \mathbf{H}) = \frac{\mu_e}{\rho} \left( H_0 \frac{\partial H_x}{\partial y}, -H_x \frac{\partial H_x}{\partial y}, -H_x \frac{\partial H_x}{\partial z} \right) \quad (3.15)$$

$$\text{Also, } \mathbf{F} = (F_x, F_y, F_z) \quad (3.16)$$

Thus the momentum equation (3.5) can be written in the Cartesian form with the help of the equation (3.15) and (3.16) as



$$\therefore \frac{\partial u}{\partial t} + u \frac{\partial u}{\partial x} + v \frac{\partial u}{\partial y} + w \frac{\partial u}{\partial z} = F_x - \frac{1}{\rho} \frac{\partial \rho}{\partial x} + v \left( \frac{\partial^2 u}{\partial x^2} + \frac{\partial^2 u}{\partial y^2} + \frac{\partial^2 u}{\partial z^2} \right) + \frac{\mu_e}{\rho} H_0 \frac{\partial H_x}{\partial y} \quad (3.17)$$

$$\therefore \frac{\partial v}{\partial t} + u \frac{\partial v}{\partial x} + v \frac{\partial v}{\partial y} + w \frac{\partial v}{\partial z} = F_y - \frac{1}{\rho} \frac{\partial \rho}{\partial y} + v \left( \frac{\partial^2 v}{\partial x^2} + \frac{\partial^2 v}{\partial y^2} + \frac{\partial^2 v}{\partial z^2} \right) - \frac{\mu_e}{\rho} H_x \frac{\partial H_x}{\partial y} \quad (3.18)$$

$$\therefore \frac{\partial w}{\partial t} + u \frac{\partial w}{\partial x} + v \frac{\partial w}{\partial y} + w \frac{\partial w}{\partial z} = F_z - \frac{1}{\rho} \frac{\partial \rho}{\partial z} + v \left( \frac{\partial^2 w}{\partial x^2} + \frac{\partial^2 w}{\partial y^2} + \frac{\partial^2 w}{\partial z^2} \right) - \frac{\mu_e}{\rho} H_x \frac{\partial H_x}{\partial z} \quad (3.19)$$

Again  $\mathbf{H} = (H_x, H_0, 0)$

and  $\mathbf{q} \cdot \nabla = u \frac{\partial}{\partial x} + v \frac{\partial}{\partial y} + w \frac{\partial}{\partial z}$

$$\begin{aligned} \therefore (\mathbf{q} \cdot \nabla) \mathbf{H} &= \left( u \frac{\partial}{\partial x} + v \frac{\partial}{\partial y} + w \frac{\partial}{\partial z} \right) (H_x \hat{i} + H_0 \hat{j} + 0 \cdot \hat{k}) \\ &= \left( u \frac{\partial H_x}{\partial x} + v \frac{\partial H_x}{\partial y} + w \frac{\partial H_x}{\partial z} \right) \hat{i} \end{aligned}$$

$$\therefore (\mathbf{q} \cdot \nabla) \mathbf{H} = \left( u \frac{\partial H_x}{\partial x} + v \frac{\partial H_x}{\partial y} + w \frac{\partial H_x}{\partial z} \right) \hat{i} \quad (3.20)$$

Again  $(\mathbf{H} \cdot \nabla) \mathbf{q} = \left[ (H_x \hat{i} + H_0 \hat{j}) \cdot \left( \hat{i} \frac{\partial}{\partial x} + \hat{j} \frac{\partial}{\partial y} + \hat{k} \frac{\partial}{\partial z} \right) \right] (u \hat{i} + v \hat{j} + w \hat{k})$

$$\begin{aligned} &= \left( H_x \frac{\partial}{\partial x} + H_0 \frac{\partial}{\partial y} \right) (u \hat{i} + v \hat{j} + w \hat{k}) \\ &= \left( H_x \frac{\partial}{\partial x} + H_0 \frac{\partial}{\partial y} \right) (u \hat{i} + v \hat{j} + w \hat{k}) \\ &= \left( H_x \frac{\partial u}{\partial x} + H_0 \frac{\partial u}{\partial y} \right) \hat{i} + \left( H_x \frac{\partial v}{\partial x} + H_0 \frac{\partial v}{\partial y} \right) \hat{j} + \left( H_x \frac{\partial w}{\partial x} + H_0 \frac{\partial w}{\partial y} \right) \hat{k} \end{aligned} \quad (3.21)$$

Also,  $\frac{1}{\mu_e \sigma'} \nabla^2 \mathbf{H} = \frac{1}{\mu_e \sigma'} \left( \frac{\partial^2}{\partial x^2} + \frac{\partial^2}{\partial y^2} + \frac{\partial^2}{\partial z^2} \right) (H_x \hat{i} + H_0 \hat{j})$

$$= \frac{1}{\mu_e \sigma'} \left( \frac{\partial^2 H_x}{\partial x^2} + \frac{\partial^2 H_x}{\partial y^2} + \frac{\partial^2 H_x}{\partial z^2} \right) \hat{i}$$

$$\therefore \frac{1}{\mu_e \sigma'} \nabla^2 \mathbf{H} = \frac{1}{\mu_e \sigma'} \left( \frac{\partial^2 H_x}{\partial x^2} + \frac{\partial^2 H_x}{\partial y^2} + \frac{\partial^2 H_0}{\partial z^2}, 0, 0 \right) \quad (3.22)$$

Thus the magnetic induction equation (3.6) yields

$$\frac{\partial H_x}{\partial t} + u \frac{\partial H_x}{\partial x} + v \frac{\partial H_x}{\partial y} + w \frac{\partial H_x}{\partial z} = H_x \frac{\partial u}{\partial x} + H_0 \frac{\partial u}{\partial y} + \frac{1}{\mu_e \sigma'} \left( \frac{\partial^2 H_x}{\partial x^2} + \frac{\partial^2 H_x}{\partial y^2} + \frac{\partial^2 H_x}{\partial z^2} \right) \quad (3.23)$$

$$0 = H_x \frac{\partial v}{\partial x} + H_0 \frac{\partial v}{\partial y} \quad (3.24)$$

$$0 = H_x \frac{\partial w}{\partial x} + H_0 \frac{\partial w}{\partial y} \quad (3.25)$$

Again,  $\mathbf{J} = \nabla \wedge \mathbf{H} = \left( 0, \frac{\partial H_x}{\partial z}, -\frac{\partial H_x}{\partial y} \right)$

$$\mathbf{J}^2 = \left[ \frac{\partial H_x}{\partial z} \hat{j} + \left( -\frac{\partial H_x}{\partial y} \right) \hat{k} \right] \cdot \left[ \frac{\partial H_x}{\partial z} \hat{j} + \left( -\frac{\partial H_x}{\partial y} \right) \hat{k} \right] = \left( \frac{\partial H_x}{\partial z} \right)^2 + \left( \frac{\partial H_x}{\partial y} \right)^2$$

$$\therefore \frac{J^2}{\rho c_p \sigma'} = \frac{1}{\rho c_p \sigma'} \left[ \left( \frac{\partial H_x}{\partial z} \right)^2 + \left( \frac{\partial H_x}{\partial y} \right)^2 \right] \quad (3.26)$$

Thus the energy equation (3.7) become

$$\frac{\partial T}{\partial t} + u \frac{\partial T}{\partial x} + v \frac{\partial T}{\partial y} + w \frac{\partial T}{\partial z} = \frac{k}{\rho c_p} \left( \frac{\partial^2 T}{\partial x^2} + \frac{\partial^2 T}{\partial y^2} + \frac{\partial^2 T}{\partial z^2} \right) + \frac{1}{\rho c_p} \phi + \frac{1}{\rho c_p \sigma'} \left[ \left( \frac{\partial H_x}{\partial z} \right)^2 + \left( \frac{\partial H_x}{\partial y} \right)^2 \right] + \frac{D_m K_T}{c_s c_p} \left( \frac{\partial^2 C}{\partial x^2} + \frac{\partial^2 C}{\partial y^2} + \frac{\partial^2 C}{\partial z^2} \right) \quad (3.27)$$

$$\text{where } \phi = \mu \left[ \left( \frac{\partial u}{\partial x} \right)^2 + \left( \frac{\partial v}{\partial y} \right)^2 + \left( \frac{\partial w}{\partial z} \right)^2 + \left( \frac{\partial u}{\partial y} + \frac{\partial v}{\partial x} \right)^2 + \left( \frac{\partial w}{\partial y} + \frac{\partial v}{\partial z} \right)^2 + \left( \frac{\partial w}{\partial x} + \frac{\partial u}{\partial z} \right)^2 \right]$$

and the species concentration equation (3.8) become

$$\frac{\partial C}{\partial t} + u \frac{\partial C}{\partial x} + v \frac{\partial C}{\partial y} + w \frac{\partial C}{\partial z} = D_m \left( \frac{\partial^2 C}{\partial x^2} + \frac{\partial^2 C}{\partial y^2} + \frac{\partial^2 C}{\partial z^2} \right) + \frac{D_m K_T}{T_m} \left( \frac{\partial^2 T}{\partial x^2} + \frac{\partial^2 T}{\partial y^2} + \frac{\partial^2 T}{\partial z^2} \right) \quad (3.28)$$

Thus in three dimensional Cartesian co-ordinate system the continuity equation, the momentum equation, the magnetic induction and the species concentration equation become

### Continuity equation

$$\frac{\partial u}{\partial x} + \frac{\partial v}{\partial y} + \frac{\partial w}{\partial z} = 0 \quad (3.29)$$

### Momentum equation

$$\therefore \frac{\partial u}{\partial t} + u \frac{\partial u}{\partial x} + v \frac{\partial u}{\partial y} + w \frac{\partial u}{\partial z} = F_x - \frac{1}{\rho} \frac{\partial \rho}{\partial x} + \nu \left( \frac{\partial^2 u}{\partial x^2} + \frac{\partial^2 u}{\partial y^2} + \frac{\partial^2 u}{\partial z^2} \right) + \frac{\mu_e}{\rho} H_0 \frac{\partial H_x}{\partial y} \quad (3.30)$$

$$\therefore \frac{\partial v}{\partial t} + u \frac{\partial v}{\partial x} + v \frac{\partial v}{\partial y} + w \frac{\partial v}{\partial z} = F_y - \frac{1}{\rho} \frac{\partial \rho}{\partial y} + \nu \left( \frac{\partial^2 v}{\partial x^2} + \frac{\partial^2 v}{\partial y^2} + \frac{\partial^2 v}{\partial z^2} \right) - \frac{\mu_e}{\rho} H_x \frac{\partial H_x}{\partial y} \quad (3.31)$$

$$\therefore \frac{\partial w}{\partial t} + u \frac{\partial w}{\partial x} + v \frac{\partial w}{\partial y} + w \frac{\partial w}{\partial z} = F_z - \frac{1}{\rho} \frac{\partial \rho}{\partial z} + \nu \left( \frac{\partial^2 w}{\partial x^2} + \frac{\partial^2 w}{\partial y^2} + \frac{\partial^2 w}{\partial z^2} \right) - \frac{\mu_e}{\rho} H_x \frac{\partial H_x}{\partial z} \quad (3.32)$$

### Magnetic induction equation

$$\frac{\partial H_x}{\partial t} + u \frac{\partial H_x}{\partial x} + v \frac{\partial H_x}{\partial y} + w \frac{\partial H_x}{\partial z} = H_x \frac{\partial u}{\partial x} + H_0 \frac{\partial u}{\partial y} + \frac{1}{\mu_e \sigma'} \left( \frac{\partial^2 H_x}{\partial x^2} + \frac{\partial^2 H_x}{\partial y^2} + \frac{\partial^2 H_x}{\partial z^2} \right) \quad (3.33)$$

$$0 = H_x \frac{\partial v}{\partial x} + H_0 \frac{\partial v}{\partial y} \quad (3.34)$$

$$0 = H_x \frac{\partial w}{\partial x} + H_0 \frac{\partial w}{\partial y} \quad (3.35)$$

### Energy equation

$$\frac{\partial T}{\partial t} + u \frac{\partial T}{\partial x} + v \frac{\partial T}{\partial y} + w \frac{\partial T}{\partial z} = \frac{k}{\rho c_p} \left( \frac{\partial^2 T}{\partial x^2} + \frac{\partial^2 T}{\partial y^2} + \frac{\partial^2 T}{\partial z^2} \right) + \frac{1}{\rho c_p} \phi + \frac{1}{\rho c_p \sigma'} \left[ \left( \frac{\partial H_x}{\partial z} \right)^2 + \left( \frac{\partial H_x}{\partial y} \right)^2 \right] + \frac{D_m K_T}{c_s c_p} \left( \frac{\partial^2 C}{\partial x^2} + \frac{\partial^2 C}{\partial y^2} + \frac{\partial^2 C}{\partial z^2} \right) \quad (3.36)$$

$$\text{where } \phi = \mu \left[ \left( \frac{\partial u}{\partial x} \right)^2 + \left( \frac{\partial v}{\partial y} \right)^2 + \left( \frac{\partial w}{\partial z} \right)^2 + \left( \frac{\partial u}{\partial y} + \frac{\partial v}{\partial x} \right)^2 + \left( \frac{\partial w}{\partial y} + \frac{\partial v}{\partial z} \right)^2 + \left( \frac{\partial w}{\partial x} + \frac{\partial u}{\partial z} \right)^2 \right]$$

### Concentration equation

$$\frac{\partial C}{\partial t} + u \frac{\partial C}{\partial x} + v \frac{\partial C}{\partial y} + w \frac{\partial C}{\partial z} = D_m \left( \frac{\partial^2 C}{\partial x^2} + \frac{\partial^2 C}{\partial y^2} + \frac{\partial^2 C}{\partial z^2} \right) + \frac{D_m K_T}{T_m} \left( \frac{\partial^2 T}{\partial x^2} + \frac{\partial^2 T}{\partial y^2} + \frac{\partial^2 T}{\partial z^2} \right) \quad (3.37)$$

The next two subsections deal with the specific problem.

### 3.1.1 Case-I: Unsteady MHD heat and mass transfer by mixed convection past an infinite vertical porous plate.

Let us consider an unsteady heat and mass transfer by mixed convection flow of an electrically conducting viscous fluid past an infinite vertical porous plate  $y = 0$ . The flow is also assumed to be in  $x$ - direction which is taken along the plate in upward direction and  $y$ - axis is normal to it. The temperature and species concentration at the plate are instantly raised from  $T_w$  and  $C_w$  to  $T_\infty$  and  $C_\infty$  respectively, which are thereafter maintained as constant, where  $T_\infty$  and  $C_\infty$  are the temperature and species concentration of the uniform flow respectively. A uniform magnetic field of strength  $\mathbf{H}$  is applied to the plate to be acting along the  $y$ -axis, which is electrically non-conducting.

In the heat and mass transfer by mixed convection flow along the vertical plate, the body force and the pressure gradient along the direction is

$$g\beta(T - T_\infty) + g\beta^*(C - C_\infty) \quad (3.38)$$

where  $g$  is the component of gravity force along the vertical direction,  $\beta$  is the coefficient of volume expansion,  $\beta^*$  is the volumetric coefficient expansion with concentration. With reference to the above assumptions, the continuity equation (3.29), the momentum equation (3.30) - (3.32) the magnetic induction equations (3.33) - (3.35), the energy equation (3.36) and the species concentration equation (3.37) become:

### Continuity equation

$$\frac{\partial u}{\partial x} + \frac{\partial v}{\partial y} + \frac{\partial w}{\partial z} = 0 \quad (3.39)$$

### Momentum equation

$$\begin{aligned} \frac{\partial u}{\partial t} + u \frac{\partial u}{\partial x} + v \frac{\partial u}{\partial y} + w \frac{\partial u}{\partial z} = g\beta(T - T_\infty) + g\beta^*(C - C_\infty) + v \left( \frac{\partial^2 u}{\partial x^2} + \frac{\partial^2 u}{\partial y^2} + \frac{\partial^2 u}{\partial z^2} \right) \\ + \frac{\mu_e}{\rho} H_0 \frac{\partial H_x}{\partial y} \end{aligned} \quad (3.40)$$

$$\therefore \frac{\partial v}{\partial t} + u \frac{\partial v}{\partial x} + v \frac{\partial v}{\partial y} + w \frac{\partial v}{\partial z} = v \left( \frac{\partial^2 v}{\partial x^2} + \frac{\partial^2 v}{\partial y^2} + \frac{\partial^2 v}{\partial z^2} \right) - \frac{\mu_e}{\rho} H_x \frac{\partial H_x}{\partial y} \quad (3.41)$$

$$\frac{\partial w}{\partial t} + u \frac{\partial w}{\partial x} + v \frac{\partial w}{\partial y} + w \frac{\partial w}{\partial z} = v \left( \frac{\partial^2 w}{\partial x^2} + \frac{\partial^2 w}{\partial y^2} + \frac{\partial^2 w}{\partial z^2} \right) - \frac{\mu_e}{\rho} H_x \frac{\partial H_x}{\partial z} \quad (3.42)$$

### Magnetic induction equation

$$\frac{\partial H_x}{\partial t} + u \frac{\partial H_x}{\partial x} + v \frac{\partial H_x}{\partial y} + w \frac{\partial H_x}{\partial z} = H_x \frac{\partial u}{\partial x} + H_0 \frac{\partial u}{\partial y} + \frac{1}{\mu_e \sigma'} \left( \frac{\partial^2 H_x}{\partial x^2} + \frac{\partial^2 H_x}{\partial y^2} + \frac{\partial^2 H_x}{\partial z^2} \right) \quad (3.43)$$

$$0 = H_x \frac{\partial v}{\partial x} + H_0 \frac{\partial v}{\partial y} \quad (3.44)$$

$$0 = H_x \frac{\partial w}{\partial x} + H_0 \frac{\partial w}{\partial y} \quad (3.45)$$

### Energy equation

$$\begin{aligned} \frac{\partial T}{\partial t} + u \frac{\partial T}{\partial x} + v \frac{\partial T}{\partial y} + w \frac{\partial T}{\partial z} = \frac{k}{\rho c_p} \left( \frac{\partial^2 T}{\partial x^2} + \frac{\partial^2 T}{\partial y^2} + \frac{\partial^2 T}{\partial z^2} \right) + \frac{1}{\rho c_p} \phi + \frac{1}{\rho c_p \sigma'} \left[ \left( \frac{\partial H_x}{\partial z} \right)^2 + \left( \frac{\partial H_x}{\partial y} \right)^2 \right] \\ + \frac{D_m K_T}{C_s c_p} \left( \frac{\partial^2 C}{\partial x^2} + \frac{\partial^2 C}{\partial y^2} + \frac{\partial^2 C}{\partial z^2} \right) \end{aligned} \quad (3.46)$$

$$\text{where } \phi = \mu \left[ \left( \frac{\partial u}{\partial x} \right)^2 + \left( \frac{\partial v}{\partial y} \right)^2 + \left( \frac{\partial w}{\partial z} \right)^2 + \left( \frac{\partial u}{\partial y} + \frac{\partial v}{\partial x} \right)^2 + \left( \frac{\partial w}{\partial y} + \frac{\partial v}{\partial z} \right)^2 + \left( \frac{\partial w}{\partial x} + \frac{\partial u}{\partial z} \right)^2 \right]$$

### Concentration equation

$$\frac{\partial C}{\partial t} + u \frac{\partial C}{\partial x} + v \frac{\partial C}{\partial y} + w \frac{\partial C}{\partial z} = D_m \left( \frac{\partial^2 C}{\partial x^2} + \frac{\partial^2 C}{\partial y^2} + \frac{\partial^2 C}{\partial z^2} \right) + \frac{D_m K_T}{T_m} \left( \frac{\partial^2 T}{\partial x^2} + \frac{\partial^2 T}{\partial y^2} + \frac{\partial^2 T}{\partial z^2} \right) \quad (3.47)$$

Since the plate occupying the plane  $y = 0$  is of infinite extent and fluid motion is unsteady, so all the physical quantities will depend only upon  $y$  and  $t$ . Thus the given governing equations (3.39) – (3.47) reduced to one-dimensional equations, which are as follows:

### Continuity equation

$$\frac{\partial v}{\partial y} = 0 \quad (3.48)$$

### Momentum equation

$$\frac{\partial u}{\partial t} + v \frac{\partial u}{\partial y} = g\beta(T - T_\infty) + g\beta^*(C - C_\infty) + v \frac{\partial^2 u}{\partial y^2} + \frac{\mu_e}{\rho} H_0 \frac{\partial H_x}{\partial y} \quad (3.49)$$

$$\frac{\partial v}{\partial t} + v \frac{\partial v}{\partial y} = v \frac{\partial^2 v}{\partial y^2} - \frac{\mu_e}{\rho} H_x \frac{\partial H_x}{\partial y} \quad (3.50)$$

### Magnetic induction equation

$$\frac{\partial H_x}{\partial t} + v \frac{\partial H_x}{\partial y} = H_0 \frac{\partial u}{\partial y} + \frac{1}{\mu_e \sigma'} \frac{\partial^2 H_x}{\partial y^2} \quad (3.51)$$

$$0 = H_0 \frac{\partial v}{\partial y} \quad (3.52)$$

### Energy equation

$$\frac{\partial T}{\partial t} + v \frac{\partial T}{\partial y} = \frac{k}{\rho c_p} \frac{\partial^2 T}{\partial y^2} + \frac{\mu}{\rho c_p} \left[ \left( \frac{\partial u}{\partial y} \right)^2 + \left( \frac{\partial v}{\partial y} \right)^2 \right] + \frac{1}{\rho c_p \sigma'} \left( \frac{\partial H_x}{\partial y} \right)^2 + \frac{D_m K_T}{c_s c_p} \frac{\partial^2 C}{\partial y^2} \quad (3.53)$$

### Concentration equation

$$\frac{\partial C}{\partial t} + v \frac{\partial C}{\partial y} = D_m \frac{\partial^2 C}{\partial y^2} + \frac{D_m K_T}{T_m} \frac{\partial^2 T}{\partial y^2} \quad (3.54)$$

Since the magnetic Reynolds number of the flow is large so that the viscosity of the fluid is small. Let  $\delta$  be the small thickness of the boundary layer and  $\varepsilon \ll 1$  be the order of magnitude of  $\delta$  i.e.  $O(\delta) = \varepsilon$ , then we can write

$$O(y) = \varepsilon, \quad O(v) = \varepsilon, \quad O(H_0) = \varepsilon$$

Also we assume that,

$$O(u) = 1, \quad O(t) = 1, \quad O(H_x) = 1$$

Hence,

$$O\left(\frac{\partial u}{\partial t}\right) = 1, \quad O\left(\frac{\partial u}{\partial y}\right) = \frac{1}{\varepsilon}, \quad O\left(\frac{\partial^2 u}{\partial y^2}\right) = \frac{1}{\varepsilon^2}, \quad O\left(\frac{\partial H_x}{\partial y}\right) = \frac{1}{\varepsilon}$$

$$O\left(\frac{\partial v}{\partial t}\right) = \varepsilon, \quad O\left(\frac{\partial v}{\partial y}\right) = 1, \quad O\left(\frac{\partial^2 v}{\partial y^2}\right) = \frac{1}{\varepsilon}$$

$$O\left(\frac{\partial H_x}{\partial t}\right) = 1, \quad O\left(\frac{\partial^2 H_x}{\partial y^2}\right) = \frac{1}{\varepsilon^2}$$

within the boundary layer. Then the equations (3.48) – (3.52) with corresponding order of each term are given below:

### Continuity equation

$$\frac{\partial v}{\partial y} = 0 \quad (3.55)$$

1

### Momentum equation

$$\frac{\partial u}{\partial t} + v \frac{\partial u}{\partial y} = g\beta(T - T_\infty) + g\beta^*(C - C_\infty) + v \frac{\partial^2 u}{\partial y^2} + \frac{\mu_e}{\rho} H_0 \frac{\partial H_x}{\partial y} \quad (3.56)$$

$$1 \quad \varepsilon \quad \frac{1}{\varepsilon} \quad \frac{1}{\varepsilon^2} \quad \varepsilon \quad \frac{1}{\varepsilon}$$

$$\frac{\partial v}{\partial t} + v \frac{\partial v}{\partial y} = v \frac{\partial^2 v}{\partial y^2} - \frac{\mu_e}{\rho} H_x \frac{\partial H_x}{\partial y} \quad (3.57)$$

$$\varepsilon \quad \varepsilon \quad 1 \quad \frac{1}{\varepsilon} \quad 1 \quad \frac{1}{\varepsilon}$$

### Magnetic induction equation

$$\frac{\partial H_x}{\partial t} + v \frac{\partial H_x}{\partial y} = H_0 \frac{\partial u}{\partial y} + \frac{1}{\mu_e \sigma'} \frac{\partial^2 H_x}{\partial y^2} \quad (3.58)$$

$$1 \quad \varepsilon \frac{1}{\varepsilon} \quad \varepsilon \frac{1}{\varepsilon} \quad \frac{1}{\varepsilon^2}$$

$$0 = H_0 \frac{\partial v}{\partial y} \quad (3.59)$$

$$\varepsilon \quad 1$$

Again let  $\delta_T$  be the thermal boundary layer thickness and let  $\varepsilon \ll 1$  be also the order of  $\delta_T$  i.e.  $O(\delta_T) = \varepsilon$ . Then we can write  $O(y) = \varepsilon$ ,  $O(v) = \varepsilon$ .

We can also write  $O(T) = 1$ ,  $O(C) = 1$ ,  $O(x) = 1$  and  $O(u) = 1$ .

Hence,

$$O\left(\frac{\partial T}{\partial t}\right) = 1, O\left(\frac{\partial T}{\partial y}\right) = \frac{1}{\varepsilon}, O\left(\frac{\partial^2 T}{\partial y^2}\right) = \frac{1}{\varepsilon^2}, O\left(\frac{\partial C}{\partial t}\right) = 1, O\left(\frac{\partial C}{\partial y}\right) = \frac{1}{\varepsilon}, O\left(\frac{\partial^2 C}{\partial y^2}\right) = \frac{1}{\varepsilon^2}$$

within the boundary layer.

Then the equations (3.53) – (3.54) with corresponding order of each term are given below:

### Energy Equation

$$\frac{\partial T}{\partial t} + v \frac{\partial T}{\partial y} = \frac{k}{\rho c_p} \frac{\partial^2 T}{\partial y^2} + \frac{\mu}{\rho c_p} \left[ \left( \frac{\partial u}{\partial y} \right)^2 + \left( \frac{\partial v}{\partial y} \right)^2 \right] + \frac{1}{\rho c_p \sigma'} \left( \frac{\partial H_x}{\partial y} \right)^2 + \frac{D_m K_T}{c_s c_p} \frac{\partial^2 C}{\partial y^2} \quad (3.60)$$

$$1 \quad \varepsilon \frac{1}{\varepsilon} \quad \frac{1}{\varepsilon^2} \quad \frac{1}{\varepsilon^2} \quad 1 \quad \frac{1}{\varepsilon^2} \quad \frac{1}{\varepsilon^2}$$

### Concentration equation

$$\frac{\partial C}{\partial t} + v \frac{\partial C}{\partial y} = D_m \frac{\partial^2 C}{\partial y^2} + \frac{D_m K_T}{T_m} \frac{\partial^2 T}{\partial y^2} \quad (3.61)$$

$$1 \quad \varepsilon \frac{1}{\varepsilon} \quad \frac{1}{\varepsilon^2} \quad \frac{1}{\varepsilon^2}$$

where we have found the order of other terms involved in the equation as follows:

$$O(g\beta(T - T_\infty)) = 1, \quad O(g\beta^*(C - C_\infty)) = 1,$$

$$O\left(\frac{\mu_e}{\rho}\right) = \varepsilon^2, \quad O(v) = \varepsilon^2, \quad O\left(\frac{1}{\mu_e \sigma'}\right) = \varepsilon^2, \quad O\left(\frac{k}{\rho c_p}\right) = \varepsilon^2, \quad O(D_m) = \varepsilon^2,$$

$$O\left(\frac{D_m K_T}{T_m}\right) = \varepsilon^2, \quad O\left(\frac{v}{c_p}\right) = \varepsilon^2, \quad O\left(\frac{1}{\rho c_p \sigma'}\right) = \varepsilon^2, \quad O\left(\frac{D_m}{c_s c_p}\right) = \varepsilon^2.$$

Since the viscosity is very small, we can neglect the terms of small orders. Thus we have from equations (3.55) – (3.61):

$$\frac{\partial v}{\partial y} = 0 \quad (3.62)$$

$$\frac{\partial u}{\partial t} + v \frac{\partial u}{\partial y} = g\beta(T - T_\infty) + g\beta^*(C - C_\infty) + v \frac{\partial^2 u}{\partial y^2} + \frac{\mu_e}{\rho} H_0 \frac{\partial H_x}{\partial y} \quad (3.63)$$

$$\frac{\partial H_x}{\partial t} + v \frac{\partial H_x}{\partial y} = H_0 \frac{\partial u}{\partial y} + \frac{1}{\mu_e \sigma'} \frac{\partial^2 H_x}{\partial y^2} \quad (3.64)$$

$$\frac{\partial T}{\partial t} + v \frac{\partial T}{\partial y} = \frac{k}{\rho c_p} \frac{\partial^2 T}{\partial y^2} + \frac{\mu}{\rho c_p} \left( \frac{\partial u}{\partial y} \right)^2 + \frac{1}{\rho c_p \sigma'} \left( \frac{\partial H_x}{\partial y} \right)^2 + \frac{D_m K_T}{C_s C_p} \frac{\partial^2 C}{\partial y^2} \quad (3.65)$$

$$\frac{\partial C}{\partial t} + v \frac{\partial C}{\partial y} = D_m \frac{\partial^2 C}{\partial y^2} + \frac{D_m K_T}{T_m} \frac{\partial^2 T}{\partial y^2} \quad (3.66)$$

The boundary conditions for the problem are as follows:

$$\left. \begin{aligned} t > 0, \quad u = U_0(t), \quad v = v(t), \quad \frac{\partial T}{\partial y} = -\frac{q}{k}, \quad \frac{\partial C}{\partial y} = -\frac{m}{D_m}, \quad H_x = H_0 \quad \text{at } y = 0 \\ t > 0, \quad u = 0, \quad T \rightarrow T_\infty, \quad C \rightarrow C_\infty, \quad H_x \rightarrow 0 \quad \text{as } y \rightarrow \infty \end{aligned} \right\} \quad (3.67)$$

where  $H_x$  is the induced magnetic field,  $H_0$  is applied constant magnetic field at the plate and  $m$  is the coefficient of mass flux per unite area.

### 3.1.2 Case-II: Steady MHD heat and mass transfer by mixed convection flow past a semi-infinite vertical porous plate

Let us consider a steady heat and mass transfer by mixed convection flow of an electrically conducting viscous fluid past a semi-infinite vertical porous plate  $y = 0$ . The flow is also assumed to be in  $x$ -direction which is taken along the plate is upward direction and  $y$ -axis is normal to it. The detailed descriptions of the present problem are similar to those of Case –I. In the heat and mass transfer by mixed convection flow along the vertical plate, the body force and pressure gradient along the direction is

$$g\beta(T - T_\infty) + g\beta^*(C - C_\infty) \quad (3.68)$$

where  $g$  is the component of gravity force along the vertical direction,  $\beta$  is the coefficient of volume expansion,  $\beta^*$  is the volumetric coefficient expansion with concentration. With reference to the above assumptions, the continuity equation (3.29), the momentum equations (3.30) – (3.32), the magnetic induction equations (3.33) – (3.35), the energy equation (3.36) and the species concentration equation (3.37) become:

### Continuity equation

$$\frac{\partial u}{\partial x} + \frac{\partial v}{\partial y} + \frac{\partial w}{\partial z} = 0 \quad (3.69)$$

### Momentum equation

$$u \frac{\partial u}{\partial x} + v \frac{\partial u}{\partial y} + w \frac{\partial u}{\partial z} = g\beta(T - T_\infty) + g\beta^*(C - C_\infty) + \nu \left( \frac{\partial^2 u}{\partial x^2} + \frac{\partial^2 u}{\partial y^2} + \frac{\partial^2 u}{\partial z^2} \right) + \frac{\mu_e}{\rho} H_0 \frac{\partial H_x}{\partial y} \quad (3.70)$$

$$u \frac{\partial v}{\partial x} + v \frac{\partial v}{\partial y} + w \frac{\partial v}{\partial z} = \nu \left( \frac{\partial^2 v}{\partial x^2} + \frac{\partial^2 v}{\partial y^2} + \frac{\partial^2 v}{\partial z^2} \right) - \frac{\mu_e}{\rho} H_x \frac{\partial H_x}{\partial y} \quad (3.71)$$

$$u \frac{\partial w}{\partial x} + v \frac{\partial w}{\partial y} + w \frac{\partial w}{\partial z} = \nu \left( \frac{\partial^2 w}{\partial x^2} + \frac{\partial^2 w}{\partial y^2} + \frac{\partial^2 w}{\partial z^2} \right) - \frac{\mu_e}{\rho} H_x \frac{\partial H_x}{\partial z} \quad (3.72)$$

### Magnetic induction equation

$$u \frac{\partial H_x}{\partial x} + v \frac{\partial H_x}{\partial y} + w \frac{\partial H_x}{\partial z} = H_x \frac{\partial u}{\partial x} + H_0 \frac{\partial u}{\partial y} + \frac{1}{\mu_e \sigma'} \left( \frac{\partial^2 H_x}{\partial x^2} + \frac{\partial^2 H_x}{\partial y^2} + \frac{\partial^2 H_x}{\partial z^2} \right) \quad (3.73)$$

$$0 = H_x \frac{\partial v}{\partial x} + H_0 \frac{\partial v}{\partial y} \quad (3.74)$$

$$0 = H_x \frac{\partial w}{\partial x} + H_0 \frac{\partial w}{\partial y} \quad (3.75)$$

### Energy equation

$$\frac{\partial T}{\partial t} + u \frac{\partial T}{\partial x} + v \frac{\partial T}{\partial y} + w \frac{\partial T}{\partial z} = \frac{k}{\rho c_p} \left( \frac{\partial^2 T}{\partial x^2} + \frac{\partial^2 T}{\partial y^2} + \frac{\partial^2 T}{\partial z^2} \right) + \frac{1}{\rho c_p} \phi + \frac{1}{\rho c_p \sigma'} \left[ \left( \frac{\partial H_x}{\partial z} \right)^2 + \left( \frac{\partial H_x}{\partial y} \right)^2 \right] + \frac{D_m K_T}{c_s c_p} \left( \frac{\partial^2 C}{\partial x^2} + \frac{\partial^2 C}{\partial y^2} + \frac{\partial^2 C}{\partial z^2} \right) \quad (3.76)$$

$$\text{where } \phi = \mu \left[ \left( \frac{\partial u}{\partial x} \right)^2 + \left( \frac{\partial v}{\partial y} \right)^2 + \left( \frac{\partial w}{\partial z} \right)^2 + \left( \frac{\partial u}{\partial y} + \frac{\partial v}{\partial x} \right)^2 + \left( \frac{\partial w}{\partial y} + \frac{\partial v}{\partial z} \right)^2 + \left( \frac{\partial w}{\partial x} + \frac{\partial u}{\partial z} \right)^2 \right]$$

### Concentration equation

$$\frac{\partial C}{\partial t} + u \frac{\partial C}{\partial x} + v \frac{\partial C}{\partial y} + w \frac{\partial C}{\partial z} = D_m \left( \frac{\partial^2 C}{\partial x^2} + \frac{\partial^2 C}{\partial y^2} + \frac{\partial^2 C}{\partial z^2} \right) + \frac{D_m K_T}{T_m} \left( \frac{\partial^2 T}{\partial x^2} + \frac{\partial^2 T}{\partial y^2} + \frac{\partial^2 T}{\partial z^2} \right) \quad (3.77)$$

Since the plate occupying the plane  $y = 0$  is of semi-infinite extent and fluid motion is unsteady, so all the physical quantities will depend only upon  $x$  and  $y$ . Thus the given governing equations (3.69) – (3.77) reduced to two-dimensional equations, which are as follows:

### Continuity equation

$$\frac{\partial u}{\partial x} + \frac{\partial v}{\partial y} = 0 \quad (3.78)$$



### Momentum equation

$$u \frac{\partial u}{\partial x} + v \frac{\partial u}{\partial y} = g\beta(T - T_\infty) + g\beta^*(C - C_\infty) + v \left( \frac{\partial^2 u}{\partial x^2} + \frac{\partial^2 u}{\partial y^2} \right) + \frac{\mu_e}{\rho} H_0 \frac{\partial H_x}{\partial y} \quad (3.79)$$

$$u \frac{\partial v}{\partial x} + v \frac{\partial v}{\partial y} = v \left( \frac{\partial^2 v}{\partial x^2} + \frac{\partial^2 v}{\partial y^2} \right) - \frac{\mu_e}{\rho} H_x \frac{\partial H_x}{\partial y} \quad (3.80)$$

### Magnetic induction equation

$$u \frac{\partial H_x}{\partial x} + v \frac{\partial H_x}{\partial y} = H_x \frac{\partial u}{\partial x} + H_0 \frac{\partial u}{\partial y} + \frac{1}{\mu_e \sigma'} \left( \frac{\partial^2 H_x}{\partial x^2} + \frac{\partial^2 H_x}{\partial y^2} \right) \quad (3.81)$$

$$0 = H_x \frac{\partial v}{\partial x} + H_0 \frac{\partial v}{\partial y} \quad (3.82)$$

### Energy equation

$$u \frac{\partial T}{\partial x} + v \frac{\partial T}{\partial y} = \frac{k}{\rho c_p} \left( \frac{\partial^2 T}{\partial x^2} + \frac{\partial^2 T}{\partial y^2} \right) + \frac{\mu}{\rho c_p} \left[ \left( \frac{\partial u}{\partial x} \right)^2 + \left( \frac{\partial v}{\partial y} \right)^2 + \left( \frac{\partial w}{\partial z} \right)^2 + \left( \frac{\partial u}{\partial y} + \frac{\partial v}{\partial x} \right)^2 \right] \\ + \frac{1}{\rho c_p \sigma'} \left( \frac{\partial H_x}{\partial y} \right)^2 + \frac{D_m K_T}{c_s c_p} \left( \frac{\partial^2 C}{\partial x^2} + \frac{\partial^2 C}{\partial y^2} \right) \quad (3.83)$$

### Concentration equation

$$u \frac{\partial C}{\partial x} + v \frac{\partial C}{\partial y} = D_m \left( \frac{\partial^2 C}{\partial x^2} + \frac{\partial^2 C}{\partial y^2} \right) + \frac{D_m K_T}{T_m} \left( \frac{\partial^2 T}{\partial x^2} + \frac{\partial^2 T}{\partial y^2} \right) \quad (3.84)$$

Since the magnetic Reynolds number of the flow is large enough, so that the viscosity of the fluid is small. Let  $\delta$  be the small thickness of the boundary layer and  $\varepsilon \ll 1$  be the order of magnitude of  $\delta$  i.e.  $O(\delta) = \varepsilon$ , then we can write

$$O(y) = \varepsilon, \quad O(v) = \varepsilon, \quad O(H_0) = \varepsilon$$

$$\text{Also we assume that, } O(u) = 1, \quad O(x) = 1, \quad O(H_x) = 1$$

Hence,

$$O\left(\frac{\partial u}{\partial x}\right) = 1, \quad O\left(\frac{\partial u}{\partial y}\right) = \frac{1}{\varepsilon}, \quad O\left(\frac{\partial^2 u}{\partial x^2}\right) = 1, \quad O\left(\frac{\partial^2 u}{\partial y^2}\right) = \frac{1}{\varepsilon^2}$$

$$O\left(\frac{\partial v}{\partial x}\right) = \varepsilon, \quad O\left(\frac{\partial v}{\partial y}\right) = 1, \quad O\left(\frac{\partial^2 v}{\partial x^2}\right) = \varepsilon, \quad O\left(\frac{\partial^2 v}{\partial y^2}\right) = \frac{1}{\varepsilon}$$

$$O\left(\frac{\partial H_x}{\partial x}\right) = 1, \quad O\left(\frac{\partial H_x}{\partial y}\right) = \frac{1}{\varepsilon}, \quad O\left(\frac{\partial^2 H_x}{\partial x^2}\right) = 1, \quad O\left(\frac{\partial^2 H_x}{\partial y^2}\right) = \frac{1}{\varepsilon^2}$$

within the boundary layer. Then the equations (3.78) – (3.82) with corresponding order of each term are given below:

### Continuity equation

$$\frac{\partial u}{\partial x} + \frac{\partial v}{\partial y} = 0 \quad (3.85)$$

$$1 \quad 1$$

### Momentum equation

$$u \frac{\partial u}{\partial x} + v \frac{\partial u}{\partial y} = g\beta(T - T_\infty) + g\beta^*(C - C_\infty) + \nu \left( \frac{\partial^2 u}{\partial x^2} + \frac{\partial^2 u}{\partial y^2} \right) + \frac{\mu_e}{\rho} H_0 \frac{\partial H_x}{\partial y} \quad (3.86)$$

$$1 \quad 1 \quad \varepsilon \quad \frac{1}{\varepsilon} \quad 1 \quad \frac{1}{\varepsilon^2} \quad \varepsilon \quad \frac{1}{\varepsilon}$$

$$u \frac{\partial v}{\partial x} + v \frac{\partial v}{\partial y} = \nu \left( \frac{\partial^2 v}{\partial x^2} + \frac{\partial^2 v}{\partial y^2} \right) - \frac{\mu_e}{\rho} H_x \frac{\partial H_x}{\partial y} \quad (3.87)$$

$$1 \quad \varepsilon \quad \varepsilon \quad 1 \quad \varepsilon \quad \frac{1}{\varepsilon} \quad 1 \quad \frac{1}{\varepsilon}$$

### Magnetic induction equation

$$u \frac{\partial H_x}{\partial x} + v \frac{\partial H_x}{\partial y} = H_x \frac{\partial u}{\partial x} + H_0 \frac{\partial u}{\partial y} + \frac{1}{\mu_e \sigma'} \left( \frac{\partial^2 H_x}{\partial x^2} + \frac{\partial^2 H_x}{\partial y^2} \right) \quad (3.88)$$

$$1 \quad 1 \quad \varepsilon \quad \frac{1}{\varepsilon} \quad 1 \quad 1 \quad \varepsilon \quad \frac{1}{\varepsilon} \quad 1 \quad \frac{1}{\varepsilon^2}$$

$$0 = H_x \frac{\partial v}{\partial x} + H_0 \frac{\partial v}{\partial y} \quad (3.89)$$

$$1 \quad \varepsilon \quad \varepsilon \quad 1$$

Again let  $\delta_T$  be the thermal boundary layer thickness and let  $\varepsilon \ll 1$  be also the order of  $\delta_T$  i.e.  $O(\delta_T) = \varepsilon$ . Then we can write  $O(y) = \varepsilon$ ,  $O(v) = \varepsilon$

Also we can write  $O(T) = 1$ ,  $O(C) = 1$ ,  $O(x) = 1$  and  $O(u) = 1$

$$\text{Hence } O\left(\frac{\partial T}{\partial x}\right) = 1, \quad O\left(\frac{\partial^2 T}{\partial x^2}\right) = 1, \quad O\left(\frac{\partial T}{\partial y}\right) = \frac{1}{\varepsilon}, \quad O\left(\frac{\partial^2 T}{\partial y^2}\right) = \frac{1}{\varepsilon^2}$$

$$O\left(\frac{\partial C}{\partial x}\right) = 1, \quad O\left(\frac{\partial^2 C}{\partial x^2}\right) = 1, \quad O\left(\frac{\partial C}{\partial y}\right) = \frac{1}{\varepsilon}, \quad O\left(\frac{\partial^2 C}{\partial y^2}\right) = \frac{1}{\varepsilon^2}$$

within the boundary layer. Then the equations (3.83) – (3.84) with corresponding order of each term are given below:

### Energy equation

$$u \frac{\partial T}{\partial x} + v \frac{\partial T}{\partial y} = \frac{k}{\rho c_p} \left( \frac{\partial^2 T}{\partial x^2} + \frac{\partial^2 T}{\partial y^2} \right) + \frac{\mu}{\rho c_p} \left[ \left( \frac{\partial u}{\partial x} \right)^2 + \left( \frac{\partial v}{\partial y} \right)^2 + \left( \frac{\partial w}{\partial z} \right)^2 + \left( \frac{\partial u}{\partial y} + \frac{\partial v}{\partial x} \right)^2 \right] + \frac{1}{\rho c_p \sigma'} \left( \frac{\partial H_x}{\partial y} \right)^2 + \frac{D_m K_T}{c_s c_p} \left( \frac{\partial^2 C}{\partial x^2} + \frac{\partial^2 C}{\partial y^2} \right) \quad (3.90)$$

$$1 \quad 1 \quad \varepsilon \quad \frac{1}{\varepsilon} \quad 1 \quad \frac{1}{\varepsilon^2} \quad 1 \quad 1 \quad \varepsilon^2 \quad \frac{1}{\varepsilon^2} \quad 1 \quad \frac{1}{\varepsilon^2} \quad 1 \quad \frac{1}{\varepsilon^2} \quad 1 \quad \frac{1}{\varepsilon^2}$$

### Concentration equation

$$u \frac{\partial C}{\partial x} + v \frac{\partial C}{\partial y} = D_m \left( \frac{\partial^2 C}{\partial x^2} + \frac{\partial^2 C}{\partial y^2} \right) + \frac{D_m K_T}{T_m} \left( \frac{\partial^2 T}{\partial x^2} + \frac{\partial^2 T}{\partial y^2} \right) \quad (3.91)$$

$$1 \quad 1 \quad \varepsilon \frac{1}{\varepsilon} \quad 1 \quad \frac{1}{\varepsilon^2} \quad 1 \quad \frac{1}{\varepsilon^2}$$

where we have found the order of other terms involved in the equation as follows:

$$O(g\beta(T - T_\infty)) = 1, \quad O(g\beta^*(C - C_\infty)) = 1, \quad O\left(\frac{\mu_e}{\rho}\right) = \varepsilon^2, \quad O(v) = \varepsilon^2,$$

$$O\left(\frac{1}{\mu_e \sigma'}\right) = \varepsilon^2, \quad O\left(\frac{K}{\rho C_p}\right) = \varepsilon^2, \quad O(D_m) = \varepsilon^2, \quad O\left(\frac{D_m K_T}{T_m}\right) = \varepsilon^2,$$

$$O\left(\frac{v}{c_p}\right) = \varepsilon^2, \quad O\left(\frac{1}{\rho c_p \sigma'}\right) = \varepsilon^2, \quad O\left(\frac{D_m}{c_s c_p}\right) = \varepsilon^2.$$

Since the viscosity is very small, we can neglect the terms of small orders. Thus we have from equations (3.85) – (3.91):

$$\frac{\partial u}{\partial x} + \frac{\partial v}{\partial y} = 0 \quad (3.92)$$

$$u \frac{\partial u}{\partial x} + v \frac{\partial u}{\partial y} = g\beta(T - T_\infty) + g\beta^*(C - C_\infty) + v \frac{\partial^2 u}{\partial y^2} + \frac{\mu_e}{\rho} H_0 \frac{\partial H_x}{\partial y} \quad (3.93)$$

$$u \frac{\partial H_x}{\partial x} + v \frac{\partial H_x}{\partial y} = H_x \frac{\partial u}{\partial x} + H_0 \frac{\partial u}{\partial y} + \frac{1}{\mu_e \sigma'} \frac{\partial^2 H_x}{\partial y^2} \quad (3.94)$$

$$u \frac{\partial T}{\partial x} + v \frac{\partial T}{\partial y} = \frac{k}{\rho c_p} \frac{\partial^2 T}{\partial y^2} + \frac{v}{c_p} \left( \frac{\partial u}{\partial y} \right)^2 + \frac{1}{\rho c_p \sigma'} \left( \frac{\partial H_x}{\partial y} \right)^2 + \frac{D_m K_T}{c_s c_p} \frac{\partial^2 C}{\partial y^2} \quad (3.95)$$

$$u \frac{\partial C}{\partial x} + v \frac{\partial C}{\partial y} = D_m \frac{\partial^2 C}{\partial y^2} + \frac{D_m K_T}{T_m} \frac{\partial^2 T}{\partial y^2} \quad (3.96)$$

and the boundary conditions for the problem are

$$t \leq 0, u = 0, T \rightarrow T_\infty, C \rightarrow C_\infty, H_x = 0 \text{ for all } y \quad (4.97)$$

$$\left. \begin{aligned} u = U_0, \quad v = v(x), \quad \frac{\partial T}{\partial y} = -\frac{q}{k}, \quad \frac{\partial C}{\partial y} = -\frac{m}{D_m}, \quad H_x = H_0 \text{ at } y = 0 \\ u = 0, \quad T \rightarrow T_\infty, \quad C \rightarrow C_\infty, \quad H_x \rightarrow 0 \text{ as } y \rightarrow \infty \end{aligned} \right\} \quad (3.98)$$

where  $H_x$  is the induced magnetic field,  $H_0$  is the induced magnetic field at the plate and  $m$  is the coefficient of mass flux per unite area.

## CHAPTER IV

### The Finite Difference Numerical Scheme

#### 4.1 The Governing equations

An unsteady heat and mass transfer by mixed convection flow of an electrically conducting viscous fluid past an infinite vertical porous plate have been considered. A uniform magnetic field of strength  $\mathbf{H}$  is applied to the plate to be acting along the  $y$ -axis, which is electrically non-conducting. We assumed that the magnetic Reynolds number of the flow be large enough so that the induced magnetic field is not negligible. The induced magnetic field is of the form  $\mathbf{H} = (H_x, H_0, 0)$ . The equation of the conservation of electric charge is  $\nabla \cdot \mathbf{J} = 0$ , where  $\mathbf{J} = (J_x, J_y, J_z)$ , the direction of propagation is considered only along the  $y$ -axis and does not have any variation along the  $y$ -axis and the derivative of  $\mathbf{J}$  with respect to  $y$  namely  $\frac{\partial J_y}{\partial y} = 0$ , resulting in  $J_y = \text{constant}$ . Since the plate is electrically non-conducting, this constant is zero and hence  $J_y = 0$  everywhere in the flow. Within the framework of the above stated assumptions with reference to the generalized equations as described in Chapter III, Case-I, the physical variables are functions of  $y$  and  $t$  only. Thus the problem under consideration is treated as one-dimensional problem and under the assumptions of usual Boussinesq's and boundary-layer approximations can be put in the following system of coupled non-linear partial differential equations:

$$\frac{\partial v}{\partial y} = 0 \quad (4.1)$$

$$\frac{\partial u}{\partial t} + v \frac{\partial u}{\partial y} = g\beta(T - T_\infty) + g\beta^*(C - C_\infty) + v \frac{\partial^2 u}{\partial y^2} + \frac{\mu_e}{\rho} H_0 \frac{\partial H_x}{\partial y} \quad (4.2)$$

$$\frac{\partial H_x}{\partial t} + v \frac{\partial H_x}{\partial y} = H_0 \frac{\partial u}{\partial y} + \frac{1}{\mu_e \sigma'} \frac{\partial^2 H_x}{\partial y^2} \quad (4.3)$$

$$\frac{\partial T}{\partial t} + v \frac{\partial T}{\partial y} = \frac{k}{\rho c_p} \frac{\partial^2 T}{\partial y^2} + \frac{\mu}{\rho c_p} \left( \frac{\partial u}{\partial y} \right)^2 + \frac{1}{\rho c_p \sigma'} \left( \frac{\partial H_x}{\partial y} \right)^2 + \frac{D_m K_T}{c_s c_p} \frac{\partial^2 C}{\partial y^2} \quad (4.4)$$

$$\frac{\partial C}{\partial t} + v \frac{\partial C}{\partial y} = D_m \frac{\partial^2 C}{\partial y^2} + \frac{D_m K_T}{T_m} \frac{\partial^2 T}{\partial y^2} \quad (4.5)$$

The initial and boundary conditions for the problem are as follows:

$$t \leq 0, u = 0, T \rightarrow T_\infty, C \rightarrow C_\infty, H_x = 0 \text{ for all } y \quad (4.6)$$

$$\left. \begin{aligned} t > 0, u = U_0(t), v = V_0(t), \frac{\partial T}{\partial y} = -\frac{q}{k}, \frac{\partial C}{\partial y} = -\frac{m}{D_m}, H_x = H_0 \text{ at } y = 0 \\ t > 0, u = 0, T \rightarrow T_\infty, C \rightarrow C_\infty, H_x \rightarrow 0 \text{ as } y \rightarrow \infty \end{aligned} \right\} \quad (4.7)$$

where  $u$  and  $v$  are the velocity components in  $x$ - and  $y$ - direction respectively,  $H_0$  is the applied constant magnetic field,  $H_x$  is the induced magnetic field,  $\mu_e$  is the magnetic permeability,  $q$  is the constant heat flux per unit area,  $m$  is the constant mass flux per unit area,  $\nu$  is the kinematic viscosity,  $g$  is the acceleration due to the gravity,  $\rho$  is the density,  $\beta$  is the coefficient of volume expansion,  $\beta^*$  is the volumetric coefficient expansion with concentration.  $T$  and  $T_\infty$  are the temperature of the fluid inside the thermal boundary layer and the fluid temperature in the free stream respectively, while  $C$  and  $C_\infty$  are the corresponding concentration,  $C_p$  is the specific heat at constant pressure,  $c_s$  is the concentration susceptibility,  $T_m$  is the mean fluid temperature,  $k$  is the thermal conductivity,  $K_T$  is the thermal diffusion ratio,  $D_m$  is the coefficient of mass diffusion and other symbols have their usual meaning.

## 4.2 Mathematical Formulation

Since the solutions of the governing equations (4.1) – (4.5) under the initial and boundary conditions given by (4.6) and (4.7) will be based on the implicit Finite Difference Method, it is required to transfer the equations in suitable form. For this purpose we will again introduce the following non-dimensional quantities:

$$Y = \frac{yU_0}{\nu}, U = \frac{u}{U_0}, V = \frac{v}{U_0}, \tau = \frac{tU_0^2}{\nu}, \bar{T} = \frac{T - T_\infty}{T_w - T_\infty}, \bar{C} = \frac{C - C_\infty}{C_w - C_\infty}, \bar{H}_x = \sqrt{\frac{\mu_e}{\rho}} \frac{H_x}{U_0}$$

From the above dimensionless variables, we have

$$u = U_0 U, \quad v = U_0 V, \quad y = \frac{\nu Y}{U_0}, \quad t = \frac{\nu \tau}{U_0^2}, \quad T = T_\infty + (T_w - T_\infty) \bar{T}, \quad C = C_\infty + (C_w - C_\infty) \bar{C}, \quad \text{and}$$

$$H_x = \sqrt{\frac{\rho}{\mu_e}} U_0 \bar{H}_x \quad (4.8)$$

Using these relations, we obtain the following derivatives

$$\begin{aligned}\frac{\partial u}{\partial t} &= \frac{U_0^3}{\nu} \frac{\partial U}{\partial \tau}, \quad \frac{\partial u}{\partial y} = \frac{U_0^2}{\nu} \frac{\partial U}{\partial Y}, \quad \frac{\partial^2 u}{\partial y^2} = \frac{U_0^3}{\nu^2} \frac{\partial^2 U}{\partial Y^2}, \quad \frac{\partial v}{\partial y} = U_0 \frac{\partial V}{\partial Y}, \quad \frac{\partial H_x}{\partial t} = \sqrt{\frac{\rho}{\mu_e}} \frac{U_0^3}{\nu} \frac{\partial \bar{H}_x}{\partial \tau}, \\ \frac{\partial H_x}{\partial y} &= \sqrt{\frac{\rho}{\mu_e}} \frac{U_0^2}{\nu} \frac{\partial \bar{H}_x}{\partial Y}, \quad \frac{\partial C}{\partial t} = \frac{U_0^2 (C_w - C_\infty)}{\nu} \frac{\partial \bar{C}}{\partial \tau}, \quad \frac{\partial C}{\partial y} = \frac{U_0^2 (C_w - C_\infty)}{\nu} \frac{\partial \bar{C}}{\partial Y}, \\ \frac{\partial^2 C}{\partial y^2} &= \frac{U_0^2 (C_w - C_\infty)}{\nu^2} \frac{\partial^2 \bar{C}}{\partial Y^2}, \quad \frac{\partial T}{\partial t} = \frac{U_0^2 (T_w - T_\infty)}{\nu} \frac{\partial \bar{T}}{\partial \tau}, \quad \frac{\partial T}{\partial y} = \frac{U_0^2 (T_w - T_\infty)}{\nu} \frac{\partial \bar{T}}{\partial Y} \quad \text{and} \\ \frac{\partial^2 T}{\partial y^2} &= \frac{U_0^2 (T_w - T_\infty)}{\nu^2} \frac{\partial^2 \bar{T}}{\partial Y^2}.\end{aligned}$$

Now substitute the values of the above derivatives into the equations (4.1) – (4.5) together with the initial conditions (4.6) and the boundary conditions (4.7), the following nonlinear coupled partial differential equations in terms of dimensionless variables are obtained:

$$\frac{\partial V}{\partial Y} = 0 \tag{4.9}$$

$$\begin{aligned}\frac{U_0^3}{\nu} \frac{\partial U}{\partial \tau} + \frac{U_0^3 V}{\nu} \frac{\partial U}{\partial Y} &= g\beta(T_w - T_\infty)\bar{T} + g\beta^*(C_w - C_\infty)\bar{C} + \frac{U_0^3}{\nu} \frac{\partial^2 U}{\partial Y^2} + \sqrt{\frac{\mu_e}{\rho}} \frac{U_0^2 H_0}{\nu} \frac{\partial \bar{H}_x}{\partial Y} \\ \text{or, } \frac{\partial U}{\partial \tau} + V \frac{\partial U}{\partial Y} &= \frac{g\beta\nu(T_w - T_\infty)\bar{T}}{U_0^3} + \frac{g\beta^*\nu(C_w - C_\infty)\bar{C}}{U_0^3} + \frac{\partial^2 U}{\partial Y^2} + \sqrt{\frac{\mu_e}{\rho}} \frac{H_0}{U_0} \frac{\partial \bar{H}_x}{\partial Y} \\ \text{or, } \frac{\partial U}{\partial \tau} + V \frac{\partial U}{\partial Y} &= G_r \bar{T} + G_m \bar{C} + \frac{\partial^2 U}{\partial Y^2} + M \frac{\partial \bar{H}_x}{\partial Y}\end{aligned} \tag{4.10}$$

$$\begin{aligned}\sqrt{\frac{\rho}{\mu_e}} \frac{U_0^3}{\nu} \frac{\partial \bar{H}_x}{\partial \tau} + \sqrt{\frac{\rho}{\mu_e}} \frac{U_0^3}{\nu} V \frac{\partial \bar{H}_x}{\partial Y} &= \frac{U_0^2 H_0}{\nu} \frac{\partial U}{\partial Y} + \frac{1}{\mu_e \sigma'} \sqrt{\frac{\rho}{\mu_e}} \frac{U_0^3}{\nu^2} \frac{\partial^2 \bar{H}_x}{\partial Y^2} \\ \text{or, } \frac{\partial \bar{H}_x}{\partial \tau} + V \frac{\partial \bar{H}_x}{\partial Y} &= \sqrt{\frac{\mu_e}{\rho}} \frac{H_0}{U_0} \frac{\partial U}{\partial Y} + \frac{1}{\mu_e \sigma' \nu} \frac{\partial^2 \bar{H}_x}{\partial Y^2} \\ \text{or, } \frac{\partial \bar{H}_x}{\partial \tau} + V \frac{\partial \bar{H}_x}{\partial Y} &= M \frac{\partial U}{\partial Y} + \frac{1}{P_m} \frac{\partial^2 \bar{H}_x}{\partial Y^2}\end{aligned} \tag{4.11}$$

$$\begin{aligned}
\frac{U_0^2(T_w - T_\infty)}{\nu} \frac{\partial \bar{T}}{\partial \tau} + \frac{U_0^2(T_w - T_\infty)}{\nu} V \frac{\partial \bar{T}}{\partial Y} &= \frac{k}{\rho C_p} \frac{U_0^2(T_w - T_\infty)}{\nu^2} \frac{\partial^2 \bar{T}}{\partial Y^2} + \frac{U_0^4}{C_p \nu} \left( \frac{\partial U}{\partial Y} \right)^2 \\
&+ \frac{1}{\sigma' \mu_e C_p} \frac{U_0^4}{\nu^2} \left( \frac{\partial \bar{H}_x}{\partial Y} \right)^2 + \frac{D_m K_T}{C_s C_p} \frac{U_0^2(C_w - C_\infty)}{\nu^2} \frac{\partial^2 \bar{C}}{\partial Y^2} \\
\frac{\partial \bar{T}}{\partial \tau} + V \frac{\partial \bar{T}}{\partial Y} &= \frac{k}{\nu \rho C_p} \frac{\partial^2 \bar{T}}{\partial Y^2} + \frac{U_0^2}{C_p(T_w - T_\infty)} \left( \frac{\partial U}{\partial Y} \right)^2 + \frac{1}{\sigma' \rho C_p \mu_e} \frac{U_0^2}{\nu(T_w - T_\infty)} \left( \frac{\partial \bar{H}_x}{\partial Y} \right)^2 \\
&+ \frac{D_m K_T}{C_s C_p} \frac{U_0^2(C_w - C_\infty)}{\nu(T_w - T_\infty)} \frac{\partial^2 \bar{C}}{\partial Y^2} \\
\text{or, } \frac{\partial \bar{T}}{\partial \tau} + V \frac{\partial \bar{T}}{\partial Y} &= \frac{1}{\text{Pr}} \frac{\partial^2 \bar{T}}{\partial Y^2} + E_c \left( \frac{\partial U}{\partial Y} \right)^2 + \frac{E_c}{P_m} \left( \frac{\partial \bar{H}_x}{\partial Y} \right)^2 + D_f \frac{\partial^2 \bar{C}}{\partial Y^2} \tag{4.12} \\
\frac{U_0^2(C_w - C_\infty)}{\nu} \frac{\partial \bar{C}}{\partial \tau} + \frac{U_0^2(C_w - C_\infty)}{\nu} V \frac{\partial \bar{C}}{\partial Y} &= \frac{D_m U_0^2(C_w - C_\infty)}{\nu^2} \frac{\partial^2 \bar{C}}{\partial Y^2} + \frac{D_m K_T}{T_m} \frac{U_0^2(T_w - T_\infty)}{\nu^2} \frac{\partial^2 \bar{T}}{\partial Y^2} \\
\text{or, } \frac{\partial \bar{C}}{\partial \tau} + V \frac{\partial \bar{C}}{\partial Y} &= \frac{D_m}{\nu} \frac{\partial^2 \bar{C}}{\partial Y^2} + \frac{U_0^2(T_w - T_\infty)}{\nu(C_w - C_\infty)} \frac{\partial^2 \bar{T}}{\partial Y^2} \\
\text{or, } \frac{\partial \bar{C}}{\partial \tau} + V \frac{\partial \bar{C}}{\partial Y} &= \frac{1}{S_c} \frac{\partial^2 \bar{C}}{\partial Y^2} + S_r \frac{\partial^2 \bar{T}}{\partial Y^2} \tag{4.13}
\end{aligned}$$

where  $\tau$  represents the dimensionless time,  $Y$  is the dimensionless Cartesian coordinate,  $U$  is the dimensionless primary velocity,  $\bar{T}$  is the dimensionless temperature,  $\bar{C}$  is the dimensionless concentration,

$$Gr = \frac{g\beta\nu(T_w - T_\infty)}{U_0^3} \text{ is the Grashof Number,}$$

$$Gm = \frac{g\beta^* \nu(C_w - C_\infty)}{U_0^3} \text{ is the Modified Grashof Number,}$$

$$M = \sqrt{\frac{\mu_e}{\rho}} \frac{H_0}{U_0} \text{ is the Magnetic Parameter,}$$

$$P_m = \nu \sigma' \mu_e \text{ is the Magnetic Diffusivity Number,}$$

$$Sc = \frac{\nu}{D_m} \text{ is the Schmidt Number,}$$

$$S_r = \frac{D_m k_T}{\nu T_m} \frac{(T_w - T_\infty)}{(C_w - C_\infty)} \text{ is the Soret Number,}$$

$$\text{Pr} = \frac{\nu \rho C_p}{k} \text{ is the Prandtl Number,}$$

$D_f = \frac{Dk_T(C_w - C_\infty)}{\rho c_s c_p (T_w - T_\infty)}$  is the Dufour Number, where  $D = \frac{\rho D_m}{\nu}$  is the chemical molecular diffusivity and

$Ec = \frac{U_0^2}{c_p(T_w - T_\infty)}$  is the Eckert Number.

The corresponding initial and boundary conditions are now transformed as follows:

$\tau \leq 0, U = 0, T \rightarrow T_\infty, C \rightarrow C_\infty, H_x = 0$  for all  $Y$

For  $\tau > 0, U = 1, V = \frac{V_0}{U_0} = -V_w, \frac{\partial \bar{T}}{\partial Y} = -\frac{\nu q}{kU_0(T_w - T_\infty)} = 1, \frac{\partial \bar{C}}{\partial Y} = -\frac{\nu m}{D_m U_0(C_w - C_\infty)} = 1,$

$\bar{H}_x = \sqrt{\frac{\mu_e}{\rho}} \frac{H_0}{U_0 M} = 1$  at  $Y = 0$ , where  $q = -\frac{kU_0(T_w - T_\infty)\nu}{\nu}, m = -\frac{D_m U_0(C_w - C_\infty)}{\nu}$  are the

coefficient of heat transfer and mass flux, respectively and  $V_w = -\frac{V_0}{U_0}$  is the Suction

Parameter.

Also for  $\tau > 0, U = 0, V = 0, \bar{T} = 0, \bar{C} = 0, \bar{H}_x = 0$  as  $Y \rightarrow \infty$ .

Thus after introducing the dimensionless quantities and proper simplification, the obtained nonlinear coupled partial differential equations in terms of dimensionless variables (by omitting the bar on each term in practice) are as follows:

$$\frac{\partial U}{\partial \tau} - V_w \frac{\partial U}{\partial Y} = G_r T + G_m C + \frac{\partial^2 U}{\partial Y^2} + M \frac{\partial H_x}{\partial Y} \quad (4.14)$$

$$\frac{\partial T}{\partial \tau} - V_w \frac{\partial T}{\partial Y} = \frac{1}{Pr} \frac{\partial^2 T}{\partial Y^2} + E_c \left( \frac{\partial U}{\partial Y} \right)^2 + \frac{E_c}{P_m} \left( \frac{\partial H_x}{\partial Y} \right)^2 + D_f \frac{\partial^2 C}{\partial Y^2} \quad (4.15)$$

$$\frac{\partial C}{\partial \tau} - V_w \frac{\partial C}{\partial Y} = \frac{1}{S_c} \frac{\partial^2 C}{\partial Y^2} + S_r \frac{\partial^2 T}{\partial Y^2} \quad (4.16)$$

$$\frac{\partial H_x}{\partial \tau} - V_w \frac{\partial H_x}{\partial Y} = M \frac{\partial U}{\partial Y} + \frac{1}{P_m} \frac{\partial^2 H_x}{\partial Y^2} \quad (4.17)$$

with the corresponding initial and boundary conditions:

$$\tau \leq 0, U = 0, T \rightarrow T_\infty, C \rightarrow C_\infty, H_x = 0 \text{ for all } Y \quad (4.18)$$

$$\tau > 0, U = 1, V = -V_w, \frac{\partial T}{\partial Y} = 1, \frac{\partial C}{\partial Y} = 1, H_x = 1 \text{ at } Y = 0 \quad (4.19)$$

and  $U = 0, V = 0, T = 0, C = 0, H_x = 0$  as  $Y \rightarrow \infty$



### 4.3 The Finite Difference Numerical Solution

In this section, we are now attempted to find the solution of the governing second order nonlinear coupled dimensionless partial differential equations (4.14) – (4.17) subject to the associated initial and boundary conditions (4.18) – (4.19) using the Finite Difference

**Method:** For solving a transient free convection flow problem with mass transfer past a semi-infinite plate, Callahan and Marner (1976) used the explicit Finite Difference Method which is relatively simple and computationally fast but conditionally stable. On the other hand, the same problem was studied by Soundalgekar and Ganesan (1980) by an implicit Finite Difference Method which is unconditionally stable. However, the above two methods produced the same results.

To solve the non-dimensional system by the Finite Difference technique, it is required to find a set finite difference equations corresponding to the given system of partial differential equations (4.14) – (4.17). Thus, to obtain the difference equations, region within the boundary layer is divided by some lines perpendicular to the  $Y$ -axis, where  $Y$ -axis is normal to the plate as shown in Figure 4.3.1. Here it is also assumed that the maximum thickness of boundary layer is  $Y_{\max} = 50$  as corresponds to  $Y \rightarrow \infty$  i.e.  $Y$  varies from 0 to 50 and the number of grids in  $Y$  directions is  $N = 1000$  and hence the constant mesh size along  $Y$  axis becomes  $\Delta Y = 0.05 (0 \leq Y \leq 50)$  with a smaller time-step  $\Delta \tau = 0.005$ .

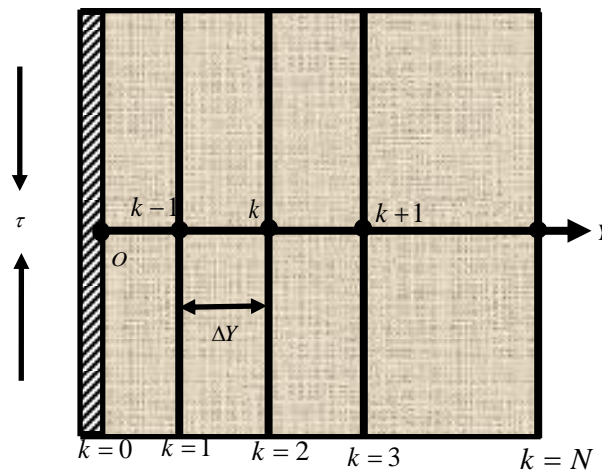


**Figure 4.3.1:** Implicit finite difference system grid.

Let  $U^n$ ,  $C^n$ ,  $H_x^n$  and  $T^n$  denote the values of  $U$ ,  $C$ ,  $H_x$  and  $T$  at the end of  $n$ th time-step respectively. Using the implicit finite difference approximation, the following relations are obtained as:

$$\begin{aligned} \left(\frac{\partial U}{\partial \tau}\right)_k &= \frac{U_k^{n+1} - U_k^n}{\Delta \tau}, & \left(\frac{\partial U}{\partial Y}\right)_k &= \frac{U_{k+1}^n - U_k^n}{\Delta Y}, & \left(\frac{\partial^2 U}{\partial Y^2}\right)_k &= \frac{U_{k+1}^n - 2U_k^n + U_{k-1}^n}{(\Delta Y)^2}, \\ \left(\frac{\partial C}{\partial \tau}\right)_k &= \frac{C_k^{n+1} - C_k^n}{\Delta \tau}, & \left(\frac{\partial H_x}{\partial \tau}\right)_k &= \frac{H_k^{n+1} - H_k^n}{\Delta \tau}, & \left(\frac{\partial H_x}{\partial Y}\right)_k &= \frac{H_{k+1}^n - H_k^n}{\Delta Y}, \\ \left(\frac{\partial^2 H_x}{\partial Y^2}\right)_k &= \frac{H_{k+1}^n - 2H_k^n + H_{k-1}^n}{(\Delta Y)^2}, & \left(\frac{\partial C}{\partial Y}\right)_k &= \frac{C_{k+1}^n - C_k^n}{\Delta Y}, & \left(\frac{\partial^2 C}{\partial Y^2}\right)_k &= \frac{C_{k+1}^n - 2C_k^n + C_{k-1}^n}{(\Delta Y)^2}, \\ \left(\frac{\partial T}{\partial \tau}\right)_k &= \frac{T_k^{n+1} - T_k^n}{\Delta \tau}, & \left(\frac{\partial T}{\partial Y}\right)_k &= \frac{T_{k+1}^n - T_k^n}{\Delta Y} \text{ and } \left(\frac{\partial^2 T}{\partial Y^2}\right)_k &= \frac{T_{k+1}^n - 2T_k^n + T_{k-1}^n}{(\Delta Y)^2}. \end{aligned}$$

Substituting above values into equations (4.14) – (4.17), we obtain

$$\frac{U_k^{n+1} - U_k^n}{\Delta \tau} - V_w \frac{U_{k+1}^n - U_k^n}{\Delta Y} = \frac{U_{k+1}^n - 2U_k^n + U_{k-1}^n}{(\Delta Y)^2} + M \frac{H_{k+1}^n - H_k^n}{\Delta Y} + G_r T_k^n + G_m C \quad (4.21)$$

$$\begin{aligned} \frac{T_k^{n+1} - T_k^n}{\Delta \tau} - V_w \frac{T_{k+1}^n - T_k^n}{\Delta Y} &= \frac{1}{Pr} \frac{T_{k+1}^n - 2T_k^n + T_{k-1}^n}{(\Delta Y)^2} + E_c \left( \frac{U_{k+1}^n - U_k^n}{\Delta Y} \right)^2 + \frac{E_c}{P_m} \left( \frac{H_{k+1}^n - H_k^n}{\Delta Y} \right)^2 \\ &+ D_f \frac{C_{k+1}^n - 2C_k^n + C_{k-1}^n}{(\Delta Y)^2} \end{aligned} \quad (4.22)$$

$$\frac{C_k^{n+1} - C_k^n}{\Delta \tau} - V_w \frac{C_{k+1}^n - C_k^n}{\Delta Y} = \frac{1}{Sc} \frac{C_{k+1}^n - 2C_k^n + C_{k-1}^n}{(\Delta Y)^2} + S_r \frac{T_{k+1}^n - 2T_k^n + T_{k-1}^n}{(\Delta Y)^2} \quad (4.21)$$

$$\frac{H_k^{n+1} - H_k^n}{\Delta \tau} - V_w \frac{H_{k+1}^n - H_k^n}{\Delta Y} = \frac{1}{P_m} \frac{H_{k+1}^n - 2H_k^n + H_{k-1}^n}{(\Delta Y)^2} + M \frac{U_{k+1}^n - U_k^n}{\Delta Y} \quad (4.22)$$

$$\text{Corresponding to the initial conditions: } U_0^0 = 0, T_0^0 = 0, C_0^0 = 0, H_0^0 = 0 \quad (4.23)$$

and the corresponding boundary conditions:

$$U_0^n = 1, T_0^n = T_1^n \Delta Y, H_0^n = 1, C_0^n = C_1^n \Delta Y \quad (4.24)$$

$$U_L^n = 0, T_L^n = 0, C_L^n = 0, H_L^n = 0 \text{ where } L \rightarrow \infty$$

Here the subscript  $k$  designates the grid points with  $Y$  coordinate and the superscript  $n$  represents a value of time,  $\tau = n\Delta\tau$ , where  $n = 0, 1, 2, \dots$ . The velocity ( $U$ ), temperature

( $T$ ), concentration ( $C$ ) distributions and the induced magnetic field at all interior nodal points may be computed by successive applications of the above finite difference equations. The obtained values are shown graphically and in tabular form in CHAPTER V.

## CHAPTER V

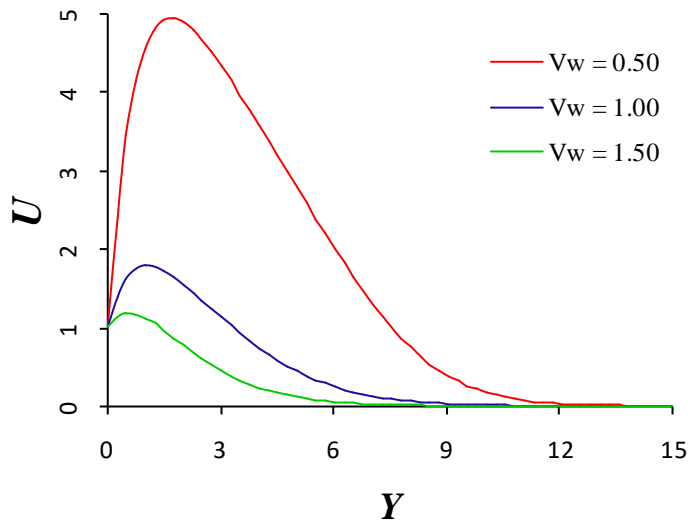
### Numerical Solution and Results Discussions

The solution of the system of coupled nonlinear partial differential equations (4.14) – (4.17) and the corresponding initial and boundary conditions (4.18) and (4.19), respectively are obtained by using implicit Finite Difference numerical technique. In order to get insight into the physical phenomena of the problem, the numerical values regarding the velocity, temperature, induced magnetic field and concentration profiles have been carried out for different selected values of the established dimensionless parameters like the suction parameter ( $V_w$ ), Dufour number ( $D_f$ ), magnetic parameter ( $M$ ), Soret number ( $S_r$ ), Grashof number ( $G_r$ ), modified Grashof number ( $G_m$ ) for mass transfer, the Prandtl number ( $Pr$ ), Eckert number ( $E_c$ ) magnetic diffusivity ( $P_m$ ) and Schmidt number ( $S_c$ ).

To observe the effect of one parameter on field variables, the values of all other parameters are chosen to be fixed. The fixed values are taken to be as  $V_w = 0.5$ ,  $D_f = 1.0$ ,  $M = 1.0$ ,  $S_r = 2.0$ ,  $G_r = 5.0$ ,  $G_m = 2.0$ ,  $Pr = 0.71$ ,  $E_c = 0.5$ ,  $P_m = 1.0$  and  $S_c = 0.6$  respectively. The values of Grashof number  $G_r$  is taken to be large ( $G_r = 5.0$ ), since this value corresponds to a cooling problem that is generally encountered in nuclear engineering in connection with the cooling of reactors. Since the two most important fluids are atmospheric air and water, the values of the Prandtl number ( $Pr$ ) are limited to 0.71 corresponds to air (at 20<sup>o</sup>C), 1.0 corresponds to electrolyte solution like saline water and 7.0 corresponds to water (at 20<sup>o</sup>C) throughout the numerical investigation.

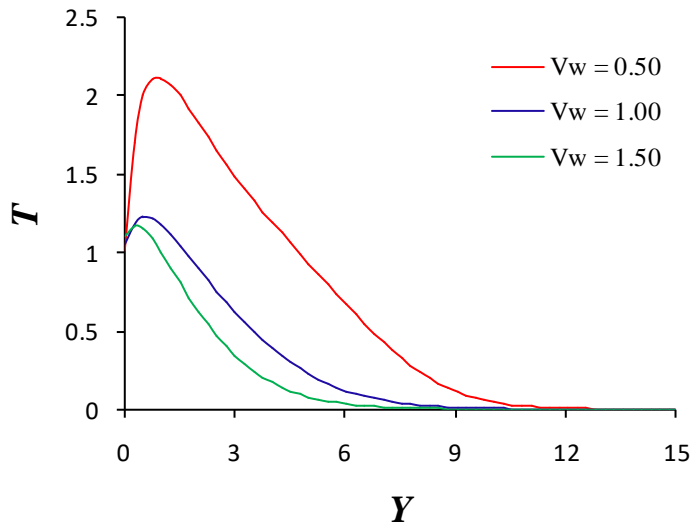
The values of  $S_c$  are considered as 0.22, 0.30, 0.6 and 0.78 which represent specific condition of the flow; in particular, 0.22 corresponds to hydrogen, 0.30 corresponds to helium, 0.60 corresponds to water vapor that represents a diffusivity chemical species of most common interest in air while 0.78 represents ammonia at 25<sup>o</sup>C and 1 atmospheric pressure. The other values of parameters  $V_w$ ,  $D_f$ ,  $M$ ,  $S_r$ ,  $G_r$ ,  $G_m$ ,  $E_c$ , and  $P_m$  are however chosen arbitrarily. With the above mentioned parameters the velocity and temperature profiles, the variation of mass concentration and induced magnetic field are presented in the following Figures (Figures 5.1 – 5.40).

Figures 5.1 – 5.4 show the effect of suction parameter ( $V_w$ ) on the velocity and temperature profiles, the mass concentration and the induced magnetic field respectively. From Figures 5.1 – 5.3, we observed that an increase in the suction parameter lead to decrease the velocity, temperature and concentration profiles. The usual stabilizing effect of the suction parameter on the boundary layer growth is also conformed from these figures. We see that the effect of suction is to reduce the velocity profiles. This is because of sucking decelerated fluid particles through the porous wall reduce growth of the fluid boundary layer as well as thermal and concentration boundary layers. From these Figures, it is clear that the dimensionless temperature and concentration decrease due to fluid suction.

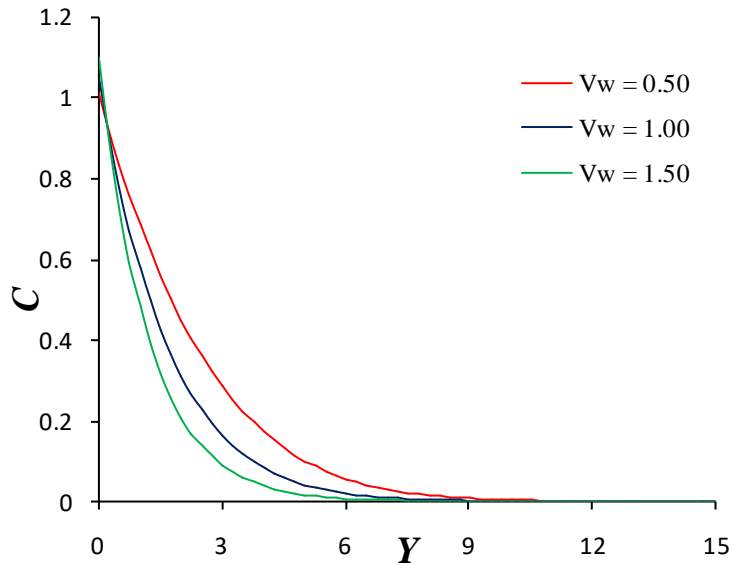


**Figure 5.1:** Velocity profiles for different values of  $V_w$  (for  $D_f = 2.0$ ,  $M = 1.0$ ,  $S_r = 2.0$ ,  $G_r = 5.0$ ,  $G_m = 2.0$ ,  $Pr = 0.71$ ,  $P_m = 1.0$ ,  $E_c = 0.5$  and  $S_c = 0.6$ ).

It is observed from Figure 5.4 that the induced magnetic field decrease with increasing  $V_w$  within a certain interval very close to the plate ( $0 < Y < 1.2$  (approx.)) whereas after that interval ( $Y > 1.2$  (approx.)) they become negative and asymptotically tends to zero away from the plate surface. In this negative region, the induced magnetic fields increase with the increase of  $V_w$ .

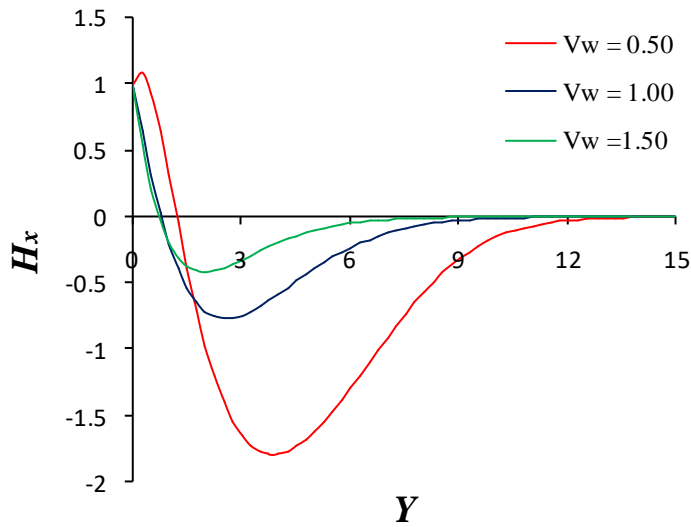


**Figure 5.2:** Temperature profiles for different values of  $V_w$  (for  $D_f = 2.0$ ,  $M = 1.0$ ,  $S_r = 2.0$ ,  $G_r = 5.0$ ,  $G_m = 2.0$ ,  $Pr = 0.71$ ,  $P_m = 1.0$ ,  $E_c = 0.5$  and  $S_c = 0.6$ ).

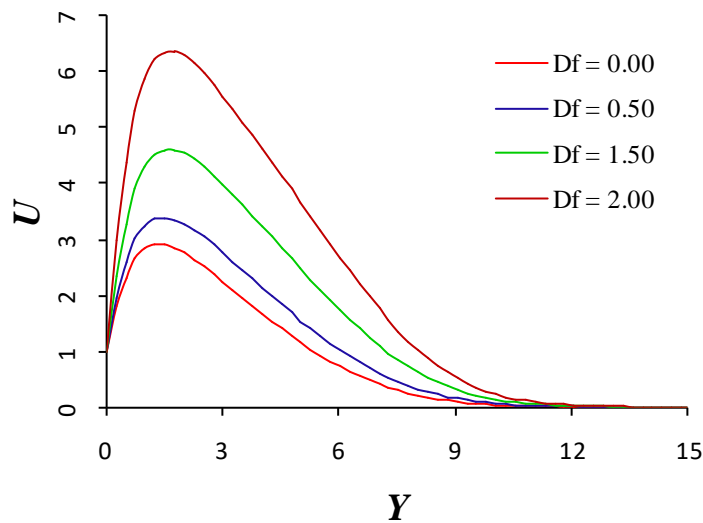


**Figure 5.3:** Variation of concentration for different values of  $V_w$  (for  $D_f = 2.0$ ,  $M = 1.0$ ,  $S_r = 2.0$ ,  $G_r = 5.0$ ,  $G_m = 2.0$ ,  $Pr = 0.71$ ,  $P_m = 1.0$ ,  $E_c = 0.5$  and  $S_c = 0.6$ ).

Figures 5.5 – 5.8 depict the influence of the Dufour parameter ( $D_f$ ) on the dimensionless velocity, temperature and concentration distributions and the induced magnetic fields. It can be clearly seen from Figures 5.5 that as the Dufour effects increase, the velocity profiles increases.



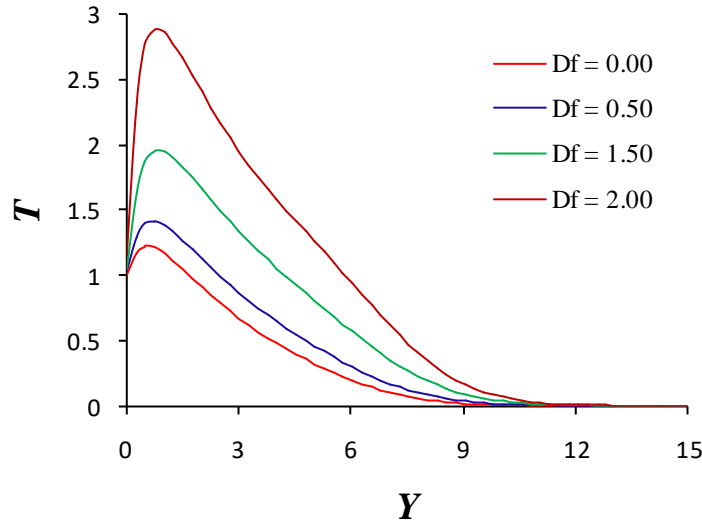
**Figure 5.4:** Variation of induced magnetic field for different values of  $V_w$  (for  $D_f = 2.0$ ,  $M = 1.0$ ,  $S_r = 2.0$ ,  $G_r = 5.0$ ,  $G_m = 2.0$ ,  $Pr = 0.71$ ,  $P_m = 1.0$ ,  $E_c = 0.5$  and  $S_c = 0.6$ ).



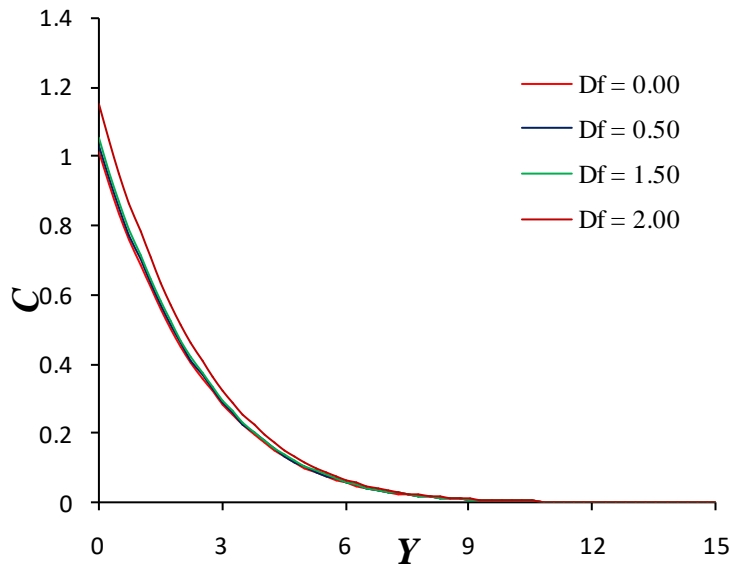
**Figure 5.5:** Velocity profiles for different values of  $D_f$  (for  $V_w = 0.5$ ,  $M = 1.0$ ,  $S_r = 2.0$ ,  $G_r = 5.0$ ,  $G_m = 2.0$ ,  $Pr = 0.71$ ,  $P_m = 1.0$ ,  $E_c = 0.5$  and  $S_c = 0.6$ ).

It is observed in Figures 5.6 that diffusion-thermo effects greatly affect the fluid temperature. As the values of the Dufour parameter increase, the fluid temperature also

increases. We also observe in Figures 5.7 that increasing values of the Dufour parameter ( $D_f$ ) leads to increase the concentration of the fluid flow. It is also observed from Figure 5.8 that, close to the plate surface, the induced magnetic fields increase with the increase of Dufour parameter and a reverse effect is observed adjacent to the plate.

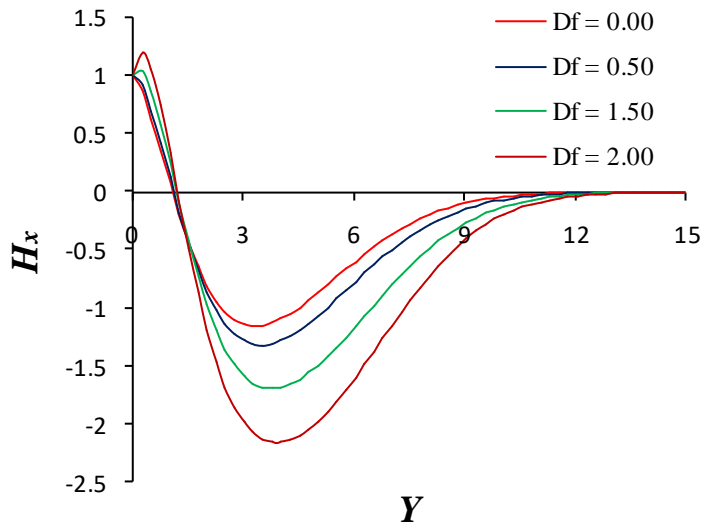


**Figure 5.6:** Temperature profiles for different values of  $D_f$  (for  $V_w = 0.5$ ,  $M = 1.0$ ,  $S_r = 2.0$ ,  $G_r = 5.0$ ,  $G_m = 2.0$ ,  $Pr = 0.71$ ,  $P_m = 1.0$ ,  $E_c = 0.5$  and  $S_c = 0.6$ ).

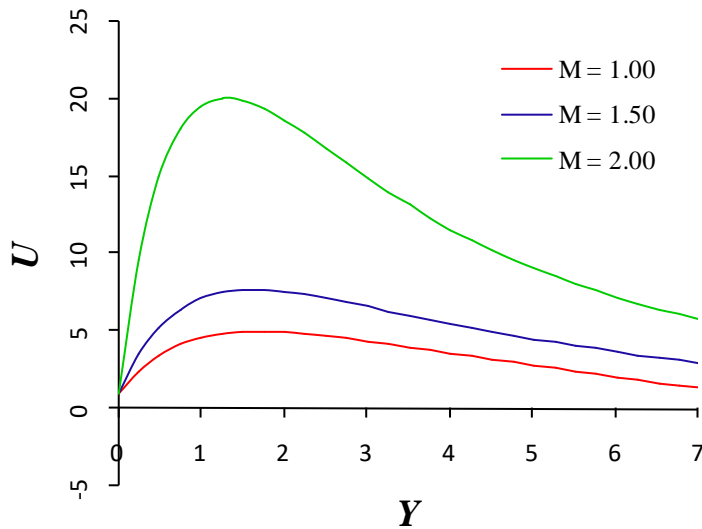


**Figure 5.7:** Variation of concentration for different values of  $D_f$  (for  $V_w = 0.5$ ,  $M = 1.0$ ,  $S_r = 2.0$ ,  $G_r = 5.0$ ,  $G_m = 2.0$ ,  $Pr = 0.71$ ,  $P_m = 1.0$ ,  $E_c = 0.5$ , and  $S_c = 0.6$ ).



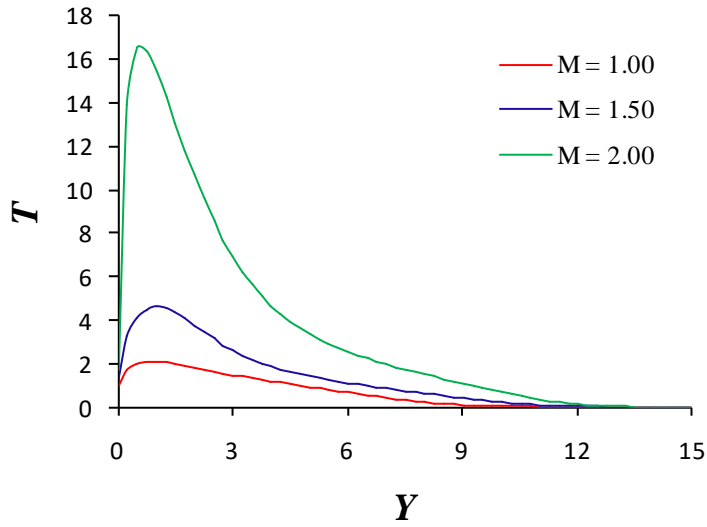


**Figure 5.8:** Variation of induced magnetic field for different values of  $D_f$  (for  $V_w = 0.5$ ,  $M = 1.0$ ,  $S_r = 2.0$ ,  $G_r = 5.0$ ,  $G_m = 2.0$ ,  $Pr = 0.71$ ,  $P_m = 1.0$ ,  $E_c = 0.5$  and  $S_c = 0.6$ ).

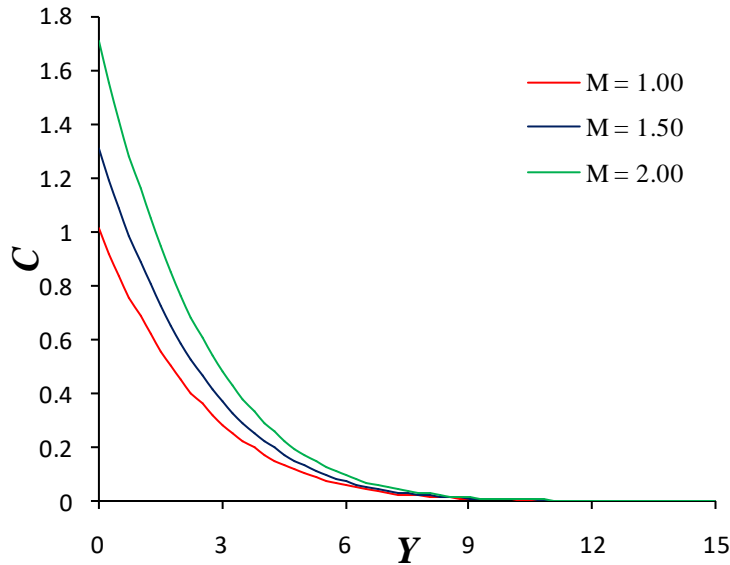


**Figure 5.9:** Velocity profiles for different values of  $M$  (for  $V_w = 0.5$ ,  $D_f = 1.0$ ,  $S_r = 2.0$ ,  $G_r = 5.0$ ,  $G_m = 2.0$ ,  $Pr = 0.71$ ,  $P_m = 1.0$ ,  $E_c = 0.5$  and  $S_c = 0.6$ ).

Figure 5.9 – 5.12 show the effect of magnetic parameter ( $M$ ) on the velocity and temperature fields, mass concentration and induced magnetic field. As  $M$  increases, velocity, temperature and concentration observed to increase in Figure 5.9 – 5.11.

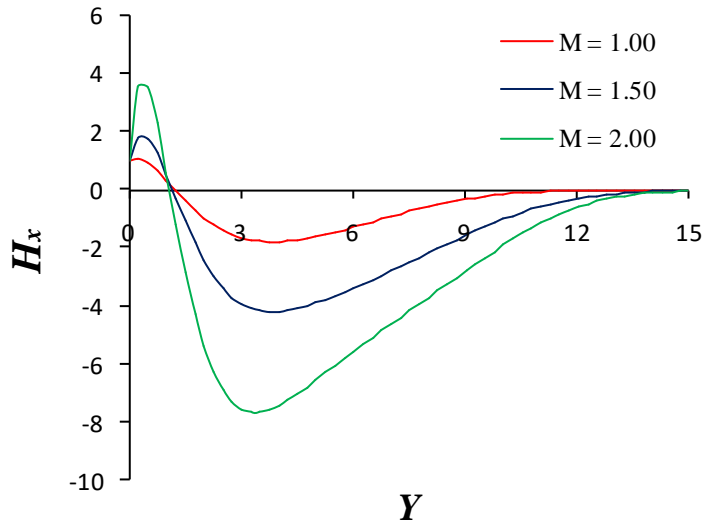


**Figure 5.10:** Temperature profiles for different values of  $M$  (for  $V_w = 0.5$ ,  $D_f = 1.0$ ,  $S_r = 2.0$ ,  $G_r = 5.0$ ,  $G_m = 2.0$ ,  $Pr = 0.71$ ,  $P_m = 1.0$ ,  $E_c = 0.5$  and  $S_c = 0.6$ ).



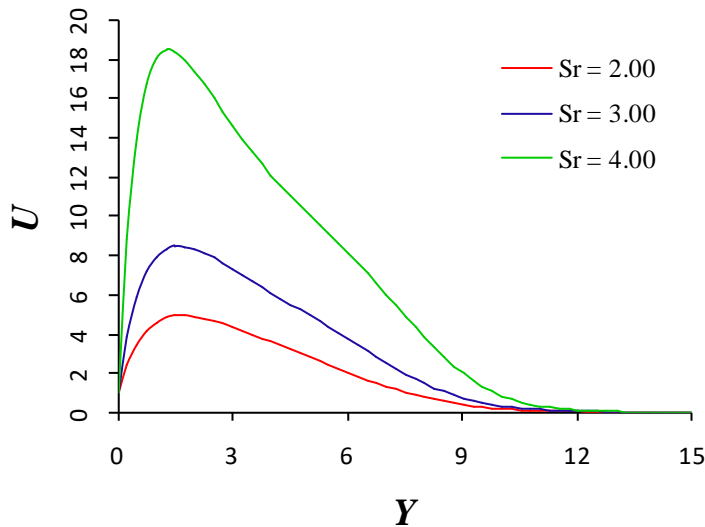
**Figure 5.11:** Variation of concentration for different values of  $M$  (for  $V_w = 0.5$ ,  $D_f = 1.0$ ,  $S_r = 2.0$ ,  $G_r = 5.0$ ,  $G_m = 2.0$ ,  $Pr = 0.71$ ,  $P_m = 1.0$ ,  $E_c = 0.5$  and  $S_c = 0.6$ ).

Figure 5.12 shows that, close to the plate surface, the induced magnetic fields increase with the increase of  $M$  whereas the reverse effect is observed away from the plate surface before asymptotically approaches to zero.



**Figure 5.12:** Variation of induced magnetic field for different values of  $M$  (for  $V_w = 0.5$ ,  $D_f = 1.0$ ,  $S_r = 2.0$ ,  $G_r = 5.0$ ,  $G_m = 2.0$ ,  $Pr = 0.71$ ,  $P_m = 1.0$ ,  $E_c = 0.5$  and  $S_c = 0.6$ ).

The effects the Soret number ( $S_r$ ) on the dimensionless velocity, temperature and concentration distributions and induced magnetic field are displayed in Figures 5.13 – 5.16. We observe that the velocity, temperature and concentration profiles increase with increasing values of the Soret parameter  $S_r$ . It is observed that increasing the Soret number ( $S_r$ ) increases the boundary layer thickness for the concentration.



**Figure 5.13:** Velocity profiles for different values of  $S_r$  (for  $V_w = 0.5$ ,  $D_f = 1.0$ ,  $M = 1.0$ ,  $G_r = 5.0$ ,  $G_m = 2.0$ ,  $Pr = 0.71$ ,  $P_m = 1.0$ ,  $E_c = 0.5$  and  $S_c = 0.6$ ).

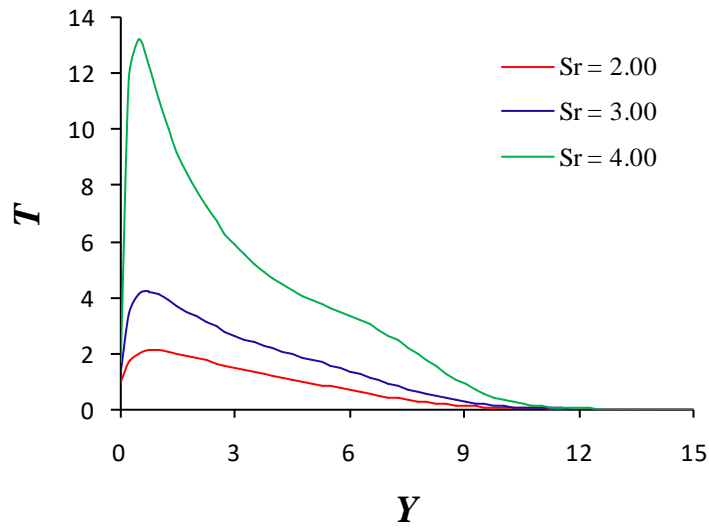


**Figure 5.14:** Temperature profiles for different values of  $S_r$  (for  $V_w = 0.5$ ,  $D_f = 1.0$ ,  $M = 1.0$ ,  $G_r = 5.0$ ,  $G_m = 2.0$ ,  $Pr = 0.71$ ,  $P_m = 1.0$ ,  $E_c = 0.5$  and  $S_c = 0.6$ ).

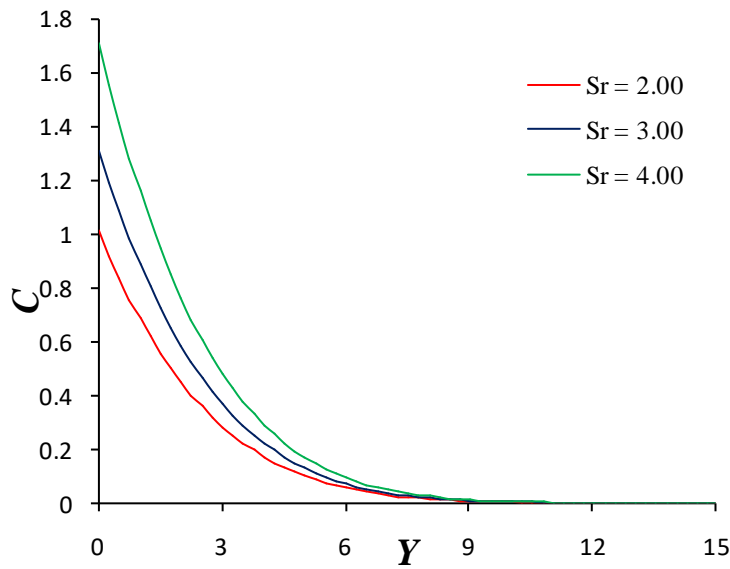


**Figure 5.15:** Variation of concentration for different values of  $S_r$  (for  $V_w = 0.5$ ,  $D_f = 1.0$ ,  $M = 1.0$ ,  $G_r = 5.0$ ,  $G_m = 2.0$ ,  $Pr = 0.71$ ,  $P_m = 1.0$ ,  $E_c = 0.5$  and  $S_c = 0.6$ ).

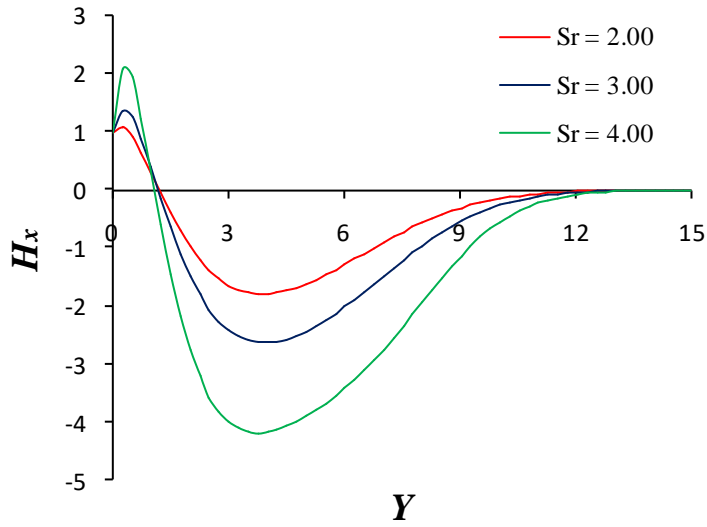


**Figure 5.16:** Variation of induced magnetic field for different values of  $S_r$  (for  $V_w = 0.5$ ,  $D_f = 1.0$ ,  $M = 1.0$ ,  $G_r = 5.0$ ,  $G_m = 2.0$ ,  $Pr = 0.71$ ,  $P_m = 1.0$ ,  $E_c = 0.5$  and  $S_c = 0.6$ ).

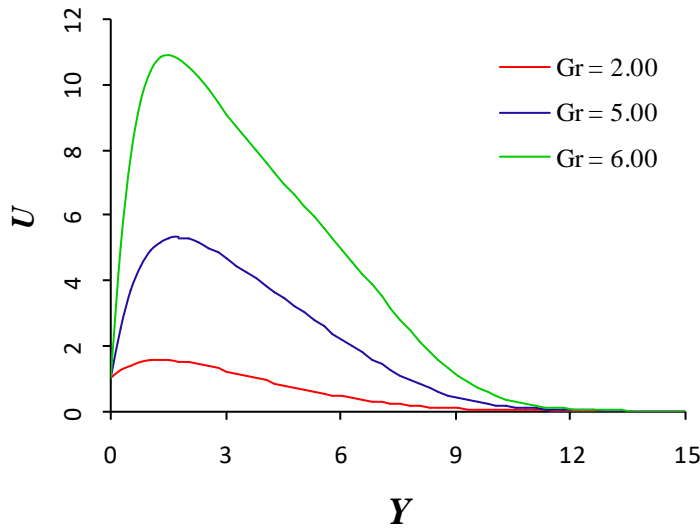


**Figure 5.17:** Velocity profiles for different values of  $G_r$  (for  $V_w = 0.5$ ,  $D_f = 1.0$ ,  $M = 1.0$ ,  $S_r = 2.0$ ,  $G_m = 2.0$ ,  $Pr = 0.71$ ,  $P_m = 1.0$ ,  $E_c = 0.5$  and  $S_c = 0.6$ ).

From Figure 5.16 we see that, close to the plate surface, the induced magnetic fields increase with the increase of  $S_r$  but the reverse effect is observed little bit away from the plate surface as before.

Figures 5.17 – 5.20 depict the influence of Grashof number ( $G_r$ ) on the velocity, temperature, concentration profiles and induced magnetic field. Figures show that both velocity and temperature increase rapidly with the increase of  $G_r$ , but the effect of  $G_r$  on the concentration distribution is found very small. Here concentration profiles increases a little with the increase of  $G_r$ .

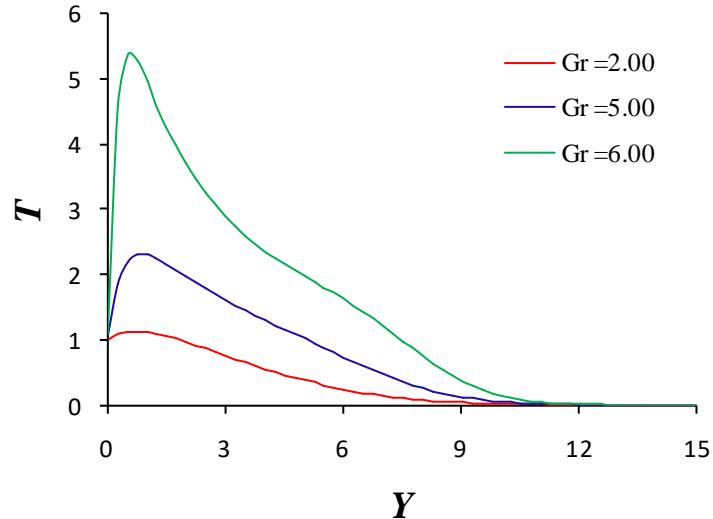


**Figure 5.18:** Temperature profiles for different values of  $G_r$  (for  $V_w = 0.5$ ,  $D_f = 1.0$ ,  $M = 1.0$ ,  $S_r = 2.0$ ,  $G_m = 2.0$ ,  $Pr = 0.71$ ,  $P_m = 1.0$ ,  $E_c = 0.5$  and  $S_c = 0.6$ ).

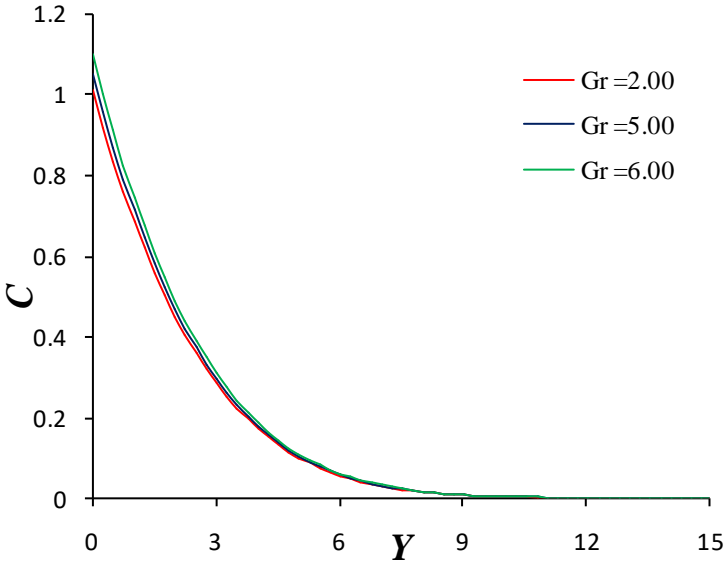


**Figure 5.19:** Variation of concentration for different values of  $G_r$  (for  $V_w = 0.5$ ,  $D_f = 1.0$ ,  $M = 1.0$ ,  $S_r = 2.0$ ,  $G_m = 2.0$ ,  $Pr = 0.71$ ,  $P_m = 1.0$ ,  $E_c = 0.5$  and  $S_c = 0.6$ ).

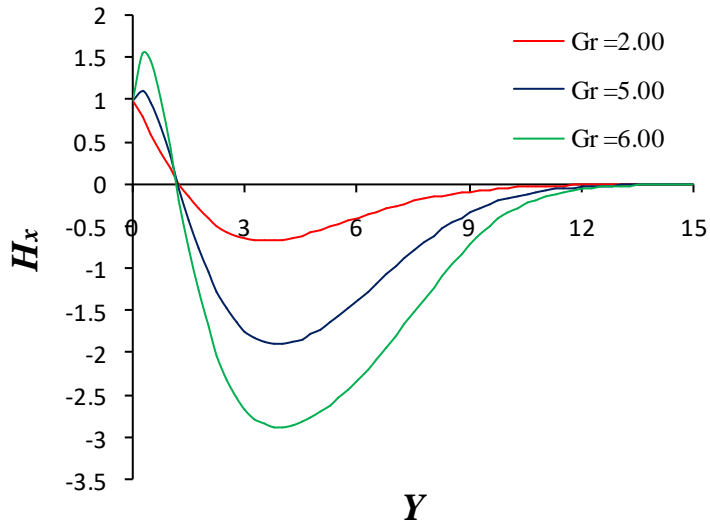


**Figure 5.20:** Variation of induced magnetic field for different values of  $G_r$  (for  $V_w = 0.5$ ,  $D_f = 1.0$ ,  $M = 1.0$ ,  $S_r = 2.0$ ,  $G_m = 2.0$ ,  $Pr = 0.71$ ,  $P_m = 1.0$ ,  $E_c = 0.5$  and  $S_c = 0.6$ ).

Figure 5.20 we see that, close to the plate surface, the induced magnetic fields increase with the increase of  $G_r$  but as before, induced magnetic field decreases with increasing values of  $G_r$  bit away from the plate surface.

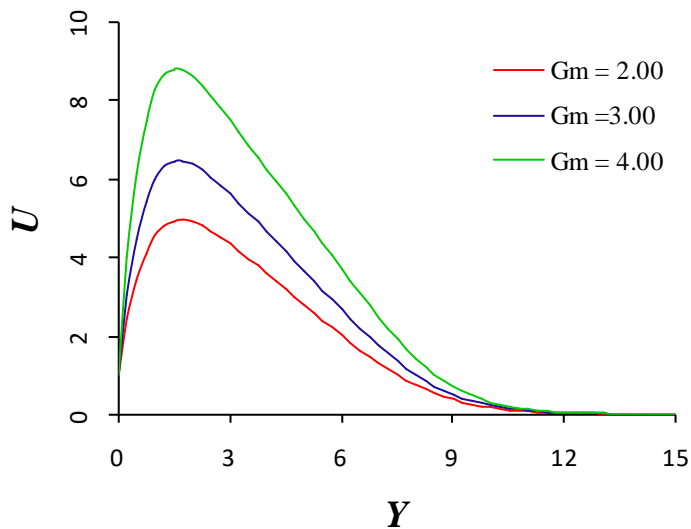


**Figure 5.21:** Velocity profiles for different values of  $G_m$  (for  $V_w = 0.5$ ,  $D_f = 1.0$ ,  $M = 1.0$ ,  $S_r = 2.0$ ,  $G_r = 5.0$ ,  $Pr = 0.71$ ,  $P_m = 1.0$ ,  $E_c = 0.5$  and  $S_c = 0.6$ ).

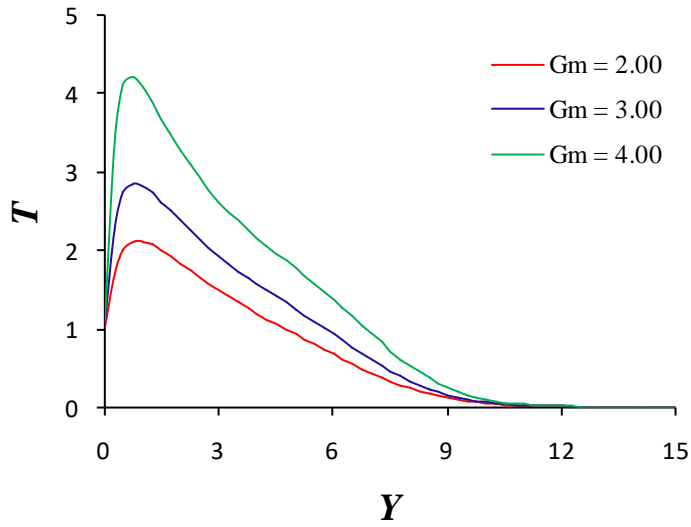


**Figure 5.22:** Temperature profiles for different values of  $G_m$  (for  $V_w = 0.5$ ,  $D_f = 1.0$ ,  $M = 1.0$ ,  $S_r = 2.0$ ,  $G_r = 5.0$ ,  $Pr = 0.71$ ,  $P_m = 1.0$ ,  $E_c = 0.5$  and  $S_c = 0.6$ ).

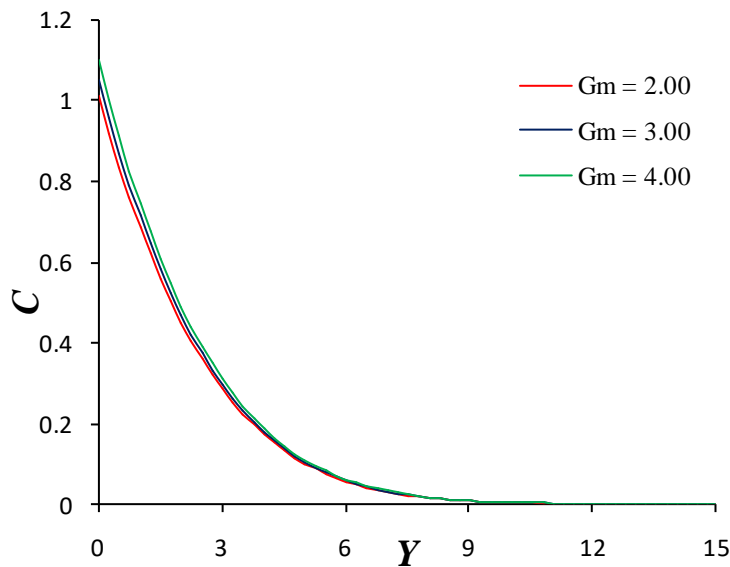


**Figure 5.23:** Variation of concentration for different values of  $G_m$  (for  $V_w = 0.5$ ,  $D_f = 1.0$ ,  $M = 1.0$ ,  $S_r = 2.0$ ,  $G_r = 5.0$ ,  $Pr = 0.71$ ,  $P_m = 1.0$ ,  $E_c = 0.5$  and  $S_c = 0.6$ ).

The effect of modified Grashof number ( $G_m$ ) on velocity, temperature, concentration profiles and induced magnetic field are given in Figure 5.21 – 5.24 respectively. It is seen that both velocity and temperature increase with the increase of modified Grashof number



$G_m$  but the concentration profiles slightly change with the effect of  $G_m$ . Here concentration profiles negligibly increase with the increase of  $G_m$ . The effect of  $G_m$  on induced magnetic field is as before.

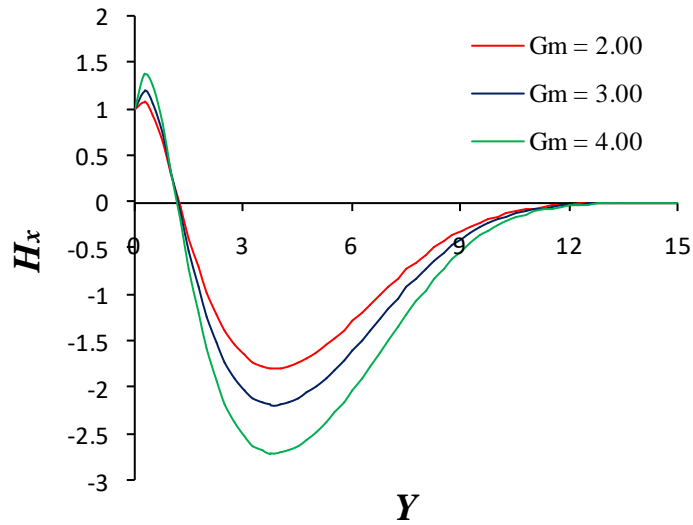


**Figure 5.24:** Variation of induced magnetic field for different values of  $G_m$  (for  $V_w = 0.5$ ,  $D_f = 1.0$ ,  $M = 1.0$ ,  $S_r = 2.0$ ,  $G_r = 5.0$ ,  $Pr = 0.71$ ,  $P_m = 1.0$ ,  $E_c = 0.5$  and  $S_c = 0.6$ ).

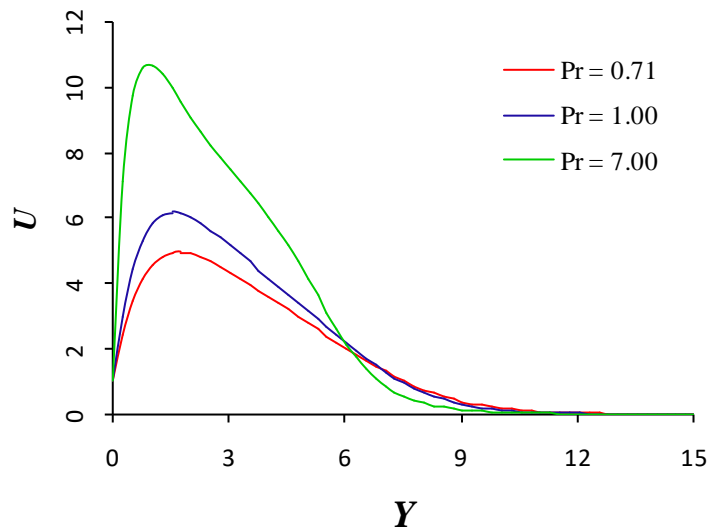


**Figure 5.25:** Velocity profiles for different values of  $Pr$  (for  $V_w = 0.5$ ,  $D_f = 1.0$ ,  $M = 1.0$ ,  $S_r = 2.0$ ,  $G_r = 5.0$ ,  $G_m = 2.00$ ,  $P_m = 1.0$ ,  $E_c = 0.5$  and  $S_c = 0.6$ ).

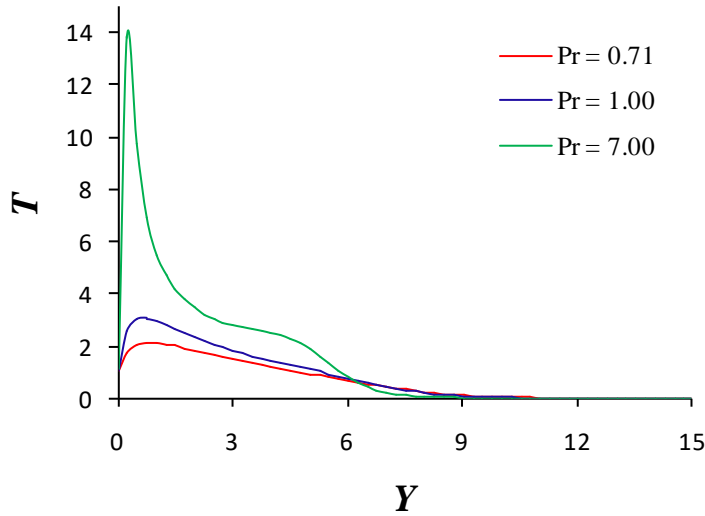


**Figure 5.26:** Temperature profiles for different values of Pr (for  $V_w = 0.5$ ,  $D_f = 1.0$ ,  $M = 1.0$ ,  $S_r = 2.0$ ,  $G_r = 5.0$ ,  $G_m = 2.00$ ,  $P_m = 1.0$ ,  $E_c = 0.5$  and  $S_c = 0.6$ ).

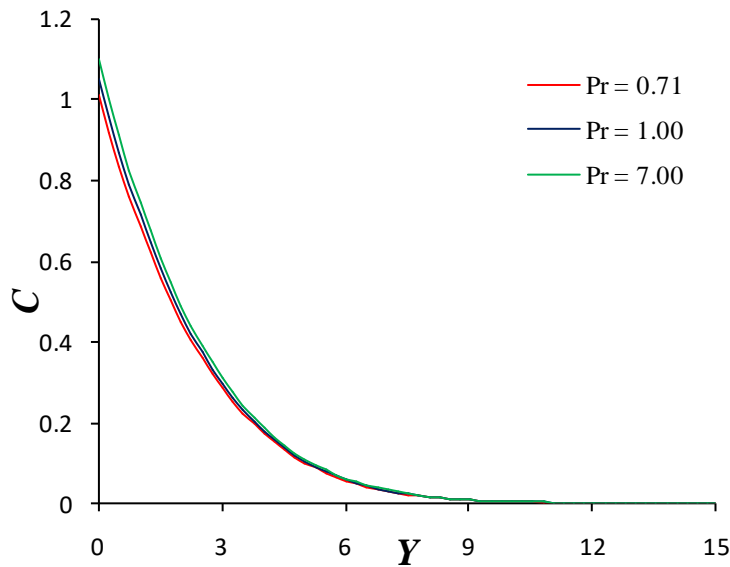


**Figure 5.27:** Variation of concentration for different values of Pr (for  $V_w = 0.5$ ,  $D_f = 1.0$ ,  $M = 1.0$ ,  $S_r = 2.0$ ,  $G_r = 5.0$ ,  $G_m = 2.00$ ,  $P_m = 1.0$ ,  $E_c = 0.5$  and  $S_c = 0.6$ ).

Displayed Figure 5.25 – 5.28 show the effect of Prandtl number (Pr) on the velocity and temperature, concentration and induced magnetic fields. For  $Pr = 0.71$  and  $Pr = 1.0$  both velocity and temperature decrease uniformly with decreasing Pr, whereas an irregular

situation is observed for both, when  $Pr = 7.0$ . Here they are found increasing first and then decrease with the increase of  $Pr$  far away before asymptotically approaches to zero.

The effect of  $Pr$  on the concentration field is very small. Here concentration increases negligibly with the increase of  $Pr$  as shown in Figure 5.27. Also the induced magnetic field decrease with the increase of  $Pr$  close to the surface, while it changes its behavior a little bit away from the surface.

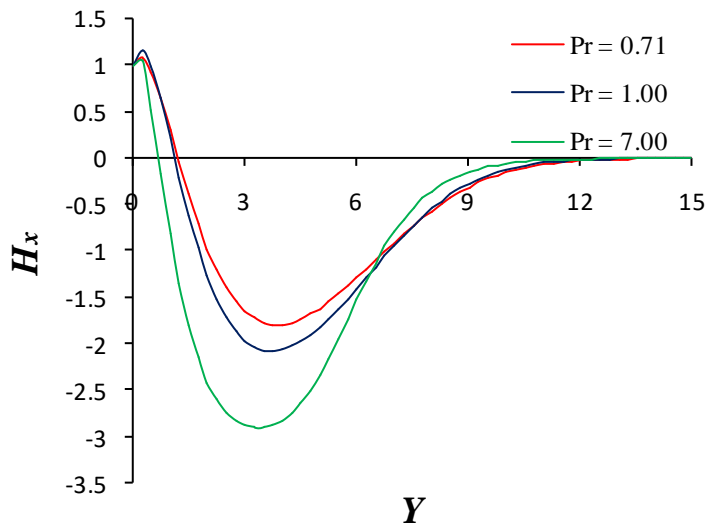


**Figure 5.28:** Variation of induced magnetic field for different values of  $Pr$  (for  $V_w = 0.5$ ,  $D_f = 1.0$ ,  $M = 1.0$ ,  $S_r = 2.0$ ,  $G_r = 5.0$ ,  $G_m = 2.00$ ,  $P_m = 1.0$ ,  $E_c = 0.5$  and  $S_c = 0.6$ ).

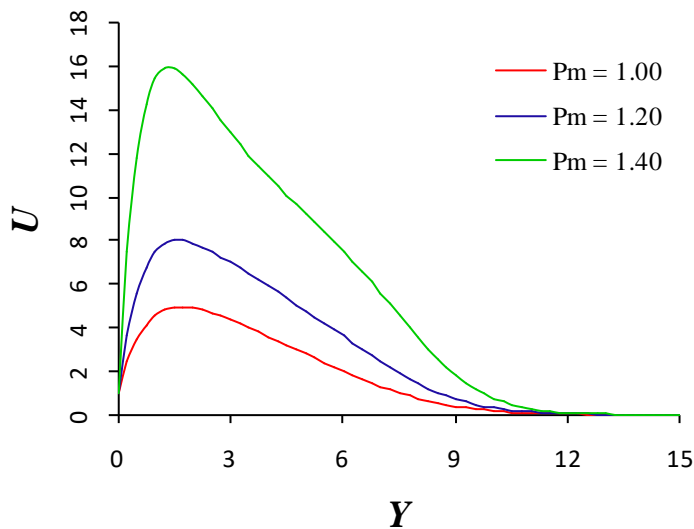


**Figure 5.29:** Velocity profiles for different values of  $P_m$  (for  $V_w = 0.5$ ,  $D_f = 1.0$ ,  $M = 1.0$ ,  $S_r = 2.0$ ,  $G_r = 5.0$ ,  $G_m = 2.00$ ,  $Pr = 0.71$ ,  $E_c = 0.5$  and  $S_c = 0.6$ ).

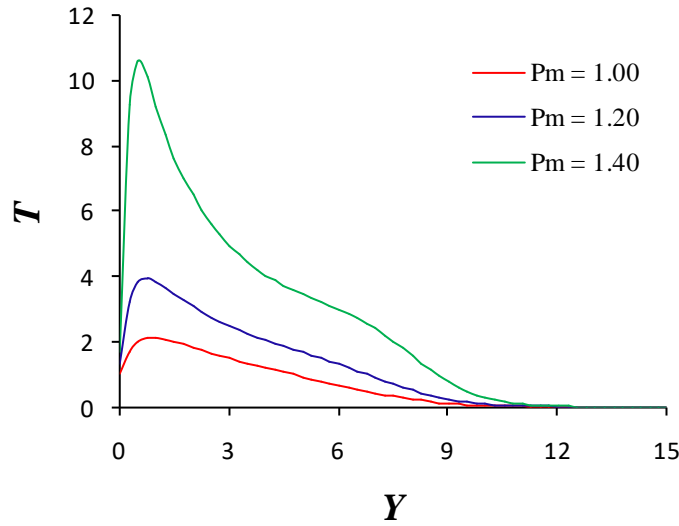


**Figure 5.30:** Temperature profiles for different values of  $P_m$  (for  $V_w = 0.5$ ,  $D_f = 1.0$ ,  $M = 1.0$ ,  $S_r = 2.0$ ,  $G_r = 5.0$ ,  $G_m = 2.00$ ,  $Pr = 0.71$ ,  $E_c = 0.5$  and  $S_c = 0.6$ ).

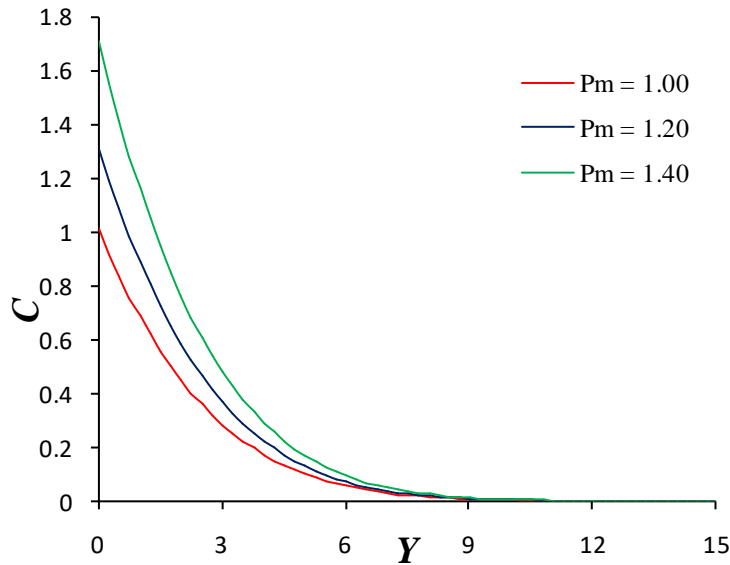


**Figure 5.31:** Variation of concentration for different values of  $P_m$  (for  $V_w = 0.5$ ,  $D_f = 1.0$ ,  $M = 1.0$ ,  $S_r = 2.0$ ,  $G_r = 5.0$ ,  $G_m = 2.00$ ,  $Pr = 0.71$ ,  $E_c = 0.5$  and  $S_c = 0.6$ ).

The influence of magnetic diffusivity parameter ( $P_m$ ) on velocity, temperature, concentration distributions and induced magnetic field are described in Figures 5.29 – 5.32. It is observed that velocity, temperature and concentration profiles are increased with the increase of  $P_m$ , but its effect on induced magnetic field is observed as usual.

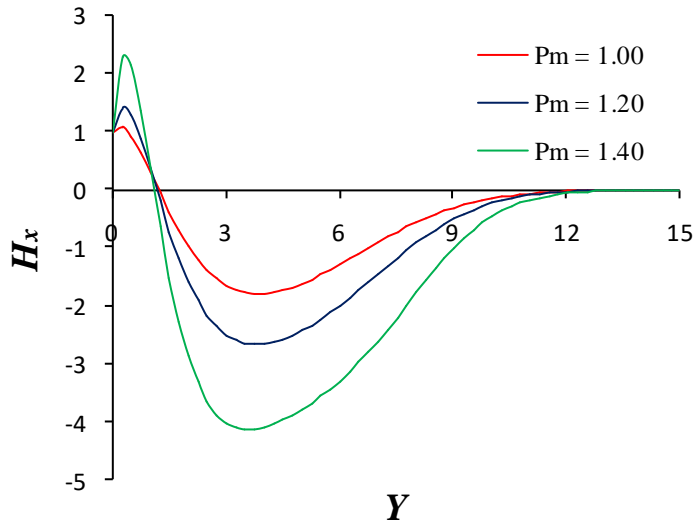


**Figure 5.32:** Variation of induced magnetic field for different values of  $P_m$  (for  $V_w = 0.5$ ,  $D_f = 1.0$ ,  $M = 1.0$ ,  $S_r = 2.0$ ,  $G_r = 5.0$ ,  $G_m = 2.00$ ,  $Pr = 0.71$ ,  $E_c = 0.5$  and  $S_c = 0.6$ ).

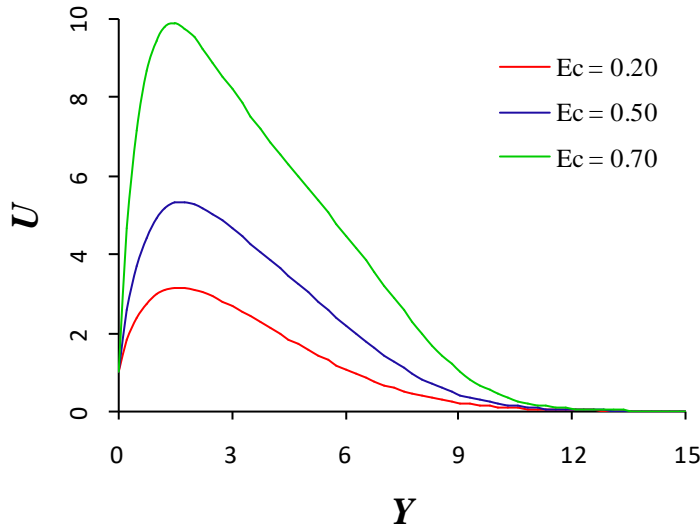


**Figure 5.33:** Velocity profiles for different values of  $E_c$  (for  $V_w = 0.5$ ,  $D_f = 1.0$ ,  $M = 1.0$ ,  $S_r = 2.0$ ,  $G_r = 5.0$ ,  $G_m = 2.00$ ,  $Pr = 0.71$ ,  $P_m = 1.0$  and  $S_c = 0.6$ ).

The effect of Eckert number  $E_c$  on the velocity, temperature, concentration and induced magnetic field are presented in Figures 5.33 – 5.36. It is observed that velocity and temperature profiles are increased with the increase of  $E_c$ . There is a small increase of

concentration profiles with increasing  $E_c$ . Here effect of  $E_c$  on induced magnetic field is observed like other cases.

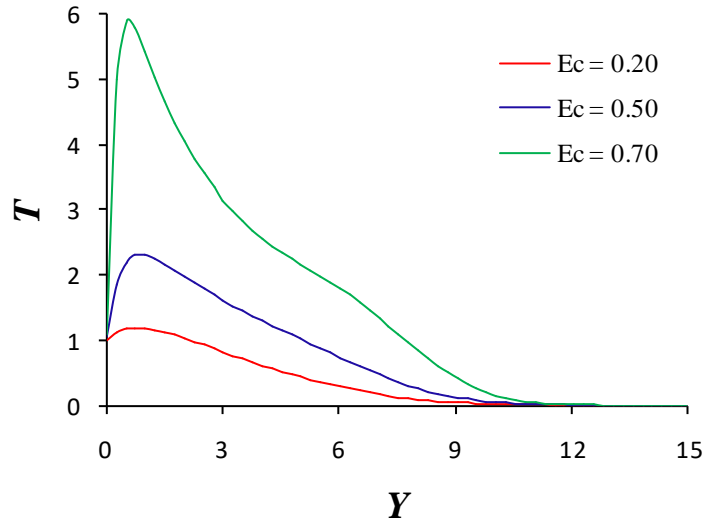


**Figure 5.34:** Temperature profiles for different values of  $E_c$  (for  $V_w = 0.5$ ,  $D_f = 1.0$ ,  $M = 1.0$ ,  $S_r = 2.0$ ,  $G_r = 5.0$ ,  $G_m = 2.00$ ,  $Pr = 0.71$ ,  $P_m = 1.0$  and  $S_c = 0.6$ ).

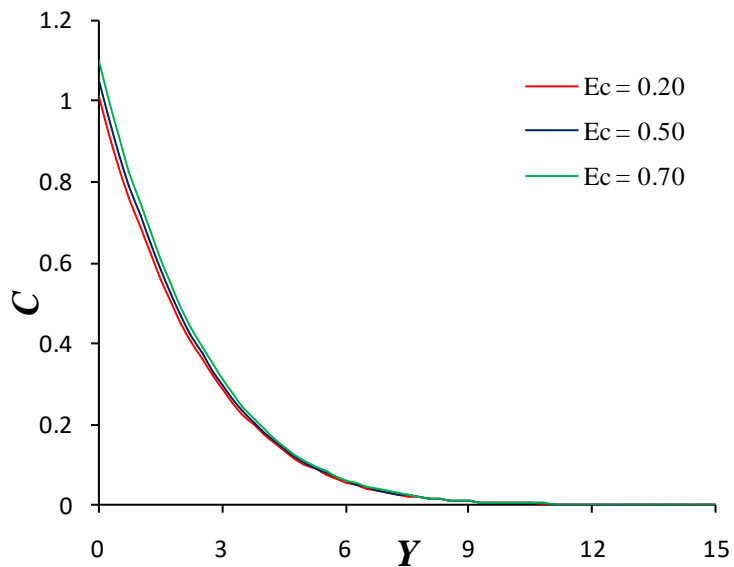


**Figure 5.35:** Variation of concentration for different values of  $E_c$  (for  $V_w = 0.5$ ,  $D_f = 1.0$ ,  $M = 1.0$ ,  $S_r = 2.0$ ,  $G_r = 5.0$ ,  $G_m = 2.00$ ,  $Pr = 0.71$ ,  $P_m = 1.0$  and  $S_c = 0.6$ ).

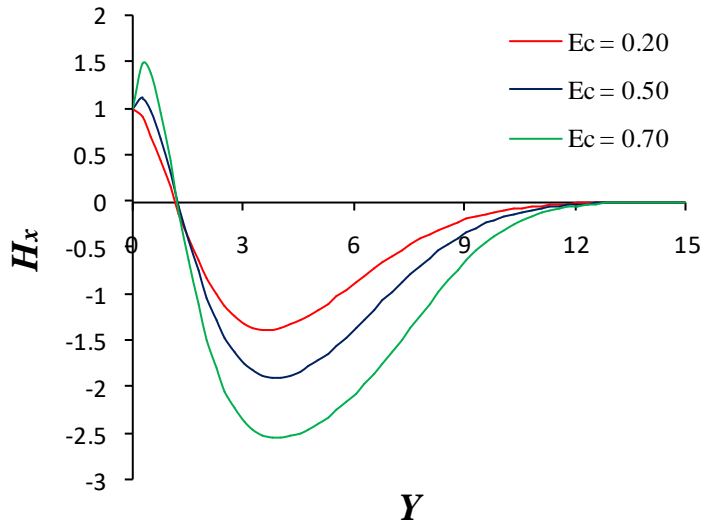


**Figure 5.36:** Variation of induced magnetic field for different values of  $E_c$  (for  $V_w = 0.5$ ,  $D_f = 1.0$ ,  $M = 1.0$ ,  $S_r = 2.0$ ,  $G_r = 5.0$ ,  $G_m = 2.00$ ,  $Pr = 0.71$ ,  $P_m = 1.0$  and  $Sc = 0.6$ ).

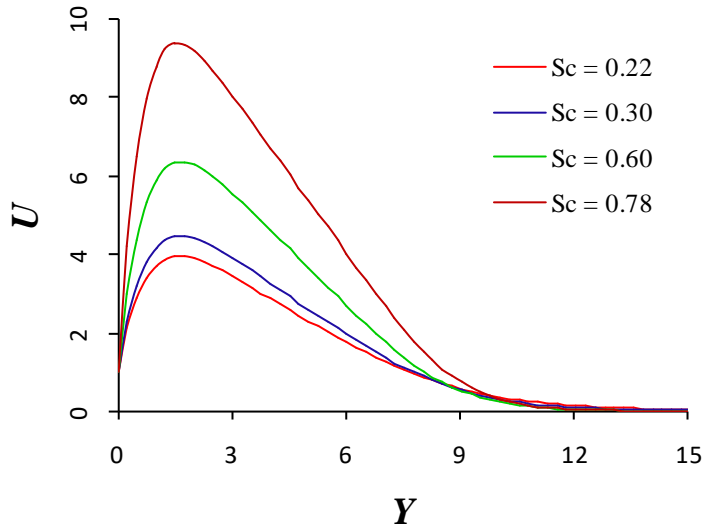


**Figure 5.37:** Velocity profiles for different values of  $Sc$  (for  $V_w = 0.5$ ,  $D_f = 1.0$ ,  $M = 1.0$ ,  $S_r = 2.0$ ,  $G_r = 5.0$ ,  $G_m = 0.6$ ,  $Pr = 0.71$ ,  $P_m = 1.0$  and  $E_c = 0.5$ ).

Finally, the effect of Schmidt number ( $Sc$ ) on the velocity, temperature and concentration distributions are presented in Figures 5.37 –5.39, whereas its effect on induced magnetic field is observed in Figure 5.40. It is observed that both velocity and temperature profiles

are increasing with the increase of  $Sc$ . Concentration increase with the increase of  $Sc$  very close to the surface but it found decreasing while increasing  $Sc$  adjacent to it. The effect of  $Sc$  on induced magnetic field is observed like other cases.

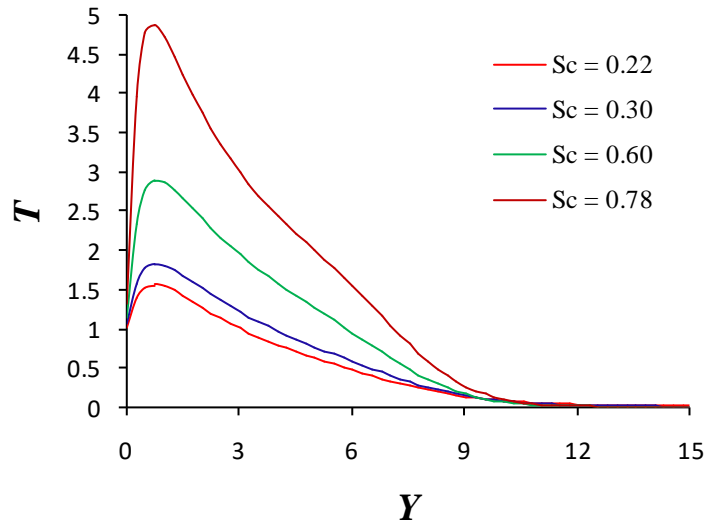


**Figure 5.38:** Temperature profiles for different values of  $Sc$  (for  $V_w = 0.5$ ,  $D_f = 1.0$ ,  $M = 1.0$ ,  $S_r = 2.0$ ,  $G_r = 5.0$ ,  $G_m = 0.6$ ,  $P_r = 0.71$ ,  $P_m = 1.0$  and  $E_c = 0.5$ ).

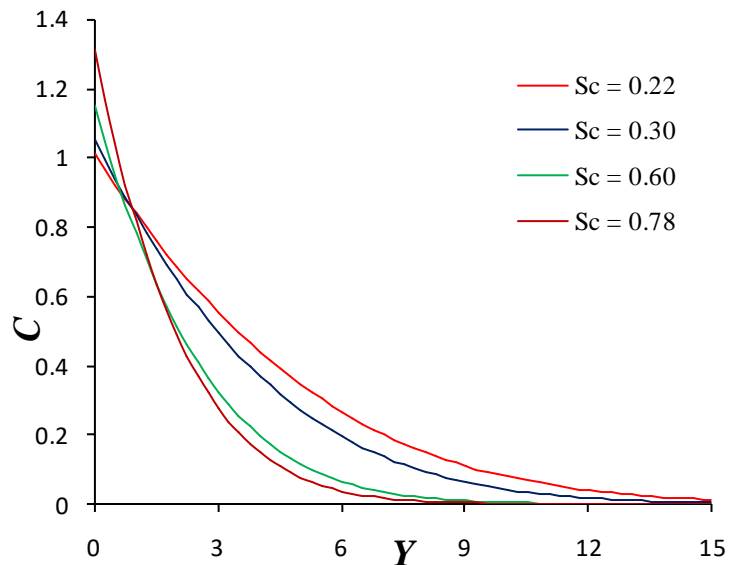


**Figure 5.39:** Variation of concentration for different values of  $Sc$  (for  $V_w = 0.5$ ,  $D_f = 1.0$ ,  $M = 1.0$ ,  $S_r = 2.0$ ,  $G_r = 5.0$ ,  $G_m = 0.6$ ,  $P_r = 0.71$ ,  $P_m = 1.0$  and  $E_c = 0.5$ ).



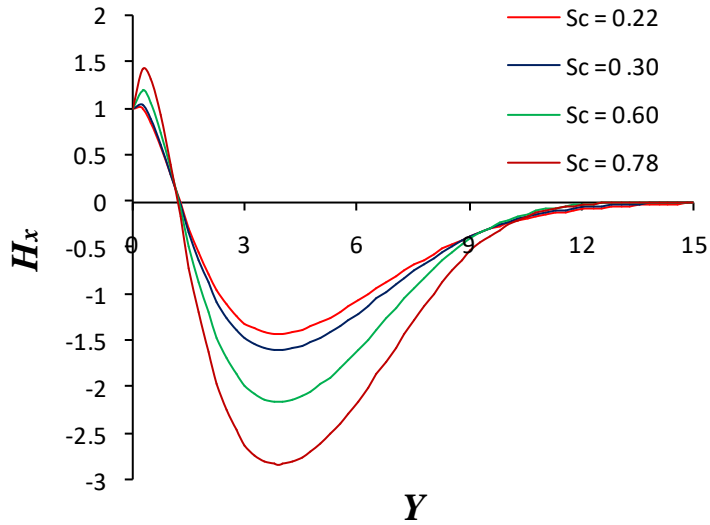


**Figure 5.40:** Variation of induced magnetic field for different values of  $S_c$  (for  $V_w = 0.5, D_f = 1.0, M = 1.0, S_r = 2.0, G_r = 5.0, G_m = 0.6, P_r = 0.71, P_m = 1.0$  and  $E_c = 0.5$ ).

The variations of the numerical values proportional to the coefficients of skin friction and heat transfer with the variation of the values of some important established dimensionless parameters are tabulated in Table (5.1) – (5.6).

**Table 5.1:** Values proportional to the coefficients of skin-friction and heat transfer for different values of suction parameter ( $V_w$ ).

$V_w$	Skin friction	Heat transfer
0.50	1.12918	1.63231
1.00	1.10182	1.77776
1.50	1.09151	2.11716

From Table 5.1, it is seen that, with the increase in  $V_w$ , the coefficient of skin friction decrease and the rate of heat transfer increases. The usual stabilizing effect of the suction parameter on the boundary layer growth is also evident from this Table.

From Table 5.2, it is seen that, with the increase in Dufour number  $D_f$ , both the coefficient of skin friction and the rate of heat transfer decreases.

**Table 5.2:** Values proportional to the coefficients of skin-friction and heat transfer for different values of Dufour parameter ( $D_f$ ).

$D_f$	Skin friction	Heat transfer
0.00	1.92917	2.17094
0.50	1.12918	2.03628
1.50	1.11181	1.76697
2.00	1.10068	1.63231

**Table 5.3:** Values proportional to the coefficients of skin-friction and heat transfer for different values of Grashof number  $G_r$ .

$G_r$	Skin friction	Heat transfer
2.00	2.24501	3.24532
5.00	1.12918	1.63231
6.00	0.98486	1.42369

It is observed from Table 5.3 that, with the increase in  $G_r$ , both the coefficient of skin friction and the rate of heat transfer decreases.

**Table 5.4:** Values proportional to the coefficients of skin-friction and heat transfer for different values of modified Grashof number ( $G_m$ ).

$G_m$	Skin friction	Heat transfer
2.00	1.12918	1.63231
3.00	1.12918	1.67122
4.00	1.12918	1.77776

It is observed from Table 5.4 that, with the increase in  $G_m$ , the coefficient of skin friction remain unchanged but and the rate of heat transfer increases.

**Table 5.5:** Values proportional to the coefficients of skin-friction and heat transfer for different values of Prandtl number (Pr).

Pr	Skin friction	Heat transfer
0.71	1.12918	1.63231
1.00	1.12918	1.74231
7.00	1.12918	1.97315

Table 5.5 exhibits that, with the increase in  $Pr$ , the coefficient of skin friction remain unchanged whereas the rate of heat transfer increases.

**Table 5.6:** Values proportional to the coefficients of skin-friction and heat transfer for different values of Schmidt number ( $S_c$ ).

$S_c$	Skin friction	Heat transfer
0.22	-1.12918	1.63231
0.30	-1.12918	1.69696
0.60	-1.12918	1.85859
0.78	-1.12918	2.11716

From Table 5.6 it is seen that, with the increase in  $S_c$ , the coefficient of skin friction remains unchanged whereas the rate of heat transfer gradually increases.

## CHAPTER VI

### Conclusions and Recommendations

An analysis of the steady MHD mixed convection heat and mass transfer flow of viscous incompressible electrically conducting fluid above a vertical porous plate have been studied in the presence of induced magnetic field. The thermal diffusion (Soret) effect as well as the diffusion-thermo (Dufour) effect are taken into account. An implicit Finite Difference numerical technique is used to obtain the solutions regarding the velocity, temperature, mass concentration and induced magnetic field and are presented for different selected values of the established dimensionless parameters.

On the basis of the figures, some important observations are as follows:

- a. An increase in the suction parameter leads to decrease the velocity, temperature and concentration.
- b. The induced magnetic fields decrease within a certain interval very close to the plate and then the reverse effect is observed bit away from the plate surface for the case of suction.
- c. As the values of the Dufour parameter ( $D_f$ ) increase, the fluid velocity and temperature also increases.
- d. Increasing values of the Dufour parameter lead to increase the concentration in the fluid flow.
- e. As magnetic parameter ( $M$ ) increases, the velocity, temperature and concentration increase.
- f. The fluid velocity, temperature and concentration increase with increasing values of the Soret parameter  $S_r$ .
- g. Both velocity and temperature increase rapidly with the increase of Grashof number  $G_r$  and modified Grashof number ( $G_m$ ).
- h. The effects of  $G_r$  and  $G_m$  on the concentration distribution are found very small.
- i. For  $Pr = 0.71$  and  $Pr = 1.0$  both velocity and temperature decrease uniformly with decreasing  $Pr$  but an irregular situation is observed when  $Pr = 7.0$ .
- j. The velocity, temperature and concentration profiles are increased with the increase of magnetic diffusivity parameter  $P_m$ .

- k. Both velocity and temperature profiles are increased with the increase of Eckert number  $E_c$ .
- l. A small increase of concentration profiles is found with increasing  $E_c$ .
- m. Both velocity and temperature profiles are increasing with the increase of Schmidt number  $S_c$ .
- n. Concentration increase with the increase of  $S_c$  very close to the surface but after that it found decreasing while increasing  $S_c$ .
- o. The induced magnetic fields decrease within a certain interval very close to the plate and then the reverse effect is observed bit away from the plate surface.
- p. The induced magnetic fields increase within a certain interval very close to the plate and then the reverse effect is observed bit away from the plate surface for all other parameter except suction parameter.

On the basis of the tables, the following conclusions are made:

- a. With the increase in  $V_w$ , the coefficient of skin friction decrease and the rate of heat transfer increases.
- b. With the increase in Dufour number  $D_f$ , both the coefficient of skin friction and the rate of heat transfer decreases.
- c. With the increase in  $G_r$ , both the coefficient of skin friction and the rate of heat transfer decreases.
- d. With the increase in  $G_m$ ,  $Pr$  and  $S_c$  the coefficient of skin friction remain unchanged but and the rate of heat transfer increases.

Further works are necessary to study the case of steady MHD heat and mass transfer by mixed convection flow past a semi-infinite vertical porous plate.

## REFERENCES

- Alam, MD. M. (1995): Steady MHD free convection and mass transfer flow with thermal diffusion and large suction, Ph. D. Thesis, Ch 7, 134.
- Alim, M. A., Alam, M. D. and Mamun, A. (2007): Joule heating effect on the coupling of conduction with magneto hydrodynamic free convection flow from a vertical plate, *Non-Linear Analysis: Modeling and Control*, vol. 12, no. 3, pp. 307–316.
- Asaduzzaman, MD., Islam, MD. R. and Islam, A.: (2016), Transient heat transfer flow along a vertical plate with induced magnetic field, *International Journal of Scientific & Engineering Research*, 7 (11), 10-22.
- Choudhary, R.C. and Sharma, B.K. (2006): Combined heat and mass transfer by laminar mixed convection flow from a vertical surface with induced magnetic field, *Journal of Applied Physics*, 99, 034901 (<http://dx.doi.org/10.1063/1.2161817>).
- Eckert, E. R. G. and Drake, R. M. (1974): *Analysis of Heat and Mass Transfer*, MCGraw-Hill, New York, USA.
- Gundagani, M., Sheri, S., Paul, A. and Reddy, M.C.K. (2013): Unsteady magnetohydrodynamic free convective flow past a vertical porous plate, *International Journal of Applied Science and Engineering*, 11(3), 267-275.
- Govardhan, K., Kishan, N. and Balaswamy, B. (2012): Effect of viscous dissipation and radiation on MHD gas flow and heat and mass transfer over a stretching surface with a uniform free stream, *Journal of Engineering Physics and Thermophysics*, vol. 85, no. 4, pp. 909–916.
- Hossain, M.M.T., Zaman, M.A., Rahman, F. and Hossain, M.A. (2013): Steady MHD free convection heat and mass transfer flow about a vertical porous surface with thermal diffusion and induced magnetic field, *American Institute of Physics (AIP) Conf. Proc.*, 1557, 594 – 603; doi: 10.1063/1.4824172; © 2013 AIP Publishing (<http://dx.doi.org/10.1063/1.4824172>).
- Islam, A., Islam, M.M., Rahman, M., Ali, L.E. and Khan, MD. S. (2016): Unsteady heat transfer of viscous incompressible boundary layer fluid flow through a porous plate with induced magnetic field, *Journal of Applied Mathematics and Physics*, 4, 294-306 (<http://dx.doi.org/10.4236/jamp.2016.42037>).

- Jai, S., (2012): Viscous dissipation and chemical reaction effects on flow past a stretching surface in a porous medium, *Advance Theory of Applied Mechanics*, vol. 5, pp. 323–331.
- Kafousiasis, N. G, and Williams, E. M. (1995). Thermal-diffusion and diffusion-Thermo effects on mixed free-forced convective and mass transfer boundary layer flow with temperature dependent viscosity, *International Journal of Engineering Science*, vol. 33, pp. 1369-1384.
- Khaleque, T. S. and Samad, M. A. (2010): Effects of radiation, heat generation and viscous dissipation on MHD free convection flow along a stretching sheet, *Research Journal of Applied Sciences, Engineering and Technology*, vol. 2, no. 4, pp. 368–377.
- Khan, MD. S., Wahiduzzaman, M., Karim, I., Islam, MD. S. and Alam, MD. M. (2014): Heat generation effects on unsteady mixed convection flow from a vertical porous plate with induced magnetic field, (10th International Conference on Mechanical Engineering, ICME 2013), *Procedia Engineering*, 90, 238-244.
- Makinde, O. D. (2010): On MHD heat and mass transfer over a moving vertical plate with a convective surface boundary condition, *The Canadian Journal of Chemical Engineering*, vol. 88, no. 6, pp. 983–990.
- Mansour, M. A., El-Anssary, N. F. and Aly, A. M. (2008): Effect of chemical reaction and viscous dissipation on MHD natural convection flows saturated in porous media with suction or injection, *International Journal of Applied Mathematics and Mechanics*, vol. 4, no. 2, pp. 60–70.
- Mohammad, F., Masatiro, O., Abdus, S. and Mohamud, A. (2005): Similarity solutions for MHD flow through vertical porous plate with suction, *Journal of Computational and Applied Mechanics*, 6(1), 15–25.
- Opiyo, R.O., Alfred, W.M. and Jacob, K.B. (2017): Numerical computation of steady buoyancy driven MHD heat and mass transfer past an inclined infinite flat plate with sinusoidal surface boundary conditions, *Applied Mathematical Sciences*, 11(15), 711 – 729 (<https://doi.org/10.12988/ams.2017.7127>).
- Palani, G. and Srikanth, U. (2009): MHD flow past a semi-infinite vertical plate with mass transfer, *Nonlinear Analysis: Modeling and Control*, vol. 14, no. 3, pp. 345–356.

- Pantokratoras, A. (2007): Comment on “Combined heat and mass transfer by laminar mixed convection flow from a vertical surface with induced magnetic field” *Journal of Applied Physics*, 102, 076113
- Postelnicu, A. (2010): Heat and mass transfer by natural convection at a stagnation point in a porous medium considering Soret and Dufour effects, *Heat and Mass Transfer*, vol. 46, no. 8-9, pp. 831–840.
- Raptis, A. and Kafoussias, N.G. (1982): Magnetohydrodynamic free convection flow and mass transfer through porous plate with constant heat flux, *can J. phys*, 60(12), 1725-1729.
- Reddy, V.P., Kumar, R.V.M.S.S.K., Reddy, G.V., Prasad, P.D. and Varma, S.V.K. (2015): Free convection heat and mass transfer flow of chemically reactive and radiation absorption fluid in an aligned magnetic field, (International Conference on Computational Heat and Mass Transfer-2015) *Procedia Engineering*, 127, 575-582.
- Sarada, K. and Shankar, B. (2013): The effects of Soret and Dufour on an unsteady MHD free convection flow past a vertical porous plate in the presence of suction or injection, *International Journal of Engineering and Science*, vol. 2, no. 7, pp. 13–25.
- Sattar, M. A., (1993). Free and forced convection boundary layer flow through a porous medium with large suction, *International Journal of Energy Research*, vol. 17, no. 1, pp. 1–7.
- Sattar, M.A. and Alam, M. S. and Rahman, M. M. (2006): MHD free convective heat and mass transfer flow past an inclined surface with heat generation, *Thammasat Int. J. Sc. Tech.* 11(4), 1-8.
- Usman, H. and Uwanta, I. J. (2013): Effect of thermal conductivity on MHD Heat and Mass transfer: flow past an infinite vertical plate with Soret and Dufour effects, *American Journal of Applied Mathematics*, vol. 1, no. 3, pp. 28–38.
- Uwanta, I. J. (2012): Effects of chemical reaction and radiation on Heat and Mass Transfer past a semi-infinite vertical porous plate with constant mass flux and dissipation, *European Journal of Scientific Research*, vol. 87, no. 2, pp. 190–200.
- Uwanta, I. J., Asogwa, K. K. and Ali, U. A. (2008): MHD fluid flow over a vertical plate with Dufour and Soret effects, *International Journal of Computer Applications*, vol. 45, no. 2, pp. 8–16.



Uwanta I. J. and Usman, H. (2014): On the Influence of Soret and Dufour Effects on MHD Free Convective Heat and Mass Transfer Flow over a Vertical Channel with Constant Suction and Viscous Dissipation, Hindawi Publishing Corporation, International Scholarly Research Notices, Volume 2014, Article ID 639159, 11 pages, <http://dx.doi.org/10.1155/2014/639159>.

Wahiduzzaman, M., Biswas, R., Equb, MD. A., Khan, MD. S. and Karim, I. (2015): Numerical solution of MHD convection and mass transfer flow of viscous incompressible fluid about an inclined plate with hall current and constant heat flux, Journal of Applied Mathematics and Physics, 3, 1688-1709 (<http://dx.doi.org/10.4236/jamp.2015.312195>).